THERAPEUTIC ROLE OF NEUROGENIC TRANSCRIPTION FACTORS IN SPINAL CORD INJURY

By

MISAAL N. PATEL

A dissertation submitted to the

School of Graduate Studies

Rutgers, The State University of New Jersey

In partial fulfillment of the requirements

For the degree of

Doctor of Philosophy

Graduate Program in Biomedical Engineering

Written under the direction of

Li Cai

And approved by

_____

_____

_____

_____

New Brunswick, New Jersey

OCTOBER, 2019

ABSTRACT OF THE DISSERTATION

Therapeutic role of neurogenic transcription factors in spinal cord injury

By MISAAL N. PATEL

Dissertation Director:

Li Cai, Ph.D.

Spinal cord injury (SCI) results in neuronal damage and glial scar formation, leading to loss of function and paralysis below the injury site. Although there are assistive devices in the market, there are no therapeutics that promote complete repair and regeneration after SCI. Major hurdles in neural regeneration include a limited level of neurogenesis in the adult spinal cord, an inflammatory microenvironment that inhibits neurogenesis, axon regeneration, neuronal relay formation, and myelination at the injury site. Promoting endogenous neural stem and progenitor cells (NSPCs) for tissue regeneration represents a potential strategy for the treatment of SCI. However, adult NSPCs largely differentiate into glial cells and contribute to glial scar formation in the injured spinal cord. Using virus-mediated delivery system as a potential therapeutics, we examined the effects of neurogenic factors on SCI in a mouse model. We identified that neurogenic factors promote cell proliferation and activation of NSPCs by activating Notch and Nanog signaling pathways during the acute stage of SCI. These factors promote the generation of various types of neurons (e.g., glutamatergic and cholinergic interneurons) and inhibit the generation of GABAergic interneurons in the injured spinal cord. Importantly, during the chronic stage, the treatment reduces glial scar formation and dramatically improves functional locomotion. Collectively, these findings suggest the neurogenic factors represent promising therapeutic genes for the treatment of SCI and provide molecular insight for transcription factor-mediated functional recovery.

ACKNOWLEDGEMENTS

I would like to thank my advisor, Dr. Li Cai, for allowing me to be part of his lab and his constant support and guidance for this project. I would like to thank my committee members, Dr. Bonnie Firestein, Dr. Peng Jiang, Dr. Kelvin Kwan, and Dr. Zhiping Pang for their constructive feedback. I would also like to take this opportunity to thank current and past members of the Cai lab, especially Jeremy Anderson, Shunyao Lei, Rebecca Risman, Ying Li, Sofia Castro-Pedrido, Xin Ai, and Tianyue Fu for their assistance and constructive feedback. My sincere thank go to my parents and friends for their constant support and encouragement.

TABLE OF CONTENT

LIST OF TABLES

LIST OF FIGURES

ABBREIVATIONS

SCI	spinal cord injury
NSPC	neural stem progenitor cells
GFP	green fluorescent protein
RFP	red fluorescent protein
TF	trascription factor
DPI	days post injury
CSPG	chondroitin sulfate proteoglycan
RA	reactive astrocytes
SA	scar forming astrocytes
N1CR2	Notch1CR2-GFP
CNS	central nervous system
PNS	peripheral nervous system
DEG	differenially expressed gene
NS	not significant
ND	not detected
Ms	mouse
Dk	donkey
Rb	rabbit
Gt	goat
Gp	guiana pig

Chapter I. Introduction

In the field of biomedical engineering and tissue engineering, tissue regeneration after central nervous system (CNS) injury has been one of the most prevailing topic. CNS consist of two parts: brain and spinal cord. In addition to CNS, other part of the nervous system is peripheral nervous system (PNS). PNS contains nerves and nerve cells that lies outside brain and spinal cord. PNS has the ability to spontaneously regenerate axons after injury [1-4]. However, regeneration of axons and neurons in the CNS is limited. For regenerative efforts, biomedical engineers and researchers utilize biomaterials, stem cells, cell and gene therapy, and combinational approaches. In this dissertation, stem cell and gene therapy were used in an effort to regenerate neurons after SCI. Specifically, lentivirus based gene delivery approach was used to overexpress transcription factor(s) to address the two gaps in the field of regeneration after SCI: (1) limited neurogenesis in the adult spinal cord and (2) glial scar formation.

I.1. Spinal cord and spinal cord injury

I.1.1. Spinal cord structure and function

During development, nervous system, including spinal cord, arise from ectoderm. Entire CNS develops from the neural tube. Spinal cord is an essential part of the CNS, that communicates (e.g., collects, distribute, and integrate) information between brain to the rest of the body via spinal nerves (dorsal and ventral root). Physicians Charles Bells and Francois Magendie are early pioneer in determining the role of ventral and dorsal roots in the spinal cord. Ventral roots carry information away for the spinal cord towards the body and dorsal roots carries information towards the spinal cord.

Spinal cord contains neurons and glias (e.g., oligodendrocytes and astrocytes). Neurons contains axons that transfer information as a form of electrical system across the nervous system. For instance, sensory nerves send information from outside of CNS to interneurons present in the CNS. Interneurons then sends axons to the brain to analyze the situation and forms synapse with motor neurons to command muscle contraction. At synapse junction, neurotransmitters are transferred from pre-synaptic Oligodendrocytes, which provides myelin sheaths around the axons. Myelination of the axons leads to increase in action potential conduction velocity and thus faster transfer of electrical signals. There are many types of neurons found in the spinal cord (e.g., cholinergic neurons, glutamatergic neurons, GABAergic neurons, serotonergic neurons).

I.1.2. Spinal cord injury

SCI is a damage to the part of the whole spinal cord leading to the permanent loss of function below the injury site. In some cases SCI is leads to disability, decrease life expectancy, and even death [5]. Major causes of SCI include falls (31.8%), vehicle crashes (39.3%), sports/recreation activities (8.0%), medical and surgical intervention (4.3%), and act of violence (13.5%) [6]. There are about 291,000 people in the United States currently living with SCI with about 18,000 new incidents every year [6]. SCI not only affect individual's life style and life expectancy, but also results in enormous financial burden. For instance, yearly cost due to the SCI ranges from anywhere from $43,700 to over 1 million [6]. SCI injury treatment market is already big and is expected to grow 3.7% by 2025.

I.1.3. SCI models

Numerous animals including mice, rats, dogs, rabbits, and pigs are used as a model for SCI. Pathology of human SCI is comparable to that of experimental animals, such as

mouse [7-9]. There are various advantages of using rodent as a model for SCI, such maintaining rodents is relative inexpensive compared to primate models. Furthermore, rodent models have a controlled and reproducible standard methods of behavioral analysis (e.g., Basso, Beattie, Bresnahan (BBB) scale [10] for rat model and Basso Mouse Scale (BMS) for mouse model [11]). Another standard behavioral tests includes the cylinder rearing test [12], the horizontal ladder test [12], and catwalk analysis [13].

There are numerous SCI models are used for research purpose, including but not limited to ischemia-reperfusion injury model, inflammatory model, photochemical-induced model, traumatic injury model (e.g., contusive, compressive, and tractive), and complete transected model [7]. There are different extent (incomplete vs complete) and type (tetraplegia vs paraplegia) of SCI, out which incomplete tetraplegia is most prevalent (47.6%) in clinics [6].

I.1.4. Primary and Secondary physiology of the SCI

The mechanism behind spinal cord injury is divided into two stages: primary injury and secondary injury. The primary injury, an acute stage, includes the immediate effect of the trauma (e.g., compression, contusion, and shear activity) [14]. Whereas, the secondary injury, a sub-acute stage, usually follows the primary injury and could involves breakdown of blood-spinal cord barrier, cellular dysfunction, oxidative stress, free-radical formation, ischemia, inflammation, edema, and/or excitotoxicity that lead to cell necrosis or apoptosis [14].

I.1.5. Limited extent of neurogenesis after SCI

Major hurdles in neural regeneration in the injured spinal cord include a limited level of neurogenesis in the adult spinal cord, an inflammatory microenvironment that inhibits neurogenesis and axon regeneration, neuronal relay formation and myelination at the injury site [15-18]. SCI leads to loss of both neurons and glial cells after injury. In comparison to PNS, CNS spontaneously does not regenerate sufficient amount of neurons and axons after injury in the adult [1-4]. Injury activates neural stem cells (NSCs) in the ependymal layer of the spinal cord [19-21]. NSCs migrate from ependymal layer towards superficial dorsal horn layers along the lamina IV as they differentiate to mature neurons. Level of NSCs activation and migration is significantly increase after an injury [21, 22]. The migration of NSCs to superficial dorsal horn layers takes up to a month and within that time NSCs gradually differentiate into mature neurons [21-23]. Typically in adult spinal cord, NSCs differentiate through multiple stages characterize by Skp2, Nestin, Mash1, Ngn2, Notch3, doublecortin (DCX), Calretinin (CR), and eventually into NeuN expressing mature neurons [21].

I.1.6. Gliogenesis and glial scar

SCI causes activation of the local immune cells, microglia, and astrocytes, which lead to glial scar formation. Glial scar is mostly composed of reactive astrocytes, NG2-glia, and non-neuronal cells (e.g., pericytes and meningeal cells) and proteoglycan rich extracellular matrix (ECM) [24, 25]. Injury activated astrocytes (also called reactive astrocytes) release chondroitin sulfaphate proteoglycans (CSPGs) into the extra cellular matrix (ECM). Reactive astrocytes and CSPGs form glial scars, which act as a major physical barrier in inhibition of an axonal regrowth and connections after SCI. There are several studies that

are targeting astrocytes [26] and CSPGs [27, 28] to reduce the formation of glial scar, in order to improve locomotion after SCI.

I.2. Current research on SCI

Currently on the market, there are assistive devices, rehabilitation therapies, and drugs that can reduce the pain and maintain stabilization. Unfortunately, there are no therapeutics that promote complete repair and regeneration after SCI.

I.2.1. Cell transplantation

Although there are several molecular and genetics factors known for spinal cord regeneration after injury, reliable regenerative therapy has not been developed. Transplantation of embryonic stem cells (ESCs) or induced pluripotent stem cells (iPSCs) derived NSPCs after SCI lead to some functional recovery in animal models, but the mechanism is poorly understood [29, 30]. Although NSPCs are believed to give rise to all types including oligodendrocytes, astrocytes, and neurons in the CNS, transplanted NSPCs mostly give rise to astrocytes and some oligodendrocytes with little known generation of neurons [31]. Furthermore, transplantation based cell therapies faces multiple major challenges to be applicable for clinical usage due to the time required to prepare the cells for the transplantation. Many transplanted studies have shown some functional recovery when cells are transplanted in sub-acute phase, but not when they are transplanted in the chronic phase [32, 33].

I.2.2. *In vivo* reprogramming for promoting neurogenesis and attenuating glial scar formation

As an alternative to transplantation, researchers are focusing on *in vivo* reprogramming. The *in vivo* reprogramming approach uses transcription factors to target internal terminally differentiated cells (e.g., astrocytes and oligodendrocytes) to program and regenerate target cells (e.g., neurons) for tissue repair after injury. Currently, there are many *in vivo* reprogramming research being performed to promote neurogenesis after central nervous system injury, however most of them are in the brain [34-41]. There are few studies conducted to promote neurogenesis after SCI [42, 43], however these studies have not shown any functional/locomotion recovery in mice.

I.2.3. Stem cell therapy has potential to repair and regenerate spinal cord after injury

Identification NSPCs and their role in injured spinal cords have provided promising opportunities for spinal cord regeneration. Stem cell therapy relies on the differentiation of injury activated endogenous NSPCs to neurons, astrocytes, and oligodendrocytes [44-46]. Endogenously generated neurons have ability to mature and integrate into the surrounding environment [45, 47]. However, adult NSPCs mostly generate astrocytes and oligodendrocytes [31]. Therefore amount of neurogenesis through endogenous NSPCs is not sufficient to replenish all the neurons lost due to the injury [48, 49].

I.3. Limitation of current approach in SCI research

Although there are various strategies that are already developed to repair and regenerate the spinal cord after injury using NSPCs, no studies are successful in regeneration of a functional spinal cord [50]. This is partially due to lack of a comprehensive understanding about the activation and differentiation of NSPCs into specific sub-types of interneurons

and about the factors that reduces glial scar after SCI. Previous approaches for the SCI treatment have targeted glial scar [26-28] or native spinal cord cell source [42, 43] (e.g., astrocytes and oligodendrocytes) to induce neurogenesis and functional recovery. Some of these studies were successful in inducing neurogenesis or functional recovery, however the amount and the specific sub-type of interneuron was not sufficient to replenish all the neurons lost due to the injury [48, 49]. Our proposed approach targets both glial scar and native cells, in an aim to identify a novel therapeutic target, Gsx1, for SCI that is sufficient enough to reduce glial scar and promote NSPCs differentiation into specific type of interneurons essential for locomotion recovery after SCI. Having a therapeutic that has the ability to reduce glial scar, regenerate specific types of interneurons, and enhance locomotion function after SCI will be a breakthrough therapy in the SCI field.

I.4. Importance of gene therapy for the treatment of the SCI

I.4.1. Lentivirus mediated gene delivery system

To deliver these factors, *in vivo*, we will be using a lentivirus, a type of retrovirus, as a mediated delivery method. Retroviruses are believed to infect the dividing cells (e.g., progenitor cells and reactive glial cells) and not infect non-dividing cells (e.g., neurons) [51]. Additionally, gene delivered through lentivirus integrate are stable and long term can into host genome. We are using lentivirus carrying gene of interest to target Notch signaling pathway.

I.4.2. Notch signaling pathway

Notch1 gene is one of four important genes in Notch1 signaling pathway. The Notch signaling pathway is a highly conserved signaling pathway in most multicellular organism and plays important role in promotion of gliogenesis, inhibition of premature neurogenesis,

and regeneration of NSPCs [52, 53]. Gsx1 and Nkx6.1 bind and interact with the CR2 (conserved non-coding fragment in the second intron) region of Notch1 gene, also is one of Notch1 enhancer [54]. Previous study have indicated that an increase in Nkx6.1 expression leads to an increase in Notch1 expression and knockdown of Nkx6.1 leads to a decrease in Notch1 expression [54]. Notch is required for NSPC proliferation and maintenance [53, 55] and dendritic arborization in the central nervous system (CNS). In spinal cord, Notch pathway also plays pivotal role in induction and maintained of the neuropathic pain [56]. Thus, targeting Notch pathway can also be used to identify therapeutics for neuropathic pain. In Zebrafish, after SCI, Notch signaling pathway leads to generation of motor neurons [57].

I.4.3. Nkx6.1

NK6 Homeobox 1 (Nkx6.1) is widely expressed by NSPC within the neural tube, plays critical roles in ventral neural patterning, controls lineage specification of both neurons and glia during spinal cord development [58, 59]. In addition, Nkx6.1^{+} ependymal cells in the adult mouse spinal cords retain the proliferative property of NSPCs [60]. In the injured spinal cord of zebrafish, V2 interneurons can be generated from Pax6 and Nkx6.1 expressing progenitors [61]. Furthermore, Nkx6.1 is known to differentiate into neurons during development [62] and after spinal cord injury in turtles [63].

I.4.4. Gsx1

In addition to Nkx6.1, we are also studying the role of GS Homeobox 1 (Gsx1, also called Gsh1) in the spinal cord after hemisection spinal cord injury. The homeodomain transcription factor Gsx1 is known to play an essential roles during spinal cord development [64, 65]. Gsx1 expression is found in the dorsal region of the embryonic

developing spinal cord and is involved in regulating early NSPCs [64]. In adult normal and injured spinal cord, Gsx1 expression is low or not detectable. Since normal development of the spinal cord requires Gsx1 function, we hypothesize that upregulation of Gsx1 in injured spinal cord initiates and promotes neurogenesis and regenerates damaged spinal cord.

Chapter II. Gsx1 Promotes Functional Recovery after Spinal Cord Injury

Note: This Chapter is reproduced from the manuscript that is submitted to Nature Communication.

Misaal Patel, Jeremy Anderson, Shunyao Lei, Yi Lisa Lyu, and Li Cai. Gsx1 Promotes Functional Recovery after Spinal Cord Injury. Nature Communication (Submitted).

II.1. Abstract

Promoting endogenous neural stem and progenitor cells (NSPCs) for tissue regeneration represents a potential strategy for the treatment of spinal cord injury (SCI). However, adult NSPCs largely differentiate into glial cells and contribute to glial scar formation in the injured spinal cord. Here we show that lentivirus-mediated Gsx1 expression (Gsx1 treatment) promotes cell proliferation and activation of NSPCs, increases the generation of glutamatergic and cholinergic interneurons, and inhibits the generation of GABAergic interneurons in mice with lateral hemisection SCI. Importantly, Gsx1 treatment reduces reactive astrogliosis and glial scar formation and dramatically improves locomotor function. Genome-wide transcriptome analysis reveals that Gsx1 induces signaling pathways associated with neurogenesis and inhibits genes associated with reactive and scar forming astrocytes. These gene expression changes correlate with NSPC activation, neuronal differentiation, and attenuation of scar formation. Collectively, our study identifies Gsx1 treatment as a promising therapy for SCI and provides molecular insight for Gsx1-mediated functional recovery.

II.2. Introduction

To restore function after spinal cord injury (SCI), it is necessary to repair and reconstruct the damaged local circuitry. Major hurdles in neural regeneration include a limited level of

neurogenesis in the adult spinal cord, an inflammatory microenvironment that inhibits neurogenesis, axon regeneration, neuronal relay formation, and myelination at the injury site [15-18]. SCI activates endogenous neural stem and progenitor cells (NSPCs) that reside around the central canal in the ependymal region [20, 66, 67], which provides potential cell source for damage repair and regeneration. However, adult NSPCs in the spinal cord largely differentiate into astrocytes and oligodendrocytes with only a very small portion into neurons [19, 20, 31, 68-70]. Transplantation of many cell types have been tested for their potential to treat SCI, however, the efficacy and safety of this approach has not been established [18]. More recently, it has been demonstrated that new neurons can be generated by cell reprogramming with forced expression of neurogenic transcription factors (e.g., Sox2, NeuroD1, and Olig2) in the injured spinal cord [42, 43, 71, 72]. However, these approaches provide limited or no functional improvement. Furthermore, injury-induced reactive astrocytes produce chondroitin sulfate proteoglycans (CSPGs), which are known to prevent axonal growth and sprouting, and result in permanent functional deficits. Attempts to attenuate glial scar formation have shown the potential to promote axonal regeneration [27, 73-75]. Nevertheless, reducing scar tissue alone does not promote sufficient functional improvement. In addition, SCI induces over-inhibition by the GABAergic neurons causing the spared axons non-functional [76, 77]. By reducing the excitability of inhibitory interneurons or re-establishing the excitation/inhibition ratio, the dormant relay pathways can be reactivated, which leads to an improved locomotor function [78].

Genomic Screened Homeo Box 1 (Gsx1 or Gsh1) is a neurogenic factor highly expressed in the central nervous system at the embryonic stage [79]. During the development of the spinal cord, Gsx1 and its homolog Gsx2 regulate proliferation and differentiation of neural stem/progenitor cells (NSPCs) [64, 80-84]. Gsx1 is also involved in controlling cell fate

determination between excitatory and inhibitory interneurons [64, 65]. In the adult spinal cord, Gsx1 expression is low or not detected [79, 85]. These findings raise the possibility that reactivating Gsx1 expression at the lesion site may promote neurogenesis to generate neurons native to the spinal cord for injury repair and functional recovery.

In this study, we use a lentivirus-mediated gene expression system to transduce Gsx1 (Gsx1 treatment) into the adult mouse spinal cord with a lateral hemisection injury. We found that Gsx1 treatment promotes cell proliferation and activation of NSPCs at the injury site. Furthermore, Gsx1 treatment increases the number of glutamatergic and cholinergic neurons and decreases the number of GABAergic interneurons. Importantly, Gsx1 treatment attenuates glial scar formation and dramatically improves locomotor function in the injured mice. Genome-wide transcriptome analysis reveals that Gsx1 induces signaling pathways associated with NSPCs and inhibits the expression of genes associated with reactive and scar forming astrocytes. These gene expression changes correlate with NSPC activation, neuronal differentiation, attenuation of scar formation. Together, our study identifies Gsx1 treatment as a promising therapy for SCI and provides molecular insight for Gsx1-mediated functional recovery.

II.3. Materials and Methods

II.3.1. Animals

Young adult (8-12 weeks old) mice were used for this study. All the proposed animal work was conducted under compliance of the Institutional Animal Care and Use Committee (IACUC) at Rutgers University. All animals were housed in an animal care facility with 12-hour light/dark cycle. Mice under each experimental condition were assigned randomly with an equal number of male and female mice when possible.

II.3.2. Lentivirus Production

Lentiviruses encoding Gsx1 and a reporter RFP (lenti-Gsx1-RFP) and control lentiviruses (encoding only the reporter RFP, lenti-Ctrl-RFP) (ABM® LV465366 and LV084) were generated by transfecting HEK293T cells with a mixture of target vector (lenti-Gsx1-RFP or lenti-Ctrl-RFP), envelope plasmid (pMD2.G/VSVG, Addgene 12259), and 3rd generation packaging plasmids (pMDLg/pRRE, Addgene 12251 and pRSV-Rev, Addgene 12253). HEK293T cells were cultured in high glucose Dulbecco's Modified Eagle Media (DMEM) supplemented with 10% fetal bovine serum (FBS), 1% nonessential amino acid (MEM NEAA 100x Life Technology 11140050), and 1% Glutamax I 100X (Life Technology 35050061). Transfection of the HEK293T (Human Embryonic Kidney) cells was performed when the culture reaches ~ 50-60% confluency. Virus-containing supernatant was collected at day 2 and day 4 after transfection. Viruses were concentrated by precipitating the virus supernatant by polyethylene glycol 6000 (PEG6000) method [86]. Viral titer was determined by infecting HEK293T cells [86].

II.3.3. Hemisection Spinal Cord Injury and Lentivirus Injection

For hemisection SCI and lentiviral injections, mice were first anesthetized with 5% isoflurane inhalation for 3-4 minutes and then maintained at 2.5% isoflurane for the remainder of the surgery. Next, the skin was disinfected with betadine scrub and 70% ethanol wipes. Laminectomy was performed around T9-T10 to expose the spinal cord. Next, local anesthesia (0.125% Marcain) was applied and dorsal blood vessels were burned using the cauterizer. Then a lateral cut was performed to the left side of the spinal cord and the cut ends at the midline of the spinal cord for hemisection SCI. Immediately after the injury, ~1-2 µL of virus ($1x10^8$ TU/ml) was injected about 1 mm rostral and caudal to lesion epicenter. Virus was injected at about 1 µL/min and the needle was left in place for 2-3 minutes to allow diffusion and prevent leakage or backflow. For the sham animals,

skin and muscle were cut to expose the spinal cord. Muscles were sutured, and skin was stapled back together. Immediately after surgery, 1 mg/kg Meloxicam, a pain killer, and 50 mg/kg Cefazoline, an antibiotic, were administered subcutaneously.

Animals were divided into the following three groups (3-6 mice/group): 1) sham mice (exposed the spine without injury, Sham); 2) SCI mice with injection of lenti-control-RFP (SCI+Ctrl); and 3) SCI mice with lenti-Gsx1-RFP injection (SCI+Gsx1).

II.3.4. Behavioral/Locomotor Assessment

Locomotion of each animal was evaluated based on the Basso Mouse Scale (BMS) from an open field test [11]. BMS scale ranges from 0 (completely paralyzed) to 9 (normal) locomotion. The BMS score assessment was given by three independent observers who are blinded to the type of treatment after a 2-3 minutes observation per animal. The BMS assessment is performed before the injury and then twice a week for up to 8 weeks after injury.

II.3.5. Tissue Processing

Spinal cord tissues at 3, 7, 14, and 56 days post-injury (DPI) were harvested after intracardial perfusion with 1x phosphate buffer saline (PBS) followed by 4% (w/v) paraformaldehyde (PFA). Spinal cord tissue was then microsurgically dissected and fixed overnight (18-24 hours) in 4% PFA on a rotor. Fixed spinal cord tissue was washed three times with 1x PBS for 30 min and then placed in 30% (w/v) sucrose overnight until tissue sank to the bottom. Next, tissue was cryopreserved by embedding in Tissue-Tek® optimum cutting temperature (O.C.T.) and stored at -80ºC until needed. Sagittal or cross-sections (12 µm thickness) of spinal cord tissues were generated using a cryostat (ThermoScientific).

II.3.6. Immunohistochemistry

	Vendor, Catalog	Host Species	Type	RRID	Dilution
Primary Antibody					
Gsx1	Millipore Sigma, SAB2104632	Rabbit	Polyclonal	AB_10667904	1 : 200
Ki67	Abcam, ab15580	Rabbit	Polyclonal	AB_443209	1 : 1000
Nestin	Abcam, ab6142	Mouse	Monoclonal	AB_305313	1 : 200
Caspase3	Cell Signaling, 9661S	Rabbit	Polyclonal	AB_2341188	1 : 300
DCX	Santa Cruz Biotechnology, sc-8067	Goat	Polyclonal	AB_2088491	1 : 100
PDGFRa	Abcam, ab61219	Rabbit	Polyclonal	AB_2162341	1 : 100
NeuN	Millipore Sigma, MAB377	Mouse	Monoclonal	AB_2298772	1 : 300
GFAP	Millipore Sigma, G3893	Mouse	Monoclonal	AB_477010	1 : 400
Olig2	Millipore Sigma, AB9610	Rabbit	Polyclonal	AB_570666	1 : 500
vGlut2	Millipore Sigma, AB2251-I	Guinea Pig	Polyclonal	AB_2665454	1 : 1000
ChAT	Millipore Sigma, SAB2500236	Goat	Polyclonal	AB_10603616	1 : 300
GABA	Millipore Sigma, A-2052	Rabbit	Polyclonal	AB_477652	1 : 3000
CS56	Millipore Sigma, C8035	Mouse	Monoclonal	AB_476879	1 : 200
Secondary Antibody					
Alexa Fluor 488 Donkey anti Mouse	Jackson Immuno Research, 715-545-150	-	Polyclonal	AB_2340846	1 : 200
Alexa Fluor 488 Donkey anti Rabbit	Jackson Immuno Research, 711-545-152	-	Polyclonal	AB_2313584	1 : 200
Alexa Fluor 488 Donkey anti Goat	Jackson Immuno Research, 705-545-003	-	Polyclonal	AB_2340428	1 : 200
Alexa Fluor 488 Donkey anti Guinea Pig	Jackson Immuno Research, 706-545-148	-	Polyclonal	AB_2340472	1 : 200
Alexa Fluor 647 Donkey anti Mouse	Jackson Immuno Research, 715-605-150	-	Polyclonal	AB_2340862	1 : 200
Alexa Fluor 647 Donkey anti Rabbit	Jackson Immuno Research, 711-605-152	-	Polyclonal	AB_2492288	1 : 200
Alexa Fluor 647 Donkey anti Goat	Jackson Immuno Research, 705-605-003	-	Polyclonal	AB_2340436	1 : 200
Alexa Fluor 647 Donkey anti Guinea Pig	Jackson Immuno Research, 706-605-148	-	Polyclonal	AB_2340476	1 : 200

Table II.1. Primary and secondary antibodies used for immunohistochemistry.

List of primary and secondary antibodies along with the catalog, host species, type, RRID, and the dilution of each antibody used in this study.

Immunostaining was performed following a previously established protocol with minor modifications [54]. Briefly, sections were treated with cold methanol for 10 mins at room temperature for fixation and antigen retrieval. All antibodies were diluted in blocking solution containing 0.05% Triton X-100, 2% donkey serum, 3% bovine serum albumin (BSA), and PBS (1X), pH 7.4. Sections were incubated with primary antibodies (Table II.1) overnight at 4°C and washed three times for 10 min with PBS. Sections were then incubated with secondary antibodies (Table II.1) for 1 hour at room temperature and

washed three times for 10 min with PBS. For nuclear staining, 4',6-diamidino-2-phenylindole (DAPI; 200ng/ml) was added and then samples are washed three times with PBS, and sealed with Cytoseal 20 (ThermoFisher Scientific 8310-4).

II.3.7. Imaging and Image Analysis

At least five sections from each slide/animal were analyzed. Images were captured at the same exposure and threshold, and at the same intensity per condition using Zeiss LSM 800 confocal microscope or Zeiss AxioVision Imager A.1. Automatic cell counter in the ImageJ [87, 88] was used to count the total number of cells. Co-labeling of cell type specific markers with RFP was counted manually. Sample sizes were determined based on power analysis performed from previous experiments. Data are presented as mean ± standard error of the mean (SEM). All data were analyzed using GraphPad Prism version 5.0 software for Microsoft Windows. Statistical significance between two condition is calculated by Student's t-test and multi-group comparison is performed using one-way ANOVA, followed by Tukey post-hoc test. P-value of less than 0.05 is considered statistically significant.

II.3.8. RNA Extraction and Quality Control

Spinal cord tissues of 3, 14, 35 DPI ($n \geq 3$ for each time points) were dissected out and injured/injected segments (parenchymal segments spanning ~2-3 mm from each side of the lesion) were rapidly snap frozen in liquid nitrogen. Total RNA was isolated from spinal cord tissues using RNeasy Lipid Tissue Mini kit (Qiagen, #74804) following the manufacture's protocol. The concentration of the total RNA was determined using Qubit RNA BR Assay Kit (Life Technologies) and quality of the total RNA was determined using the RNA 6000 Nano chip on the 2100 Bioanalyzer automated electrophoresis system (Agilent Technologies).

II.3.9. Library Preparation and RNA-Sequencing

Library preparation and RNA-sequencing were performed by Admera Health (South Plainfield, NJ). Total RNA was used for library preparation of each sample, which was subsequently bar-coded and prepared according to manufacturer's instructions (Illumina). The libraries were prepared using an Illumina MiSeq paired-end kit and sequenced as paired-end, 2x150 bp on the Illumina MiSeq. The sequencing run was performed according to the manufacturer's instructions and generated a total of 40 million reads per sample.

II.3.10. RNA-Seq Data Analysis and Pathway Analysis

After a quality check of the raw fastq files using the FastQC (http://www.bioinformatics.babraham.ac.uk/projects/fastqc/), all sequences were aligned to the mouse reference genome, mm10, with STAR version 2.0 [89]. The raw read counts were generated using HTSeq (version 0.6.0) [90]. The DESeq2 [91, 92], a R/Bioconductor package, was used to normalize the counts and call differential gene expression on counts matrix generated by HTSeq. Differentially expressed transcripts/genes between Gsx1 treatment and control groups were defined by statistical significance (p-value) and biological relevance (fold change). Downstream pathway analysis was carried out using QIAGEN's Ingenuity Pathway Analysis (IPA, QIAGEN Redwood City, https://www.qiagenbioinformatics.com/products/ingenuity-pathway-analysis).

Gene expression of the box blot is generated from count matrix from the HTSeq using START (https://kcvi.shinyapps.io/START/) and with edgeR algorithm. Each dot on the box plot represent one biological sample.

II.3.11. Quantitative Real-Time PCR (qPCR) Analysis

Gene	Forward (5' -> 3')	Reverse (5' -> 3')
Gsx1	CTTCCCTCCCTTCGGATCG	GTCCACAGAGATGCAGTGAAA
Cd68	GGACCCACAACTGTCACTCAT	AAGCCCCACTTTAGCTTTACC
Itgam	ATGGACGCTGATGGCAATACC	TCCCCATTCACGTCTCCCA
Cd86	TGTTTCCGTGGAGACGCAAG	TTGAGCCTTTGTAAATGGGCA
Il1b	GCAACTGTTCCTGAACTCAACT	ATCTTTTGGGGTCCGTCAACT
Tnf	CCTGTAGCCCACGTCGTAG	GGGAGTAGACAAGGTACAACCC
Ki67 (Mki67)	ATCATTGACCGCTCCTTTAGGT	GCTCGCCTTGATGGTTCCT
Nestin	CCCTGAAGTCGAGGAGCTG	CTGCTGCACCTCTAAGCGA
NeuN (Hrnbp3)	AACCACGAACTCCACCCTTC	GACCTCAATTTTCCGTCCCTC
vGlut (Slc17a6)	TGGAAAATCCCTCGGACAGAT	CATAGCGGAGCCTTCTTCTCA
Th	GTCTCAGAGCAGGATACCAAGC	CTCTCCTCGAATACCACAGCC
Tph1	AACAAAGACCATTCCTCCGAAAG	TGTAACAGGCTCACATGATTCTC
Chat	CCATTGTGAAGCGGTTTGGG	GCCAGGCGGTTGTTTAGATACA
Gfap	CGGAGACGCATCACCTCTG	AGGGAGTGGAGGAGTCATTCG
Lcn2	GCAGGTGGTACGTTGTGGG	CTCTTGTAGCTCATAGATGGTGC
Serpina3n	ATTTGTCCCAATGTCTGCGAA	TGGCTATCTTGGCTATAAAGGGG
Notch1	CCCTTGCTCTGCCTAACGC	GGAGTCCTGGCATCGTTGG
Nrarp	AAGCTGTTGGTCAAGTTCGGA	CGCACACCGAGGTAGTTGG
Jag1	CCTCGGGTCAGTTTGAGCTG	CCTTGAGGCACACTTTGAAGTA
Jag2	CACTGTCCGTCAGGATGGAAC	TAGCCGCCAATCAGGTTTTTG
Dll1	CCCATCCGATTCCCCTTCG	GGTTTTCTGTTGCGAGGTCATC
Hes1	TCAGCGAGTGCATGAACGAG	CATGGCGTTGATCTGGGTCA
Cdh1	CAGGTCTCCTCATGGCTTTGC	CTTCCGAAAAGAAGGCTGTCC
Bmpr1a	TGCAAGGATTCACCGAAAGC	TGCCATCAAAGAACGGACCTAT
Col6a2	GCTCCTGATTGGGGGACTCT	CCAACACGAAATACACGTTGAC
Ctnna1	AAGTCTGGAGATTAGGACTCTGG	ACGGCCTCTCTTTTTATTAGACG
Ntng1	TGCTAAACACAGTCATTTGCGT	GCACACATTCTCATCGTCCAG
Syn1	AGCTCAACAAATCCCAGTCTCT	CGGATGGTCTCAGCTTTCAC

Table II.2. RT-qPCR primers.

Set of forward and reverse primers (5'→3') used for RT-qPCR analysis.

Complementary DNA (cDNA) was synthesized from total RNA using SuperScript III First-Strand Synthesis System (Invitrogen, 18080051) using the manufacture's protocol. qPCR was performed with Power SYBR™ Green PCR Master Mix and gene specific primers (Table II.2) using StepOnePlus Real-Time PCR system (Applied Biosystem). GAPDH is

used as a reference housekeeping gene. The Levak method is used to calculate the fold change, by normalizing it to the Sham.

II.3.12. Data Availability

The RNA-Seq data will be publically available upon publication (The accession number for the RNA-Seq data reported in this paper (NCBI GEO # will be available upon acceptance for publication).

II.4. Results

Given the role of Gsx1 in the regulation of NSPCs [64, 80-84] and cell fate determination of interneurons [64, 65] during embryonic development in the spinal cord, we hypothesize that overexpression of Gsx1 in the adult spinal cord after SCI promotes NSPC activation and neurogenesis. To test this hypothesis, we first performed a lateral hemisection from the midline to the left side of the spinal cord at the thoracic (T) 10 level. The completeness and consistency of the lateral hemisection SCI was confirmed by the observation of paralysis in the left hind limb. Immediately after the SCI, we injected 1 µL/site of lentivirus ($1x10^8$ TU/ml) encoding Gsx1 and a reporter red fluorescent protein (RFP) (lenti-Gsx1-RFP) into the injured spinal cord, approximately 1 mm rostral and caudal to the injury site (Figure II.1a). Lentivirus encoding only the RFP reporter (lenti-Ctrl-RFP) is used as a control. Animals were randomly assigned to the following three groups (3-6 mice/group): 1) sham mice (exposed the spine without injury, Sham); 2) SCI mice with injection of lenti-Ctrl-RFP (SCI+Ctrl); and 3) SCI mice with lenti-Gsx1-RFP injection (SCI+Gsx1). We confirmed that the lentivirus-mediated Gsx1 expression in the spinal cord tissue at 3 days-post injury (DPI) and 7 DPI by immunohistochemistry and RT-qPCR (Figure II.2).

Compared to the control, Gsx1 treatment significantly increased the percentage of virally transduced RFP^{+} cells with Gsx1 expression (Figure II.2).

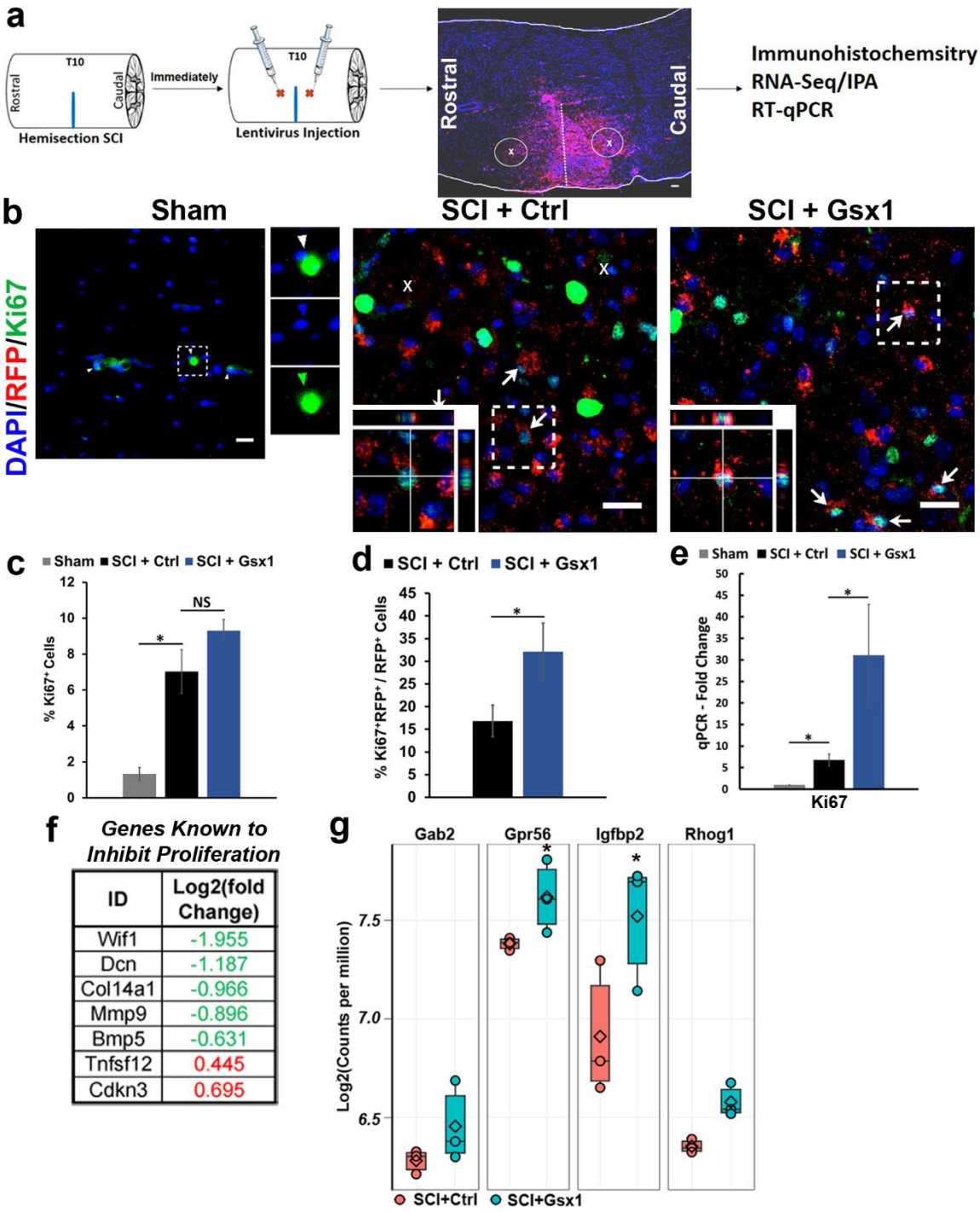

ID	Log2(fold Change)
Wif1	-1.955
Dcn	-1.187
Col14a1	-0.966
Mmp9	-0.896
Bmp5	-0.631
Tnfsf12	0.445
Cdkn3	0.695

Figure II.1. Gsx1 expression promotes cell proliferation in the injured spinal cord.

*Lateral hemisection SCI was performed on 8-12 weeks old mice around T9-T10 level immediately followed by the injection of lentivirus encoding Gsx1 along with RFP reporter (lenti-Gsx1-RFP). Lentivirus encoding only the reporter RFP was used as a control (lenti-Ctrl-RFP). Spinal cord tissues were analyzed by immunohistochemistry, RNA-Seq, Ingenuity Pathway Analysis (IPA), and RT-qPCR analysis; scale bar = 100 µm (**a**). Confocal images of sagittal sections of spinal cord tissue at 3 DPI show the expression of viral reporter RFP and cell proliferation marker Ki67 (n=3 for Sham and n=6 for SCI+Ctrl and SCI+Gsx1). Arrows indicate Ki67+/RFP+ co-labeled cells. Images in the bottom left corner show a higher magnification z-stack view of the area denoted by a dashed white box. Scale bar =20 µm (**b**). Quantification of all Ki67+ cells (**c**) and Ki67+/RFP+ cells (**d**). RT-qPCR analysis shows Ki67 mRNA expression at 3 DPI, normalized to the Sham; n=4 (**e**). List of differentially expressed genes that are known to inhibit proliferation between after lenti-Gsx1 treatment compared to lenti-Ctrl treatment from RNA-Seq analysis (n=3) (**f**). Gene expression box plot, generated by STAR and edgeR, know to promote cell proliferation; * = differentially significant (**g**). Each dot represents the gene expression as log2(count per million) for one biological replicate sample. Mean ± SEM; * = $p < 0.05$; Students' t-test.*

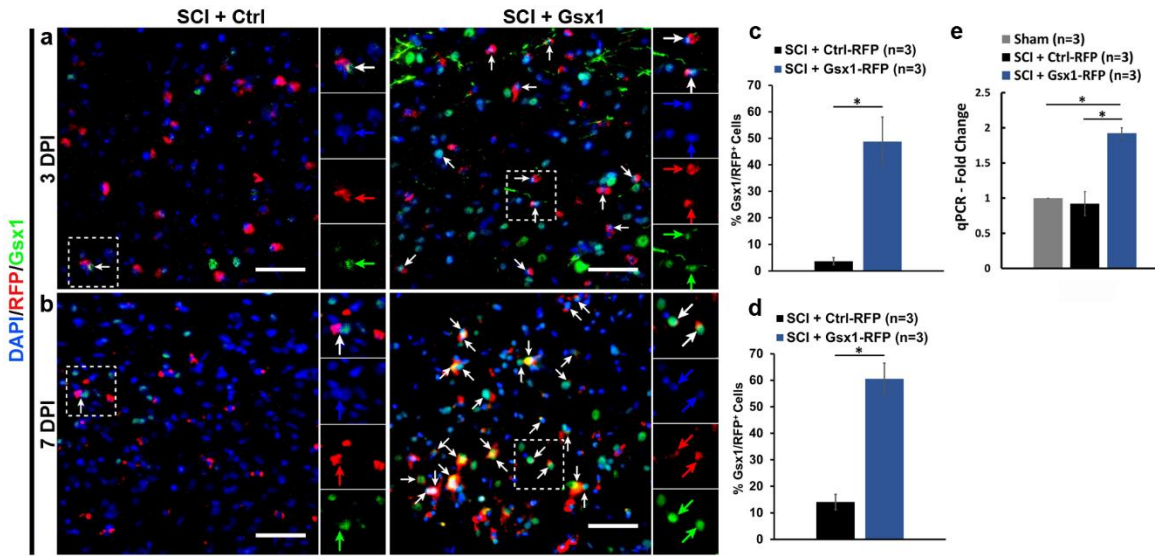

Figure II.2. Transduction of lenti-Gsx1-RFP is successful in delivering and overexpressing Gsx1 after SCI.

*Hemisection SCI was performed on 8-12 weeks old mice around T10. Immediately after lentivirus injection encoding Ctrl or Gsx1 gene along with RFP reporter. Animals were harvested 3 DPI (**a**) and 7 DPI (**b**) and sagittal sections are immunostained with Gsx1 antibody. Arrows in sagittal sections show co-expression of RFP and Gsx1 (green). Montage on the right of each of the image indicates small region (white box) of sagittal sections with separate channels (DAPI, RFP, and Gsx1) to indicates co-expression. Scale bar =50 µm. Quantification of virally transduced cells co-labeled with Gsx1 at 3 DPI (**c**) and 7 DPI (**d**). (**e**) RT-qPCR analysis indicating Gsx1 mRNA expression at 3 DPI, normalized to the Sham. n = 3; Mean ± SEM; * = p < 0.05; One-way ANOVA and Tukey post-hoc analysis. DPI = days post injury.*

II.4.1. Gsx1 treatment increases cell proliferation in mice with lateral hemisection SCI

SCI is known to increase cell proliferation at the lesion site [93]. To determine the effect of the Gsx1 treatment on cell proliferation at 3 DPI, we examined the expression of a cell proliferation marker, Ki67, by immunohistochemistry followed by confocal imaging

analysis (Figure II.1b). The RFP$^+$ and Ki67$^+$ cells were found to be located around the injection sites. We calculated the percentage of the Ki67$^+$ cells among DAPI$^+$ cells around the injury/injection areas in the following 3 control and experimental groups: Sham (n=3), SCI+Ctrl (n=6), and SCI+Gsx1 (n=6) (Figure II.1c). We observed a significant increase in the percentage of Ki67$^+$ cells in both injury groups that received viral injection compared to the Sham mice, with the highest increase in the SCI+Gsx1 group (Figure II.1c). In addition, a significantly higher percentage of Ki67$^+$/RFP$^+$ co-labeled cells among RFP$^+$ cells were found in the mice with lenti-Gsx1-RFP injections compared to mice that received lenti-Ctrl-RFP injections (Figure II.1d). Furthermore, the increase in Ki67 mRNA expression was validated by RT-qPCR analysis. Gsx1 treatment induces a significantly higher level of Ki67 mRNA level (~4-fold; Figure II.1e) in the SCI+Gsx1 group compared to the SCI+Ctrl group. These results indicate that Gsx1 treatment promotes cell proliferation in the adult injured spinal cord.

a ***RNA-Seq Sample Size***

	SCI+Ctrl	SCI+Gsx1
3 DPI	n = 3	n = 3
14 DPI	n = 3	n = 3
35 DPI	n = 4	n = 4

b ***Differentially Expressed Genes (DEGs)***

	Total DEGs	Upregulated DEGs	Downregulated DEGs
3 DPI	475	180	295
14 DPI	1447	577	870
35 DPI	2273	600	1673

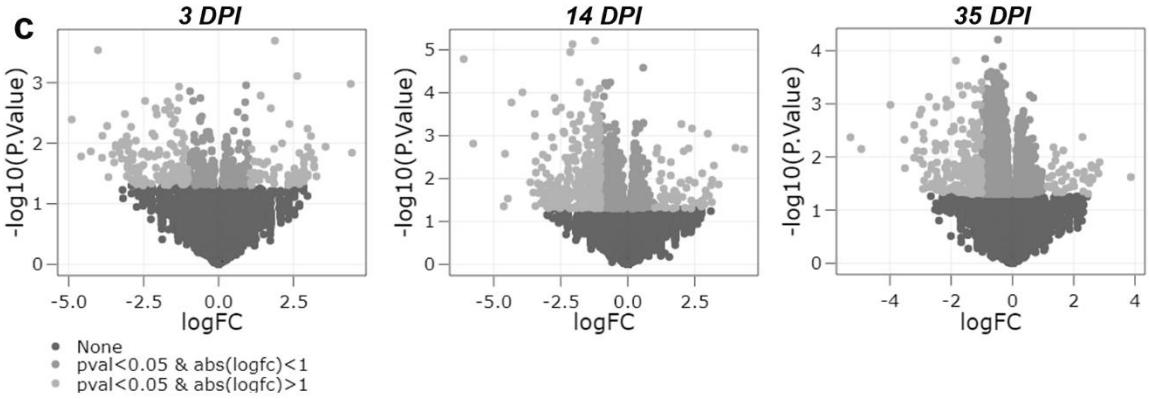

Figure II.3. Summary of RNA-Seq analysis

*(**a**) Number of biological replicates used for each group (SCI+Ctrl and SCI+Gsx1) at 3 different times points (3 DPI, 14 DPI, and 35 DPI) for RNA-Seq analysis. (**b**) Total number of differentially expressed genes (DEGs; p<0.05) that are upregulated and downregulated at 3 DPI, 14 DPI, and 35 DPI. (**c**) Volcano plot at 3 DPI, 14 DPI, and 35 DPI indicating differentially expressed genes.*

We reason that the effect of Gsx1 on promoting cell proliferation may be due to its regulation of genes associated with cell proliferation. Thus, we performed genome-wide transcriptome profiling using RNA-Seq, followed by pathway analysis using IPA (QIAGEN Inc.) [94]. RNA-Seq analysis identified 475, 1447, and 3946 differentially expressed genes (DEGs) at 3, 14, and 35 DPI, respectively (Figure II.3). The top 40 DEGs (Table II.3) were shown in heatmap at 3 DPI (Figure II.4), 14 DPI (Figure II.5), and 35 DPI (Figure II.6). Further gene ontology enrichment analysis of the 475 DEGs at 3DPI using REVIGO [95] revealed that cell proliferation is one of the key biological processes being affected by Gsx1 treatment (Figure II.7). In particular, Gsx1 treatment induced downregulation of genes known to inhibit cell proliferation (e.g., Wif1, Dcn, Mmp9; Figure II.1f) and upregulation of the genes known to promote cell proliferation (e.g., Gab, Gpr56, Igfbp2, Rhog; Figure II.1g). These data confirm that Gsx1 treatment increases cell proliferation in mice with SCI in the acute phase at 3 DPI.

	3 DPI		14 DPI		35 DPI	
Top 20 Upregulated Genes	ID	Log2(Fold Change)	ID	Log2(Fold Change)	ID	Log2(Fold Change)
	Ppef2	1.7456	Bpgm	0.6457	9330175M20Rik	0.9304
	Cnga4	1.5203	Snca	0.6409	Gm2897	0.9209
	Tmem51as1	1.4642	Fam46c	0.5624	4930525G20Rik	0.8941
	AI506816	1.3532	Gjc2	0.5451	Zfp819	0.8928
	Cdsn	1.3006	Nkx2-9	0.5346	Ripply2	0.8629
	G530011O06Rik	1.2743	Ppp1r14a	0.5226	Peg12	0.8311
	Fslp1	1.2560	Rasl11b	0.5223	Mum1l1	0.8199
	3110070M22Rik	1.2345	Prr18	0.5131	1500015L24Rik	0.8142
	Fbxw10	1.2303	Klk6	0.5103	1110015O18Rik	0.8049
	Galr3	1.2074	Ptgs1	0.5076	4930441O14Rik	0.8042
	Rn45s	1.2041	Ptp4a1	0.4919	Sox14	0.7864
	C130026I21Rik	1.1821	S100b	0.4672	Zfp804b	0.7683
	Erv3	1.1741	Bin2	0.4563	Mir331	0.7637
	Afp	1.1694	Tmem88b	0.4517	Cacna1f	0.7612
	A330048O09Rik	1.1366	Mbp	0.4422	Fgf5	0.7601
	Xlr3a	1.1299	Atp1b	0.4393	Mlpol1	0.7477
	1700001O22Rik	1.1218	Isg20	0.4377	Mir149	0.7471
	Apoa2	1.1206	AI848285	0.4364	Tmem232	0.7392
	Mir466l	1.1092	Arhgef37	0.4320	Gpr88	0.7370
	Crybb1	1.0996	Plp1	0.4288	6430584L05Rik	0.7369
Top 20 Downregulated Genes	ID	Log2(Fold Change)	ID	Log2(Fold Change)	ID	Log2(Fold Change)
	Col28a1	-2.4223	Col1a1	-2.0110	Snai1	-1.4631
	Ogn	-2.0659	Aspn	-1.8378	Wfdc17	-1.4354
	Wif1	-1.9547	Col1a2	-1.7949	Dkk2	-1.4094
	Sbspon	-1.7291	Col6a3	-1.6645	Clip2	-1.3829
	Itih4	-1.6936	Col5a1	-1.4541	H19	-1.3015
	Twist1	-1.6811	Kcnj15	-1.4052	Asgr2	-1.2978
	Sostdc1	-1.6651	Mfap5	-1.3046	Atp6v0a4	-1.2820
	Plekha4	-1.6475	Thbs1	-1.2104	Foxa1	-1.2655
	Ncmap	-1.6447	Serpinh1	-1.1806	Apoc2	-1.2628
	Aqp1	-1.6233	Ppic	-1.1093	Angpt4	-1.2556
	Gldn	-1.6205	Loxl1	-1.0945	Fam180a	-1.2413
	Prx	-1.6059	Tnc	-1.0594	Cd8b1	-1.2400
	Wnt4	-1.5861	Ltbp2	-1.0186	Twist1	-1.2251
	Cdh1	-1.5587	Cpz	-1.0108	Pl16	-1.2225
	Ngfr	-1.5471	Scara5	-0.9871	Gstm2	-1.2204
	Slc43a1	-1.5467	Scara3	-0.9867	Wnt9a	-1.1770
	Foxd1	-1.5382	Rcn3	-0.9815	Dpt	-1.1667
	Kcnj13	-1.5141	Mrc2	-0.9796	Col6a2	-1.1481
	Crlf1	-1.4928	Sh3pxd2a	-0.9693	Gpnmb	-1.1465
	Dpt	-1.4878	Tspan11	-0.9674	Ms4a7	-1.1420

Table II.3. Top 40 differentially expressed genes.

Top 20 upregulated and top 20 downregulated DEGs determined by RNA-Seq analysis from SCI+Ctrl and SC+Gsx1 groups at 3 DPI, 14 DPI, and at 35 DPI. n=3 at 3 DPI and 14 DPI; n = 4 at 35 DPI.

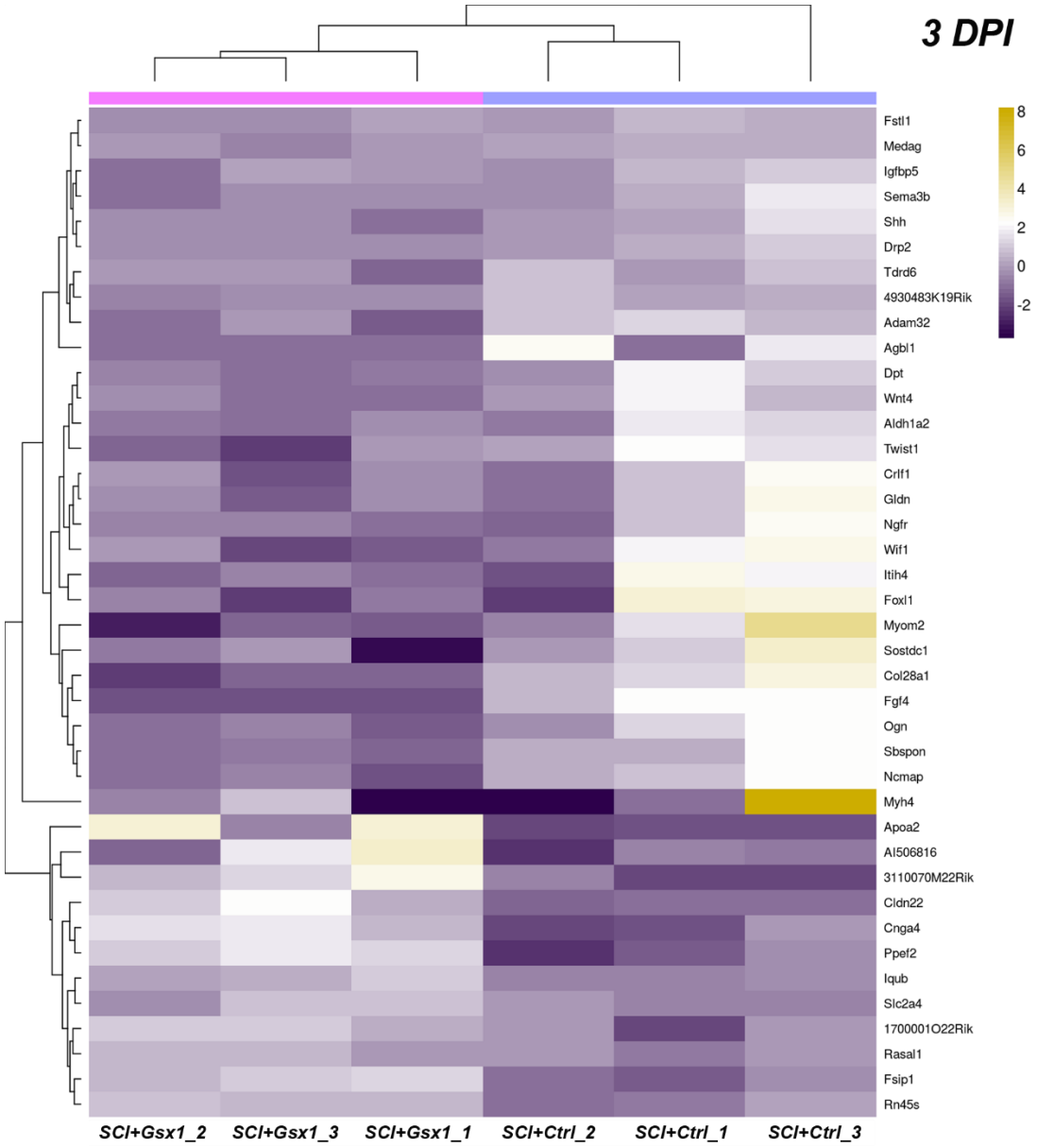

Figure II.4. Top 40 differentially expressed genes (DEGs) at 3 DPI

Heatmap of the top 40 DEGs between SCI+Ctrl and SCI+Gsx1 group at 3 DPI. Blue indicates downregulation and yellow indicates upregulation of the gene expression; n=3.

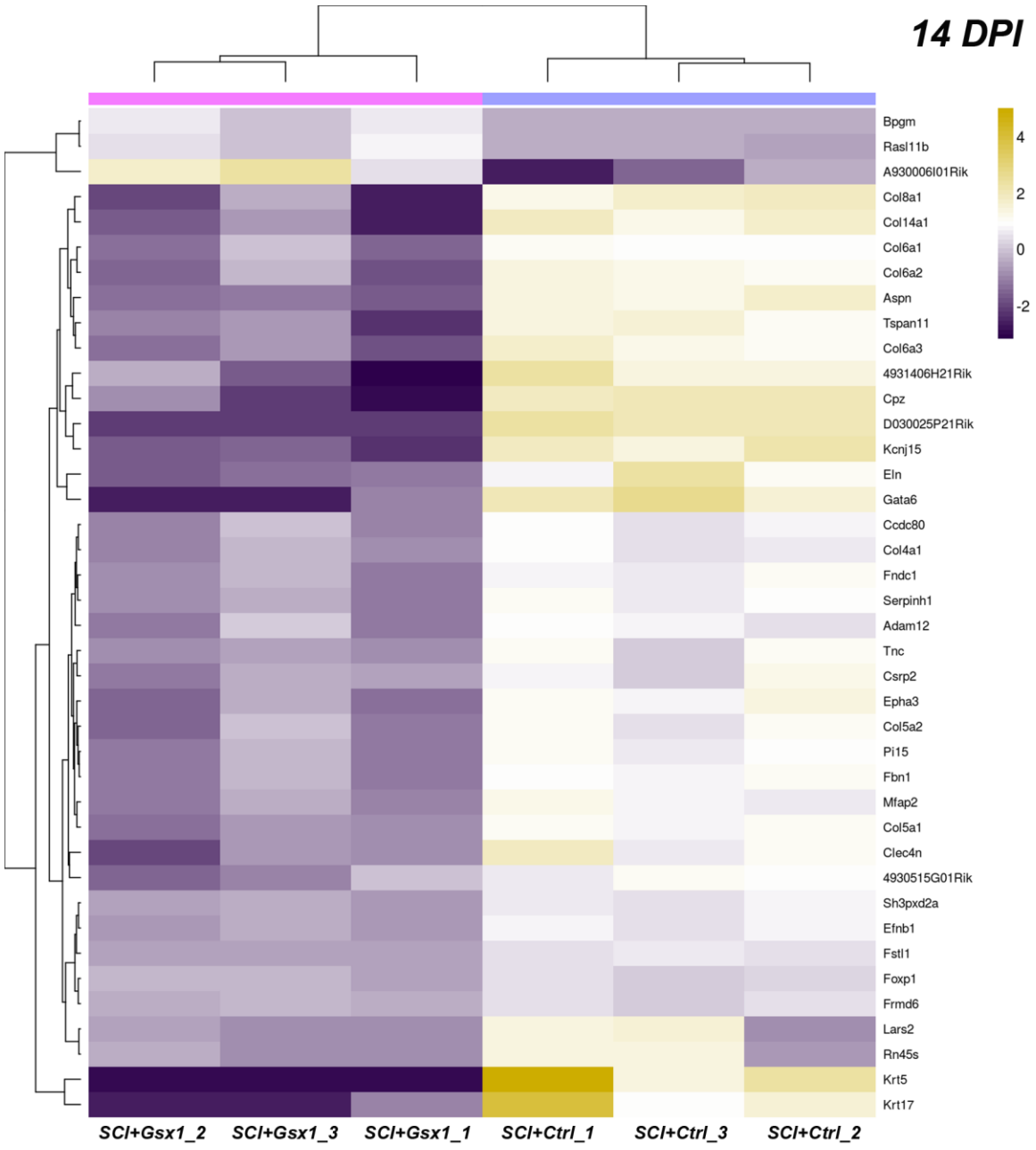

Figure II.5. Top 40 differentially expressed genes (DEGs) at 14 DPI.

Heatmap of the top 40 DEGs between SCI+Ctrl and SCI+Gsx1 group at 14 DPI. Blue indicates downregulation and yellow indicates upregulation of the gene expression; n=3.

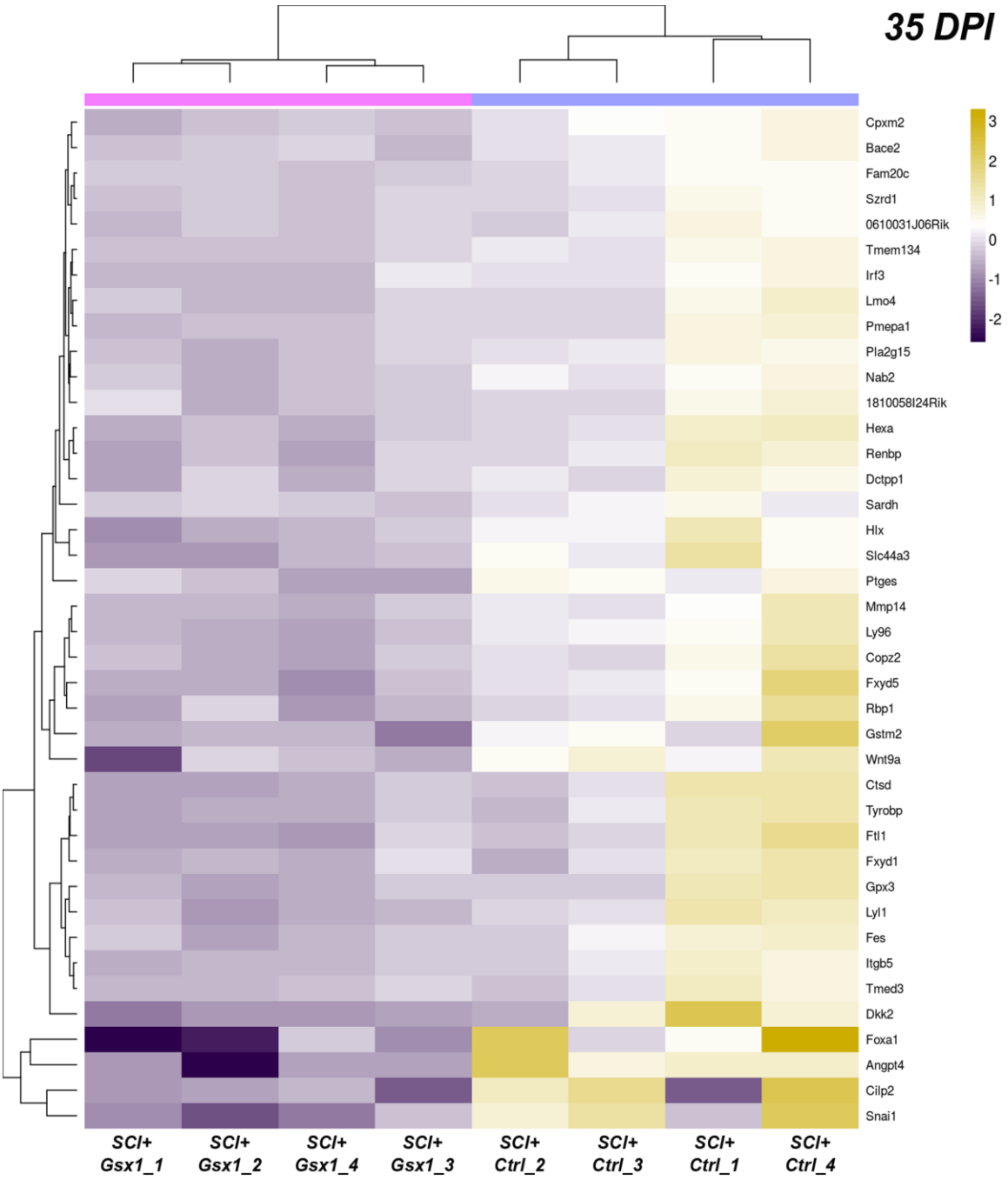

Figure II.6. Top 40 differentially expressed genes (DEGs) at 35 DPI.

Heatmap of the top 40 DEGs between SCI+Ctrl and SCI+Gsx1 group at 35 DPI. Blue indicates downregulation and yellow indicates upregulation of the gene expression; n=4.

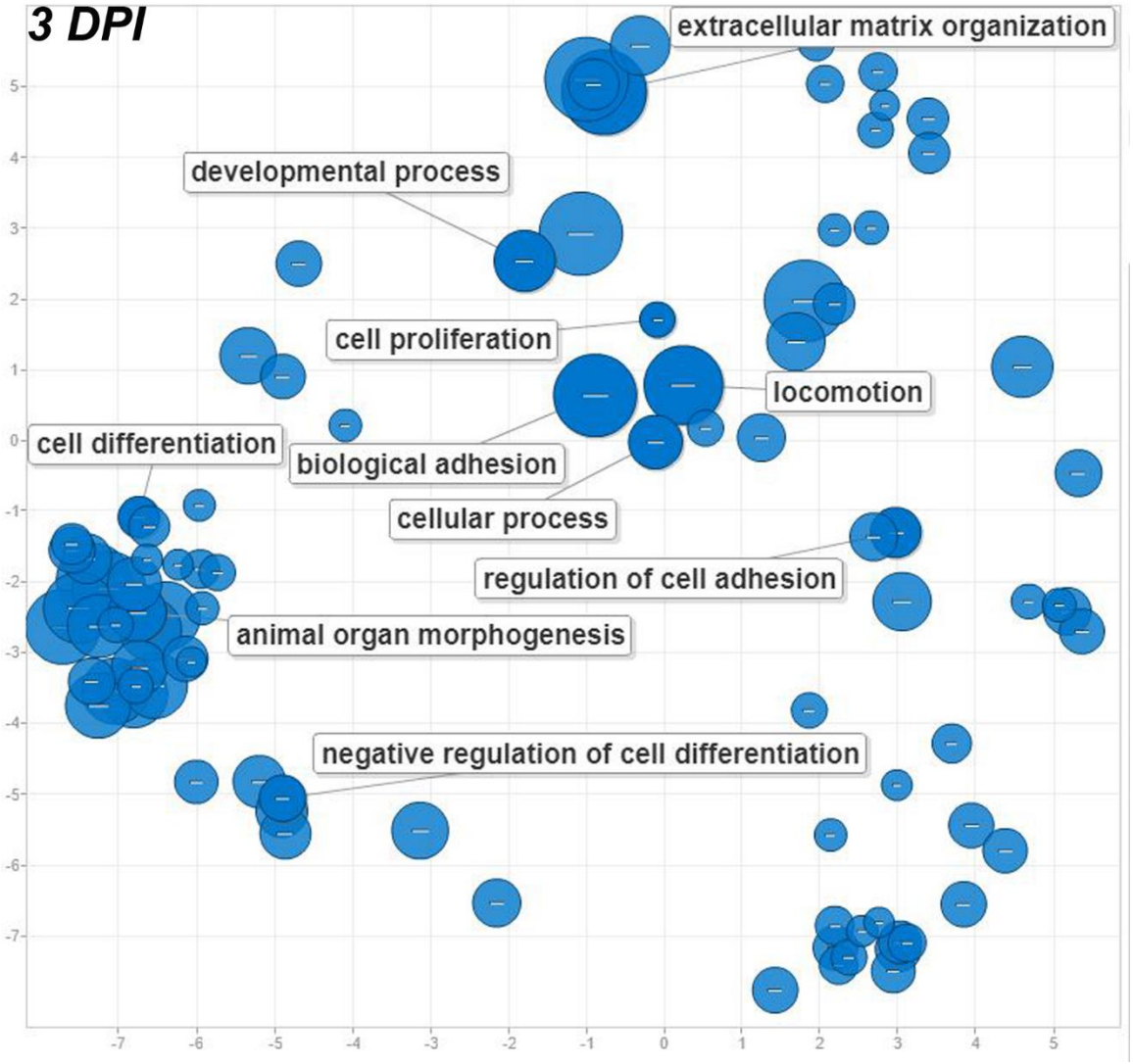

Figure II.7. Functional enrichment of gene ontology (GO) terms for differentially expressed genes (DEGs) at 3 DPI.

Enriched terms for biological process represented as a scatter plot in a two-dimensional semantic space using REVIGO. Circle size indicates the log10(p-value) of the GO terms.

II.4.2. Gsx1 treatment promotes NSPC activation after SCI

In the adult spinal cord, NSPCs exist in quiescent states under normal conditions, but become activated after injury [31, 96, 97]. To investigate the effect of Gsx1 treatment on the activation of NSPCs, we examined the expression of NSPC markers, Nestin and

Notch1, in the injured spinal cord at 3 DPI via immunohistochemistry and confocal imaging analysis. The RFP^+ and $Nestin^+$ cells were found around the injection sites (Figure II.8a). We noticed a significant increase in the percentage of $Nestin^+$ cells among $DAPI^+$ cells at the lesion site in the injury groups that received viral injection (SCI+Ctrl and SCI+Gsx1) compared to the Sham mice, with the highest increase in the SCI+Gsx1 group (Figure II.8b). Further, a significantly higher percentage of $Nestin^+/RFP^+$ co-labeled cells among RFP^+ cells were found in SCI+Gsx1 group compared to SCI+Ctrl group (Figure II.8c). In addition, RT-qPCR analysis confirmed that Gsx1 treatment significantly increased Nestin mRNA expression (Figure II.8d).

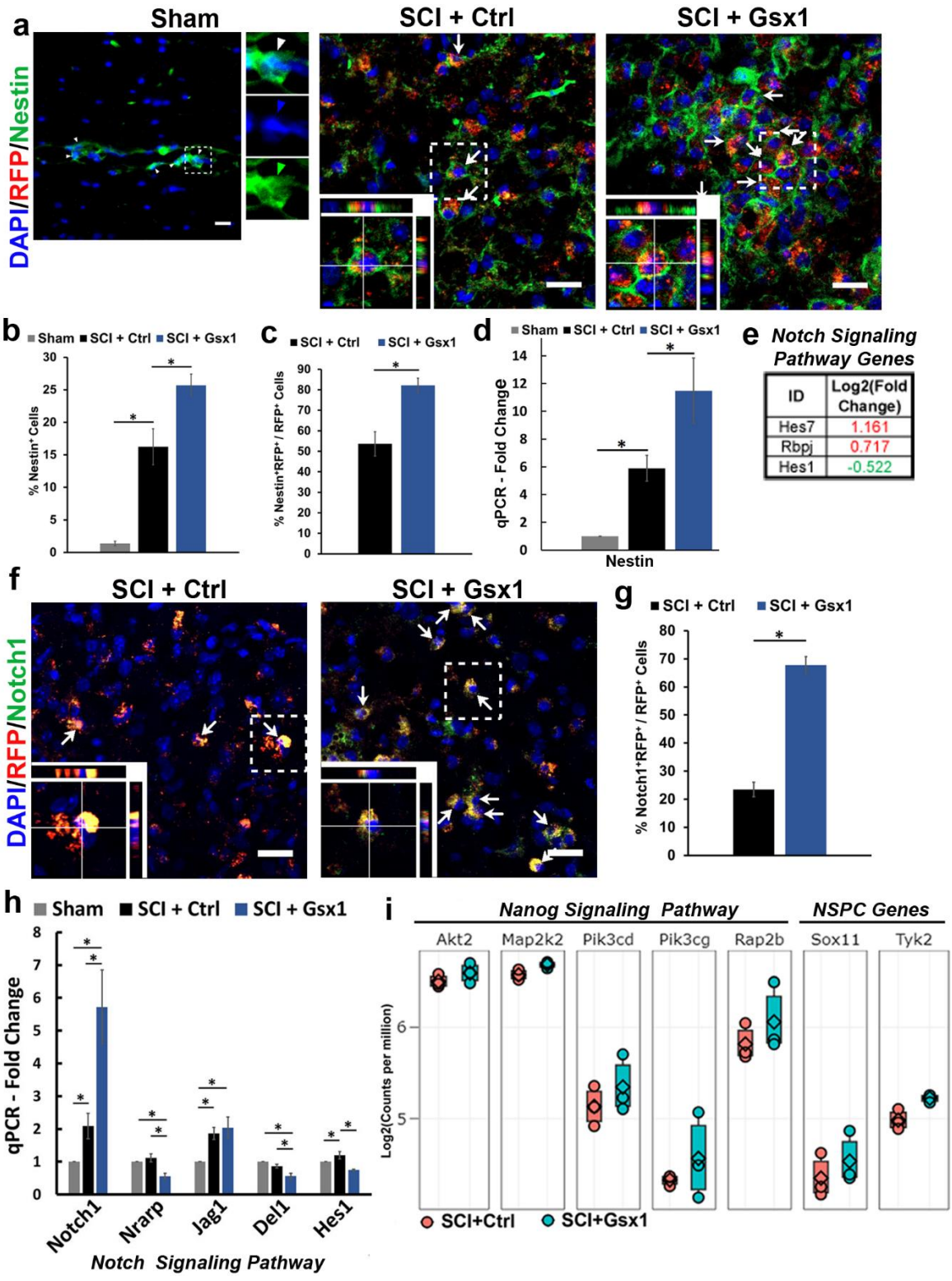
a
Sham
SCI + Ctrl
SCI + Gsx1
DAPI/RFP/Nestin
b
Sham SCI + Ctrl SCI + Gsx1
% Nestin+ Cells
c
SCI + Ctrl SCI + Gsx1
% Nestin+RFP+ / RFP+ Cells
d
Sham SCI + Ctrl SCI + Gsx1
qPCR - Fold Change
Nestin
e
Notch Signaling Pathway Genes
ID | Log2(Fold Change)
Hes7 | 1.161
Rbpj | 0.717
Hes1 | -0.522
f
SCI + Ctrl
SCI + Gsx1
DAPI/RFP/Notch1
g
SCI + Ctrl SCI + Gsx1
% Notch1+RFP+ / RFP+ Cells
h
Sham SCI + Ctrl SCI + Gsx1
qPCR - Fold Change
Notch1 Nrarp Jag1 Dll1 Hes1
Notch Signaling Pathway
i
Nanog Signaling Pathway
NSPC Genes
Akt2 Map2k2 Pik3cd Pik3cg Rap2b Sox11 Tyk2
Log2(Counts per million)
SCI+Ctrl SCI+Gsx1

Figure II.8. Gsx1 expression increases NSPC activation after SCI.

*Confocal images of sagittal sections of spinal cord tissues at 3 DPI show the expression of viral reporter RFP and NSPC marker Nestin (n=3 for Sham and n=6 for SCI+Ctrl and SCI+Gsx1). Arrows indicate Nestin$^+$/RFP$^+$ co-labeled cells. Images in the bottom left corner show a higher magnification z-stack view of the area denoted by a dashed white box. Scale bar=20 µm (**a**). Quantification of all Nestin$^+$ cells (**b**) and Nestin$^+$/RFP$^+$ co-labeled cells (**c**). RT-qPCR analysis shows Nestin mRNA expression at 3 DPI, normalized to the Sham; n=4 (**d**). List of differentially expressed genes that are known to promote Notch signaling (**e**) after lenti-Gsx1 treatment compared to lenti-Ctrl treatment from RNA-Seq analysis. Confocal images of sagittal sections of spinal cord tissues at 3 DPI show the expression of viral reporter RFP and NSPC marker Notch1 (n=4 for SCI+Ctrl and SCI+Gsx1). Arrows indicate Notch1$^+$/RFP$^+$ co-labeled cells. Images in the bottom left corner show a higher magnification z-stack view of the area denoted by a dashed white box. Scale bar=20 µm (**f**). Quantification of all Notch1$^+$ cells among RFP$^+$ cells (**g**). RT-qPCR analysis of the genes involved in the Notch signaling pathway (Notch1, Nrarp, Jag1, Del1, and Hes1) (**h**). (**i**) Gene expression box plot of the genes associated with stem cells and Nanog signaling pathway (e.g., Akt2, Map2k2, Pik3cd, Pik3cg, and Rap2b). Each dot represents the gene expression as log2(count per million) for one biological replicate sample. Mean ± SEM; * = p < 0.05; Students' t-test and One-way ANOVA followed by Tukey post-hoc test.*

To elucidate the induction in NSPC activation after Gsx1 treatment, we investigated the Gsx1-induced signaling pathways in the SCI+Ctrl (n=3) and SCI+Gsx1 (n=3) groups at 3 DPI through RNA-Seq, IPA, and gene ontology analysis using REVIGO [95]. We found that negative regulation of cell differentiation was one of the key biological processes

being affected after Gsx1 treatment (Figure II.7). IPA analysis showed a significant upregulation of the genes involved in the Notch signaling pathway (e.g., Hes7 and Rbpj) and a downregulation of the transcription repressor gene Hes1 (Figure II.8e). Immunohistochemistry analysis using anti-Notch1 antibody on sagittal sections of the spinal cord tissues at 3 DPI showed a significant increase in the number of $Notch1^{+}/RFP^{+}$ cells in Gsx1 treatment compared to the control (Figure II.8f-g). The RT-qPCR analysis confirmed a significant increase in the mRNA expression of Notch1 and Jag1 after SCI (SCI+Ctrl and SCI+Gsx1) compared to the Sham group and a further increase in Notch1 mRNA level in Gsx1 treatment compared to the control (Figure II.8h). Nrarp, a negative regulator of the Notch signaling pathway that physically interacts with Notch intracellular domain (NICD) and blocks Notch transcription [98, 99], was downregulated in the SCI+Gsx1 group (Figure II.8h). Furthermore, Gsx1 treatment decreased the expression of Del1 and Hes1 gene (Figure II.8h). Del1 promotes stem cell differentiation to glial lineage [100], while Hes1 is a transcriptional repressor [101]. The expression of Hes1 results in premature neuronal differentiation [102]. In addition, we also observed an increase in genes associated with activation of Nanog signaling pathway (e.g., Akt2, Map2k2, Pik3cd, Pik3cg, and Rap2b) (Figure II.8i). Nanog is an essential pathway in embryonic stem cells (ESCs) and the Nanog gene is commonly expressed in NSPCs [103]. In contrast, the expression of genes in Notch/Nanog signaling pathways was not detected by 35 DPI. Thus, these results suggest that Gsx1-induced transient upregulation of Notch/Nanog signaling pathways may play an important role in endogenous NSPC activation in the injured spinal cord.

II.4.3. Induction of neurogenesis in the injured spinal cord

In the adult spinal cord, injury-activated NSPCs mostly generate astrocytes and oligodendrocytes [20, 31]. To determine whether Gsx1 treatment alters cell fate

determination in NSPC, we examined the sagittal section of spinal cord tissues at 14 DPI with an early neuronal marker doublecortin (DCX) (Figure II.9a), an astrocyte marker GFAP (Figure II.9b), and an oligodendrocyte progenitor marker PDGFRa (Figure II.9c) in the SCI+Ctrl (n=6) and SCI+Gsx1 (n=6) groups. DCX is mostly expressed in neuroblasts and immature neurons [104, 105] and is associated with adult neurogenesis, but not reactive gliosis [106]. Compared to the SCI+Ctrl group, Gsx1 treatment significantly increased the percentage of DCX^+/RFP^+ co-labeled cells and decreased the percentage of $GFAP^+/RFP^+$ and $PDGFRa^+/RFP^+$ co-labeled cells among RFP^+ cells (Figure II.9d).

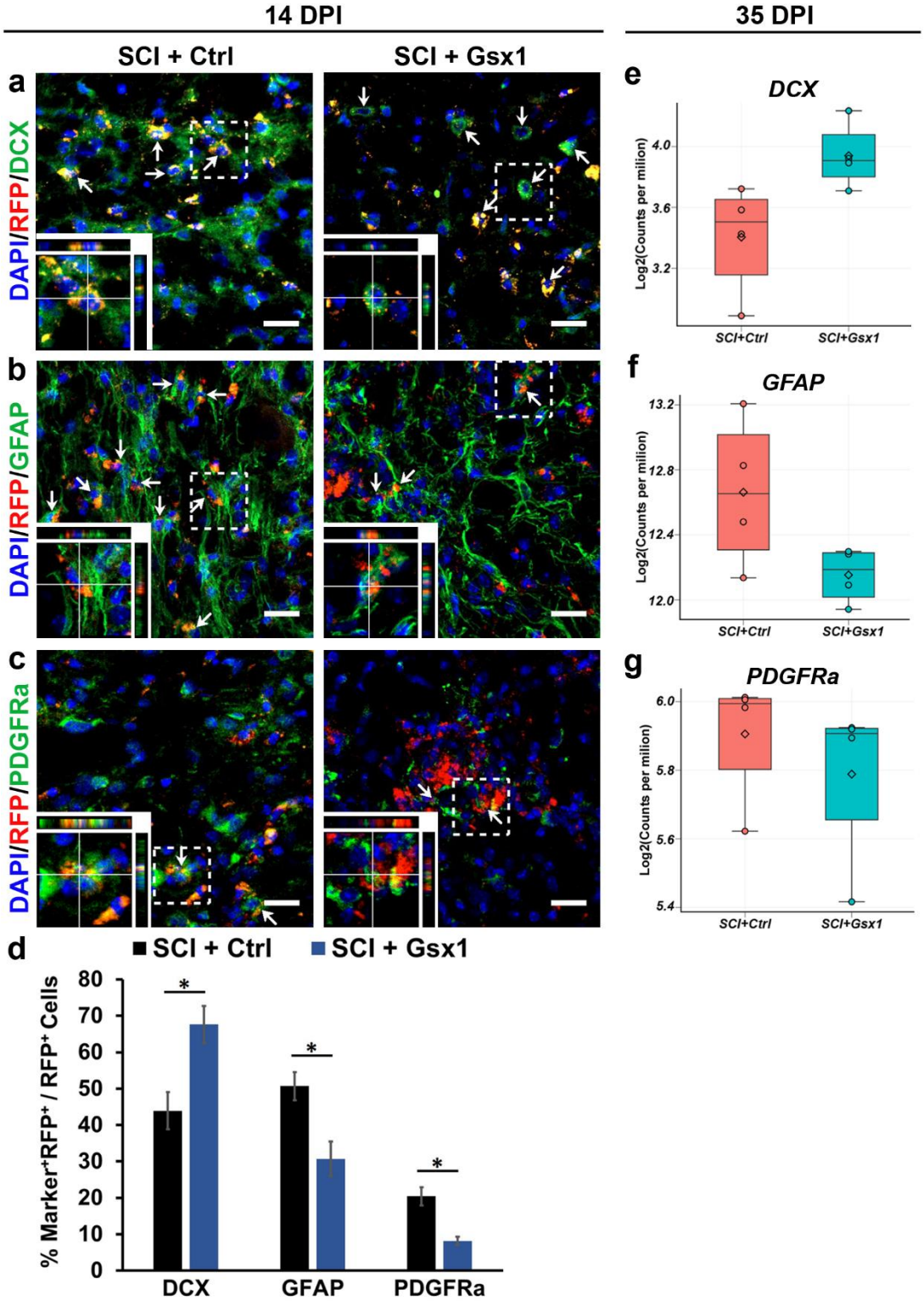
14 DPI
35 DPI
SCI + Ctrl
SCI + Gsx1
a
DAPI/RFP/DCX
b
DAPI/RFP/GFAP
c
DAPI/RFP/PDGFRa
d
SCI + Ctrl
SCI + Gsx1
% Marker+RFP+ / RFP+ Cells
DCX
GFAP
PDGFRa
e
DCX
Log2(Counts per milion)
SCI+Ctrl
SCI+Gsx1
f
GFAP
g
PDGFRa

Figure II.9. Gsx1 induces neurogenesis in the adult spinal cord after SCI.

*Confocal images of sagittal sections of spinal cord tissues at 14 DPI show the expression of viral reporter RFP and early neuronal marker Doublecortin DCX (**a**), astrocyte marker GFAP (**b**), and oligodendrocyte progenitor marker PDGFRa (**c**). Arrows indicate cell marker$^+$/RFP$^+$ co-labeled cells. Images in the bottom left corner show a higher magnification z-stack view of the area denoted by a dashed white box. Scale bar =20 µm. Quantification of virally transduced cells co-labeled DCX, GFAP, or PDGFRa (**d**); n=6. Gene expression box plot of DCX (**e**), GFAP (**f**), and PDGFRa (**g**) at 35 DPI between SCI+Ctrl and SCI+Gsx1 group. Each dot represents the gene expression as log2(count per million) for one biological replicate sample. Mean ± SEM; * = p < 0.05; Students' t-test.*

Gene ontology analysis of 1447 DEGs (identified by RNA-Seq; Figure II.3) at 14 DPI revealed that enrichment of DEGs involved in cell differentiation, neuron projection development, synapse organization, and central nervous system development as some of the key biological processes being affected after Gsx1 treatment (Figure II.10). Additionally, REVIGO [95] analysis revealed that neurogenesis and nervous system development as few of the key biological processes being affected upon Gsx1 treatment (Figure II.11). The 2273 DEGs at 35 DPI (Figure II.3) shared a similar trend in NSPC lineage classification as those of the 14 DPI, e.g., an upregulation in DCX (Figure II.9e), downregulation in GFAP (Figure II.9f) and PDGFRa (Figure II.9g) in the SCI+Gsx1 group when compared to the SCI+Ctrl group. However, there was not significant (NS) difference in Olig2$^+$/RFP$^+$ cells between the control and Gsx1 treatment groups at 56 DPI (Figure II.12). These results suggest that Gsx1 treatment induces NSPC differentiation towards neuronal over glial lineage during the chronic phase of SCI.

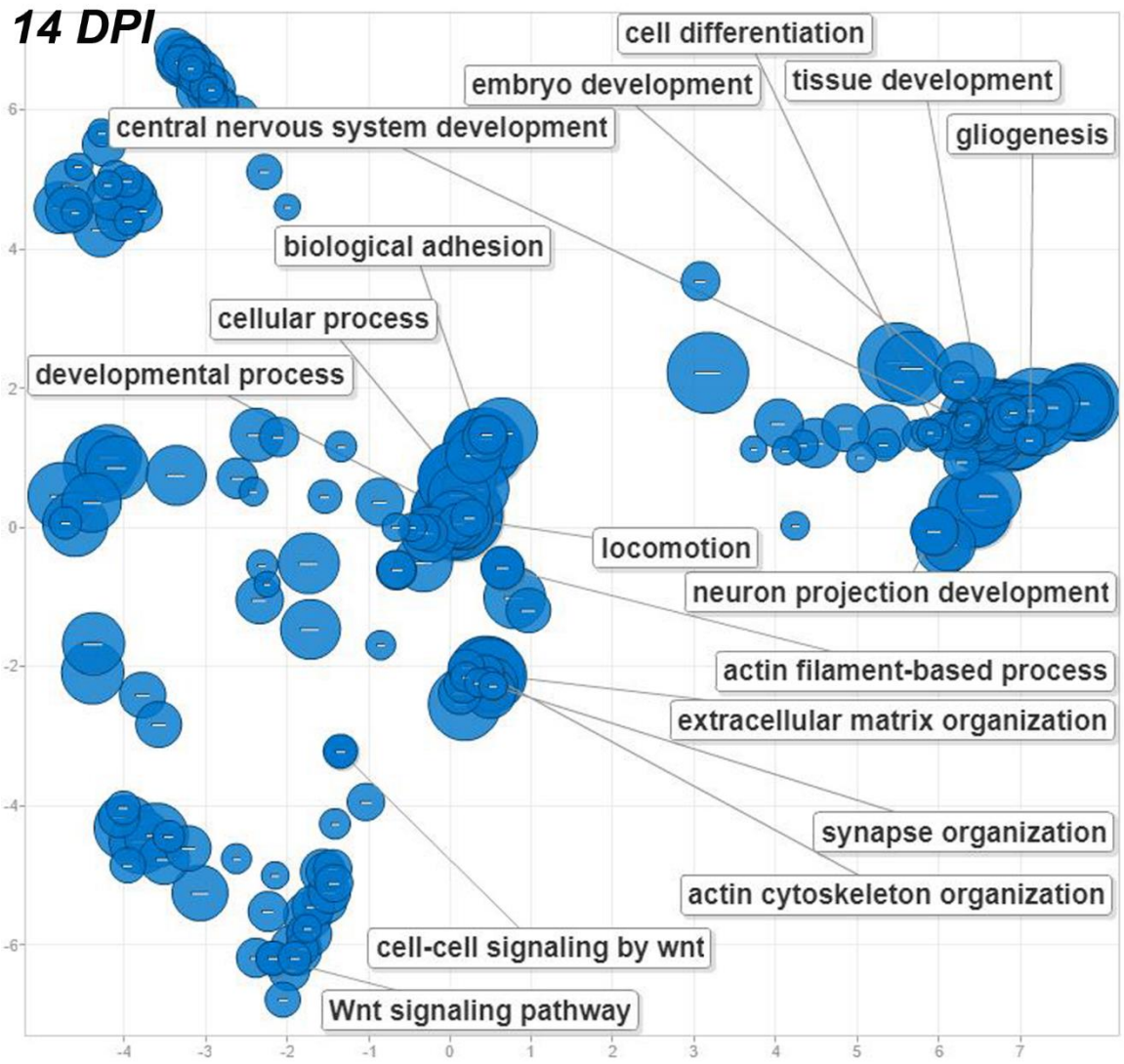

Figure II.10. Functional enrichment of gene ontology (GO) terms for differentially expressed genes (DEGs) at 14 DPI.

Enriched terms for biological process represented as a scatter plot in a two-dimensional semantic space using REVIGO. Circle size indicates the log10(p-value) of the GO terms.

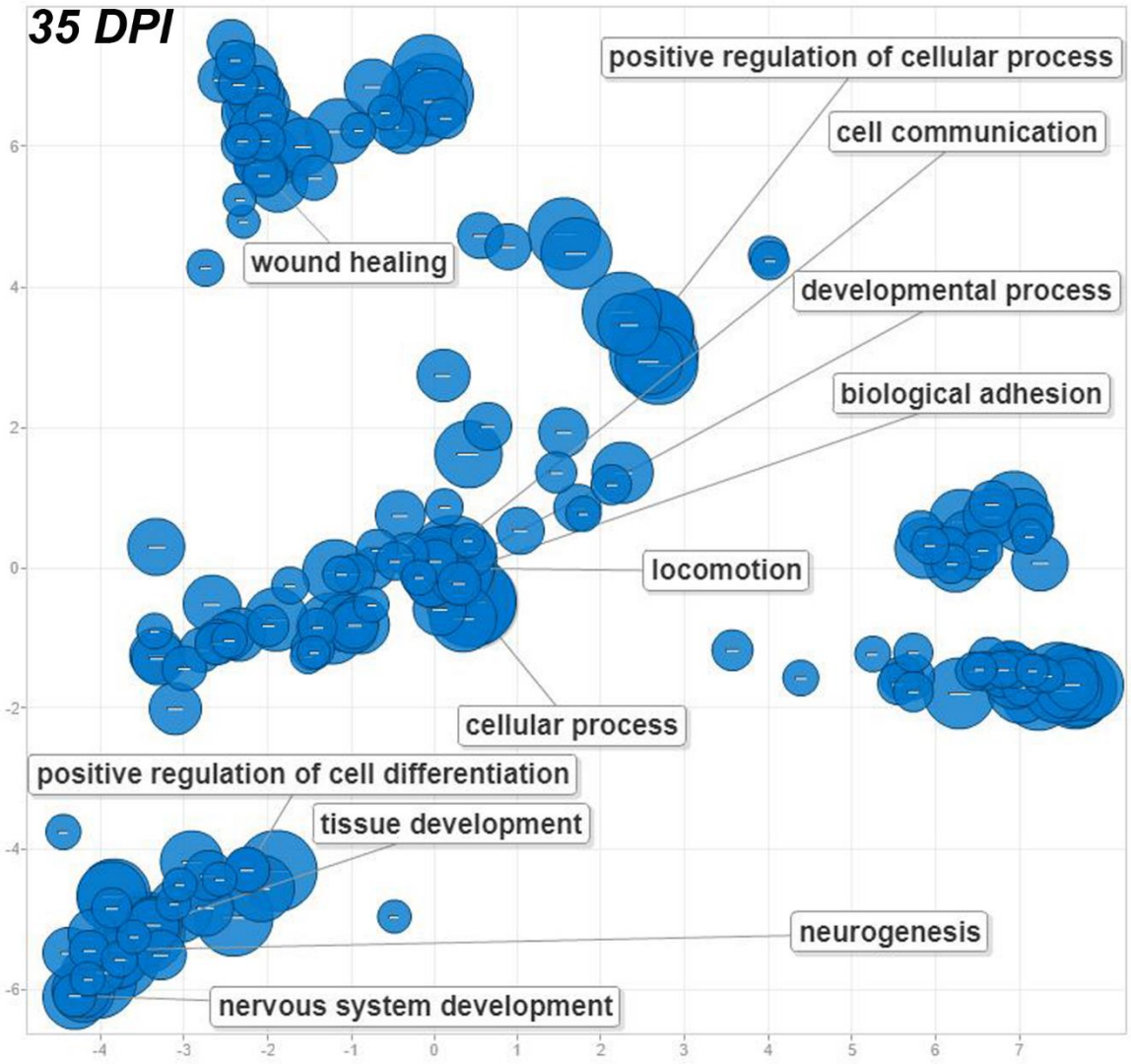

Figure II.11. Functional enrichment of gene ontology (GO) terms for differentially expressed genes (DEGs) at 35 DPI.

Enriched terms for biological process represented as a scatter plot in a two-dimensional semantic space using REVIGO. Circle size indicates the log10(p-value) of the GO terms.

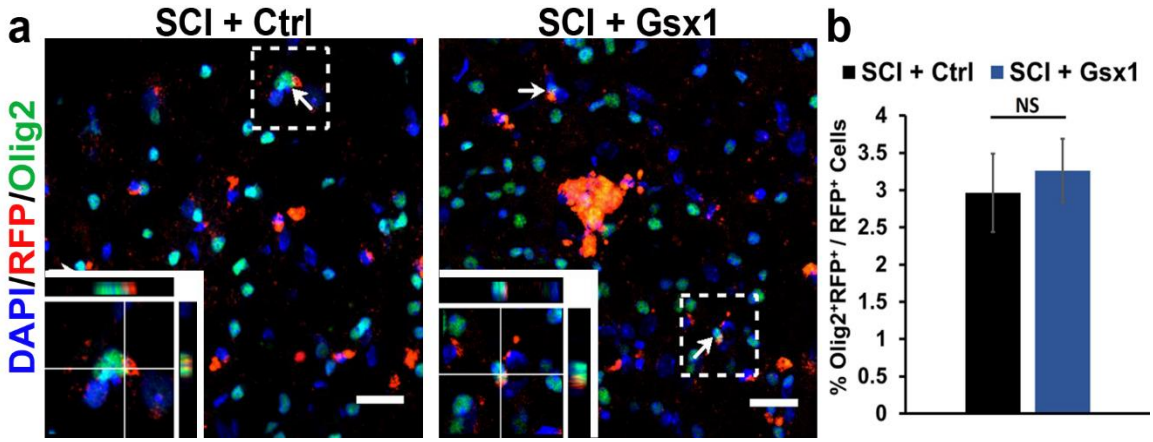

Figure II.12. Gsx1 treatment does not change the number of oligodendrocytes after SCI.

*Hemisection SCI was performed on 8-12 weeks old mice around T10. Immediately after lentivirus injection encoding Ctrl or Gsx1 gene along with RFP reporter. (**a**) Animals were harvested 56 DPI and sagittal sections are immunostained with oligodendrocyte marker, Olig2. Bottom left of the image includes the higher magnification z-stack view of the area denoted by a dashed white line to indicate co-expression. Scale bar = 20 µm. (**b**) Quantification of Olig2$^+$/RFP$^+$ at 56 DPI. n = 6; Mean ± SEM; * = p < 0.05; Students' t-test.*

II.4.4. Gsx1 treatment increases the number of specific subtypes of interneurons

Next, we asked which specific subtypes of mature neurons were induced by Gsx1 treatment. To investigate this, sagittal sections of spinal cord tissues at 56 DPI were stained with a mature neuronal marker NeuN (Figure II.13a), a cholinergic neuronal marker ChAT (Figure II.13b), a glutamatergic interneuron marker vGlut2 (Figure II.13c), and a GABAergic interneuron marker GABA (Figure II.13d). We found a significant increase in the percentage of NeuN$^+$, ChAT$^+$, and vGlut2$^+$ cells and a decrease in GABA$^+$ cells among RFP$^+$ cells in the SCI+Gsx1 group (n=6) when compared to the SCI+Ctrl group (n=6) (Figure II.13e). Further, RT-qPCR analysis of spinal cord tissues from Sham (n=4), SCI+Ctrl (n=4), and SCI+Gsx1(n=4) groups at 35 DPI (when induced cells reach maturity) showed significantly increased expression of vGlut (or Slc17a6) and Chat,

accompanied by a slightly increased mRNA expression of NeuN (or Hrnbp3) (Figure II.13f). These results indicate that Gsx1 treatment preferentially increased the number of glutamatergic and cholinergic interneurons and decreased the number of GABAergic interneurons.

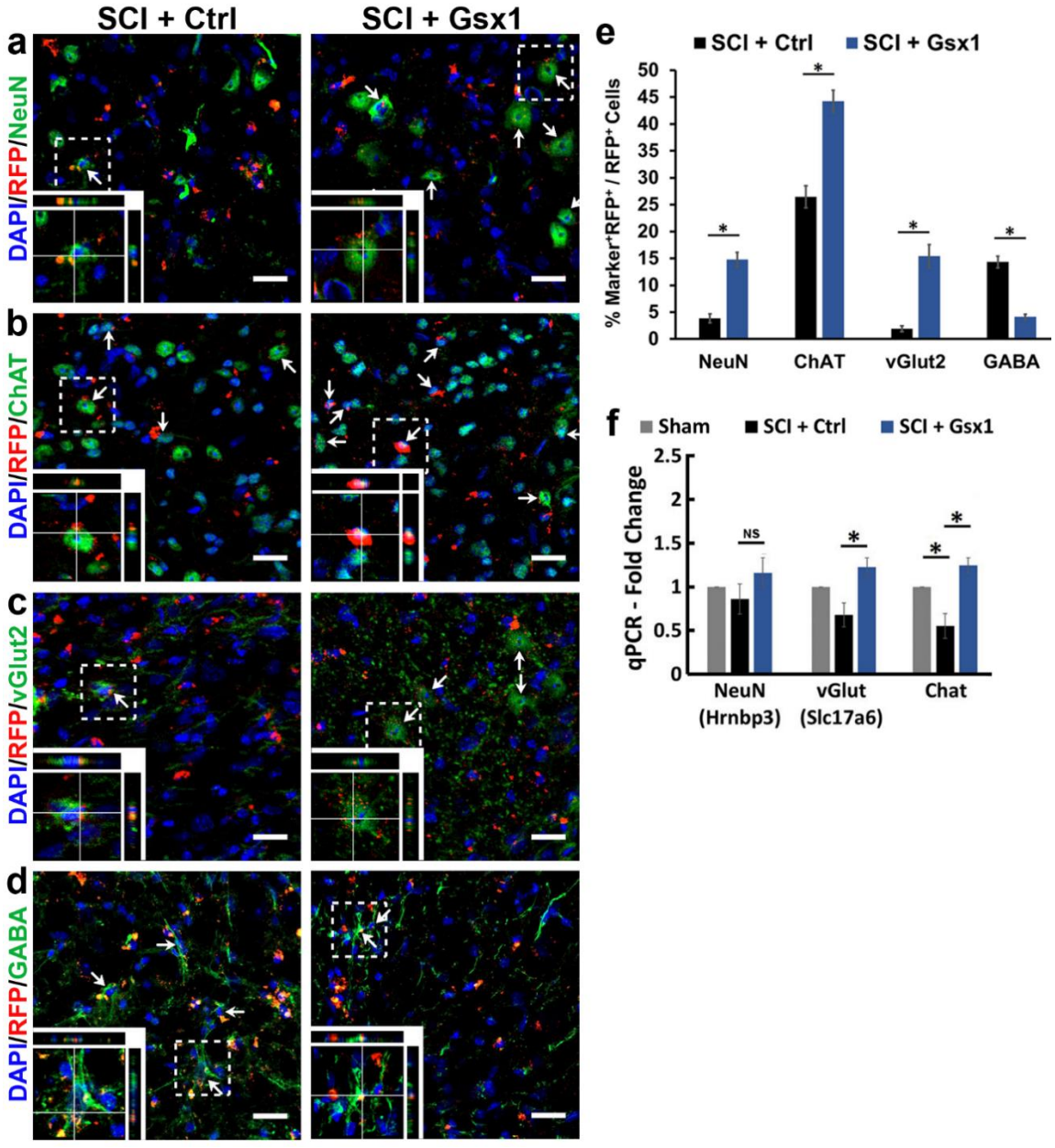

Figure II.13. Gsx1 induces glutamatergic and cholinergic interneurons and decreases GABAergic interneurons.

*Confocal images of sagittal sections of spinal cord tissues at 56 DPI show the expression of viral reporter RFP and mature neuron marker NeuN (**a**), cholinergic neuron marker ChAT (**b**), glutamatergic neuron marker vGlut2 (**c**), and GABAergic neuron marker GABA (**d**). Images in the bottom left corner show a higher magnification z-stack view of the area denoted by a dashed white box. Scale bar=20 µm. Quantification of virally transduced cells co-labeled with a cell marker (n=6) (**e**). RT-qPCR analysis measuring the mRNA level of genes (NeuN or Hrnbp3, vGlut or Slc17a6, and Chat) associated with mature neurons, normalized to the sham group (n =4) (**f**). Mean ± SEM; * = p < 0.05; Students' t-test and One-way ANOVA followed by Tukey post-hoc test and Students' t-test.*

II.4.5. Gsx1 treatment reduces glial scar formation

SCI causes activation of microglia and astrocytes, which leads to reactive astrogliosis and glial scar formation [107-109]. Glial scar is mostly composed of reactive astrocytes (RA), non-neuronal cells (e.g., pericytes and meningeal cells), and proteoglycan-rich extracellular matrix (ECM) [24, 25, 110]. Activated astrocytes secrete chondroitin sulfate proteoglycan (CSPG), which constitutes the major component of the glial scar. To investigate the role of Gsx1 in astrogliosis and scar formation, we first measured the mRNA expression level of two known marker genes, GFAP and Serpina3n, for RA involved in astrogliosis and scar formation [111] by RT-qPCR analysis. We found that SCI significantly increased the mRNA expression levels of GFAP and Serpina3n in the SCI+Ctrl (n=6) and SCI+Gsx1 (n=6) mice compared to the Sham mice (n=4) at 3 DPI (Figure II.14a) and 35 DPI (Figure II.14b), confirming that injury caused astrogliosis and scar formation. In contrast, Gsx1 treatment significantly reduced the mRNA expression of GFAP at 3DPI (Figure II.14a) and Serpina3n in the injured spinal cord at 35 DPI (Figure

II.14b). Our RNA-Seq analysis revealed that the expression of genes associated with RA (e.g., Mmp13, Mmp2, Nes, Axin2, Slit2, Plaur, and Ctnnb1), scar-forming astrocytes (SA) (e.g., Slit2 and Sox9), and both RA+SA (e.g., Gfap and Vim) [110] were downregulated at 14 DPI and 35 DPI (Figure II.14c-e).

We further determined the protein expression level of GFAP (Figure II.14f-g) and CSPG (Figure II.14h-i) by immunohistochemistry analysis using anti-GFAP and anti-CS56 antibodies, respectively. A baseline level of GFAP (Figure II.14f) but no detectable level of CSPG expression (Figure II.14h) were observed in the Sham group. In contrast, injury induced a higher protein level of GFAP (Figure II.14g) and CS56 (Figure II.14i) in the two SCI groups (i.e., SCI+Ctrl and SCI+Gsx1). Importantly, Gsx1 treatment greatly reduced $GFAP^+$ and $CS56^+$ immunostained area around the lesion site in the SCI+Gsx1 group (Figure II.14g,i). These results indicate that Gsx1 treatment reduces RA and SA, leading to attenuation of glial scar formation after SCI.

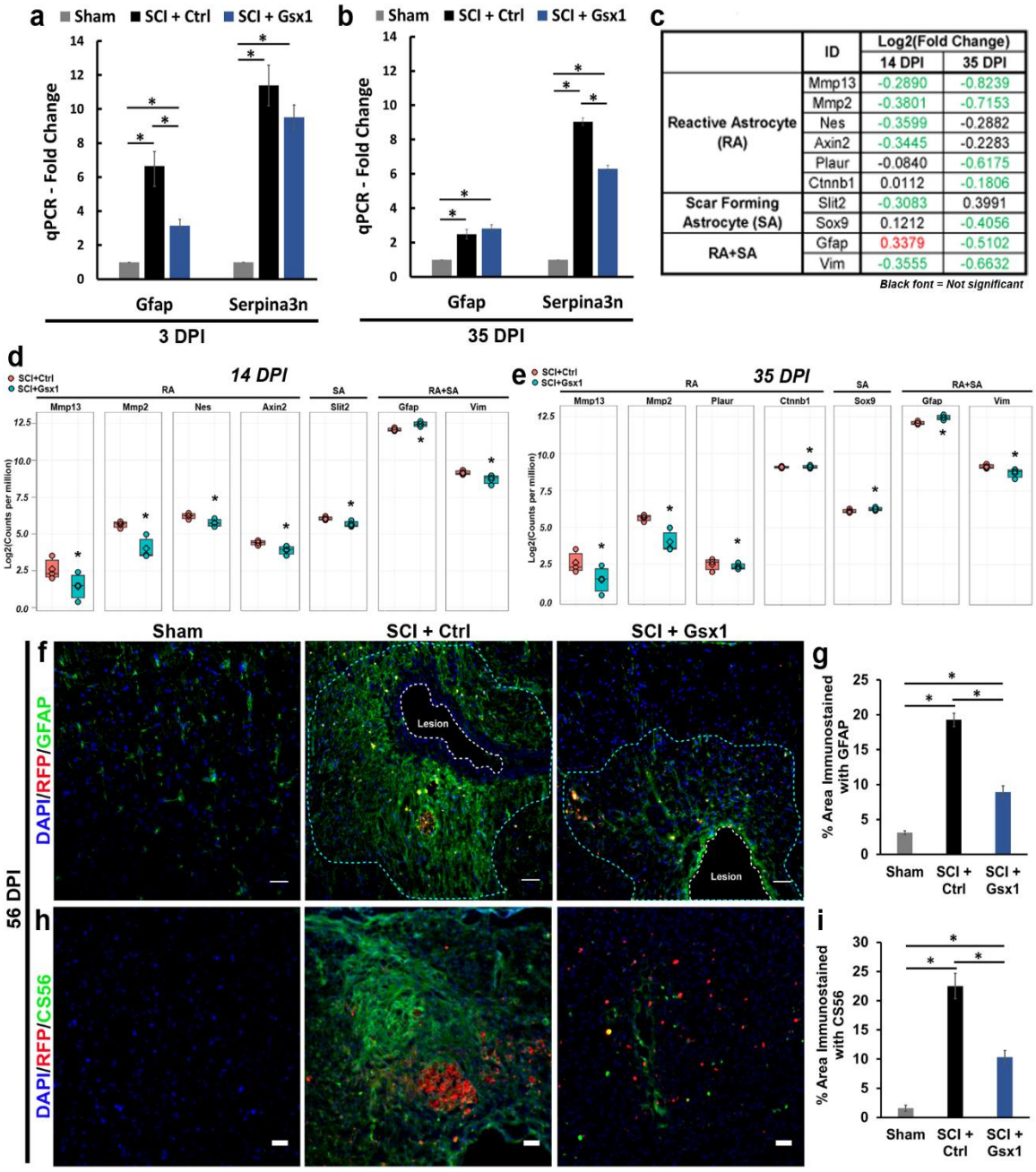

	ID	Log2(Fold Change)	
		14 DPI	35 DPI
Reactive Astrocyte (RA)	Mmp13	-0.2890	-0.8239
	Mmp2	-0.3801	-0.7153
	Nes	-0.3599	-0.2882
	Axin2	-0.3445	-0.2283
	Plaur	-0.0840	-0.6175
	Ctnnb1	0.0112	-0.1806
Scar Forming Astrocyte (SA)	Slit2	-0.3083	0.3991
	Sox9	0.1212	-0.4056
RA+SA	Gfap	0.3379	-0.5102
	Vim	-0.3555	-0.6632

Figure II.14. Attenuated astrogliosis and glial scar formation.

*The mRNA level of reactive astrocyte marker genes Gfap and Serpina3n in spinal cord tissues at 3 DPI (n=4) (**a**) at 35 DPI (n=4) (**b**) was measured by RT-qPCR. (**c**) Differentially expressed genes (DEGs) between SCI+Ctrl and SCI+Gsx1 that are known to be associated with reactive astrocytes (RA) (e.g., Mmmp13, Mmp2, Nes, Axin2, Plaur, and Ctnnb1), scar forming astrocytes (SA) (e.g., Slit2 and Sox9) and both with RA and SA*

*(e.g., Gfap and Vim) at 14 DPI and 35 DPI. Gene expression box plot representing the expression of RA and SA associated genes as a log2(counts per million) at 14 DPI (**d**) and at 35 DPI (**e**). Each dot represents the gene expression as log2(count per million) for one biological replicate sample. Images of sagittal sections of spinal cord tissues at 56 DPI show the expression of viral reporter RFP, glial scar markers GFAP (**f**) and chondroitin sulfate proteoglycan (CSPG) marker CS56 (**h**). Quantification of immunostained area with anti-GFAP (**g**) and anti-CS56 (**i**) around the injury site show reduced signals of GFAP and CS56. Scale bar =50 µm, n=4 for Sham and n=6 for SCI + Ctrl and SCI + Gsx1. Mean ± SEM; * = p < 0.05; One-way ANOVA followed by Tukey post-hoc test. DPI = days post injury.*

II.4.6. Gsx1 treatment improves locomotor function after SCI

All mice with a lateral hemisection SCI at the T10 level exhibited paralysis in the left hindlimb after injury (Figure II.15a). To determine the effect of Gsx1 treatment on functional recovery, we assessed the locomotor behavior using an established open-field locomotion test and a BMS score scale [11] starting from the day before the injury (-1 DPI) to 56 DPI (8 weeks after SCI). For each mouse, a BMS score was assigned double-blindly by three observers. BMS scores range from 0 (complete paralysis and no ankle movement) to 9 (normal walking) [11]. The Sham animals displayed a normal locomotor behavior with BMS score remained at ~ 9 from -1 to 56 DPI (Figure II.15b). Mice in the injury groups (SCI+Ctrl and SCI+Gsx1) exhibited paralysis in the left hindlimb with a BMS score of 0 on the day hemisection injury (0 DPI) (Figure II.15a-b and supplemental video), confirming the success of inducing lateral hemisection SCI. For mice in the SCI+Ctrl group (n≥6), the BMS scores gradually improved to ~3 (dorsal stepping) by 56 DPI (Figure II.15b). In contrast, mice in the SCI+Gsx1 group (n≥6) had a significantly improved locomotor function with BMS score gradually increased from ~0 to ~5 by 30 DPI (Figure

II.15b). Starting from ~30 DPI, Gsx1-treated animals showed near normal locomotion (with BMS score reaching ~ 6-7) compared to the Sham mice (Figure II.15b). Together, these results indicate that Gsx1 treatment dramatically improved locomotor functional recovery after SCI (Figure II.15a-b).

To identify the molecular basis for the improved locomotor function, we performed RT-qPCR analysis on the expression of a selected set of genes involved in axon growth. Gsx1 treatment (n=4) significantly increased mRNA level of Ctnna1 and Col6a2 compared to the SCI+Ctrl group (n=4) at 35 DPI (Figure II.15c). We further performed RNA-Seq, IPA, and gene ontology analysis on DEGs. Gsx1 treatment led to the activation of Netrin signaling (Figure II.15d; Figure II.16b) and axonal guidance pathways (Figure II.15e), and CREB signaling in neurons (Figure II.16a). CREB is an essential transcription factor responsible for axon growth and regeneration [112]. Our RNA-Seq and IPA analysis further identified an increase in the expression of genes known to promote synaptogenesis (Figure II.15f) and a decrease in the expression of genes known to inhibit synaptogenesis (Figure II.15g) in Gsx1 treatment at 35 DPI.

Neurotransmission of serotonin (5-HT) in the spinal cord is required for modulating sensory, motor, and autonomic functions [113]. After SCI, 5-HT axons caudal to the injury site degenerate, while rostral to the injury site sprout [114, 115]. Therefore, we measured the expression level of serotonergic neurons using anti-5-HT antibody in spinal cord samples at 56 DPI to determine the effect of Gsx1 treatment on the recovery of 5-HT neuronal activity. Immunostaining results show that the level of 5-HT^{+} axons was similar in the region rostral to the injury site in both the control and Gsx1 treatment. While in the region caudal region, Gsx1 treatment increased the level of 5-HT axons (Figure II.16c). This result suggests that Gsx1 promotes 5-HT neuronal activity in the injured spinal cord.

Lastly, gene ontology analysis revealed that DEGs were involved in cell communication, nervous system development, neurogenesis, and locomotion (Figure II.11). Together, these results indicate that Gsx1 treatment upregulates signaling pathways associated with axon growth and guidance, which correlate with the improved locomotor function after SCI.

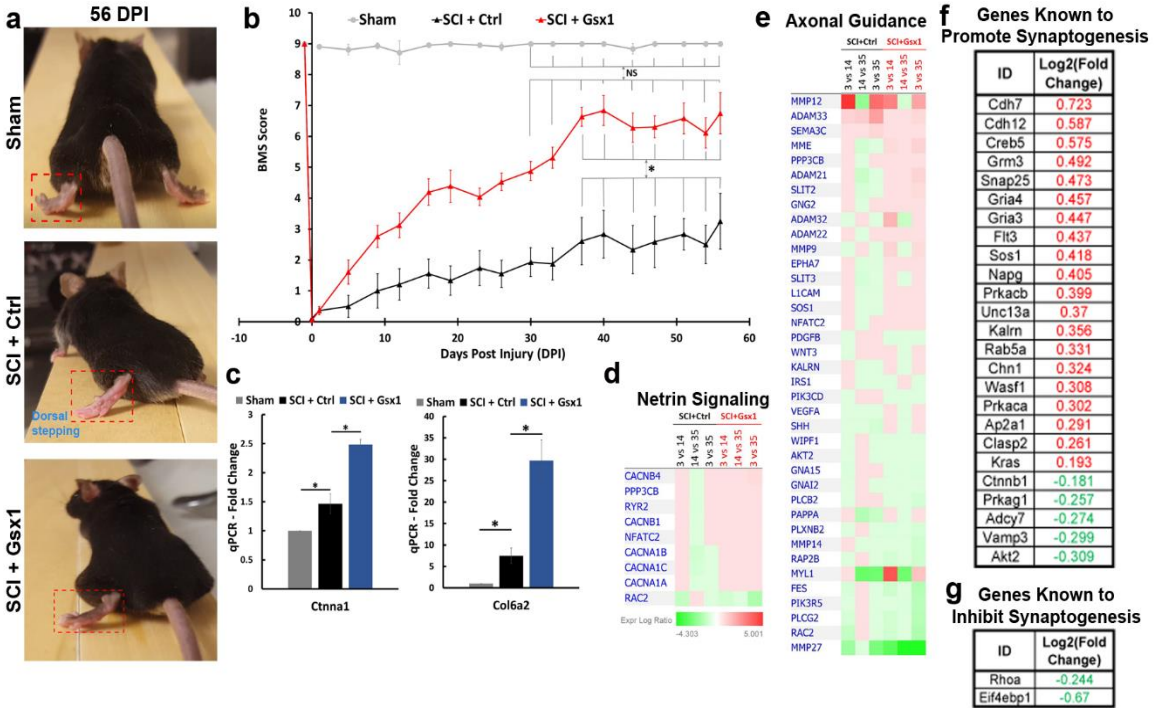

ID	Log2(Fold Change)
Cdh7	0.723
Cdh12	0.587
Creb5	0.575
Grm3	0.492
Snap25	0.473
Gria4	0.457
Gria3	0.447
Flt3	0.437
Sos1	0.418
Napg	0.405
Prkacb	0.399
Unc13a	0.37
Kalrn	0.356
Rab5a	0.331
Chn1	0.324
Wasf1	0.308
Prkaca	0.302
Ap2a1	0.291
Clasp2	0.261
Kras	0.193
Ctnnb1	-0.181
Prkag1	-0.257
Adcy7	-0.274
Vamp3	-0.299
Akt2	-0.309

ID	Log2(Fold Change)
Rhoa	-0.244
Eif4ebp1	-0.67

Figure II.15. Improved locomotor functional recovery after SCI.

*Lateral hemisection SCI was performed on 8-12 weeks old mice around T9-T10 level immediately followed by the injection of lentivirus encoding Gsx1 along with RFP reporter (lenti-Gsx1-RFP). Lentivirus encoding only the reporter RFP was used as a control (lenti-Ctrl-RFP). Locomotor function was assessed by BMS score at least twice weekly up to 56 DPI. Representative images of hindlimb walking status at 56 DPI (**a**) and the BMS scores (**b**) of left hindlimb (n ≥ 6). (**c**) RT-qPCR analysis of differentially expressed genes (Ctnna1 and Col6a2) involved in axon guidance at 35 DPI (n=4; Two-way ANOVA analysis followed by post-hoc test). Heatmaps show Gsx1 upregulated the differentially expressed genes*

*involved in Netrin signaling (**d**) and axonal guidance (**e**) from RNA-Seq analysis and IPA comparing among 3, 14, and 35 DPI groups (n≥ 3). Genes known to promote (**f**) and inhibit (**g**) synaptogenesis between Ctrl and Gsx1 treatment at 35 DPI identified using RNA-Seq and IPA analysis (n=4). Mean ± SEM * p < 0.05, Students' t-test.*

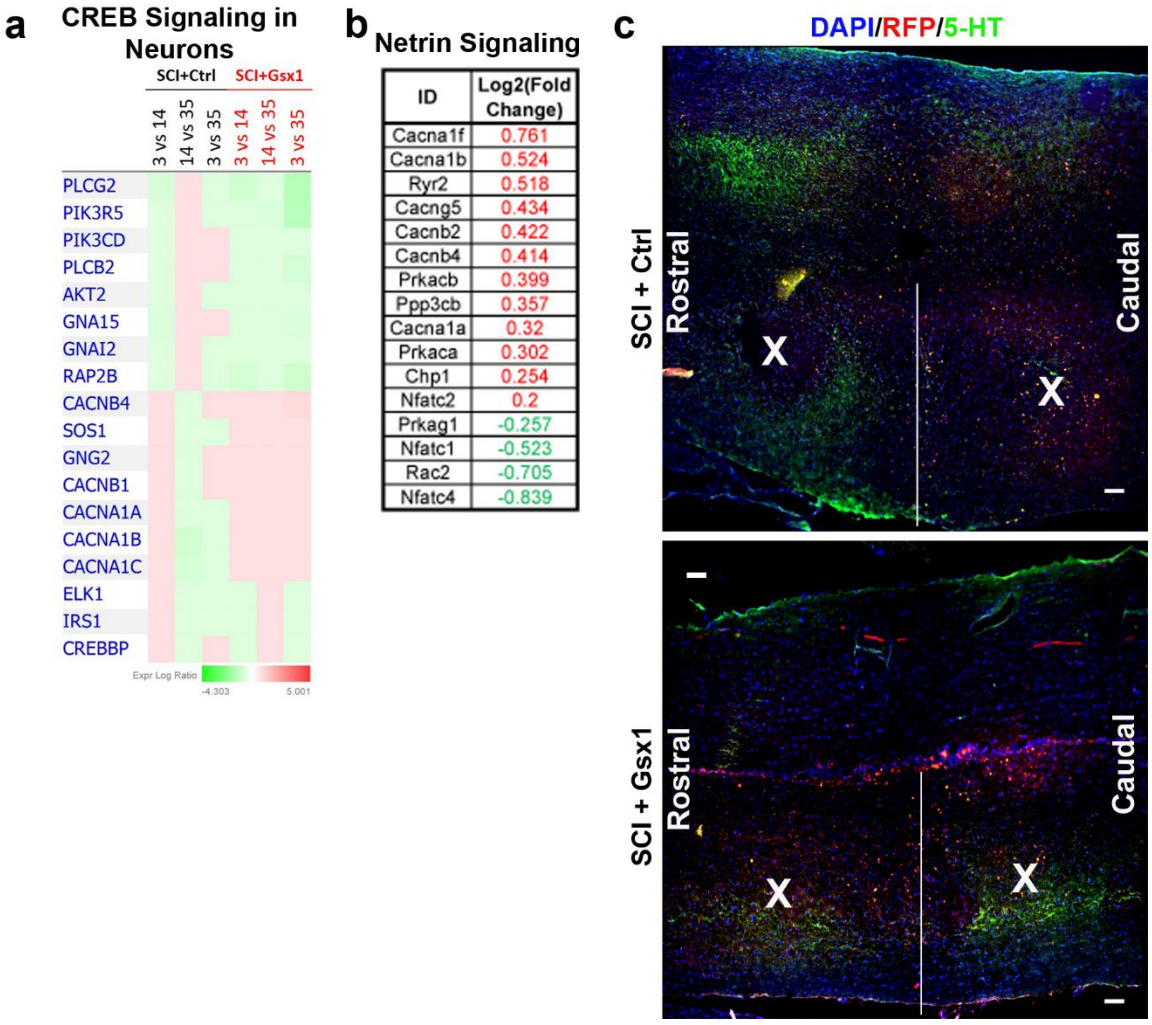

Figure II.16. Gsx1 treatment promotes signaling for axon growth and 5-HT neuronal activity after hemisection SCI.

*IPA heat map of differentially expressed genes involved in CREB signaling in neurons at 3 DPI, 14 DPI, and 35 DPI between SCI+Ctrl and SCI+Gsx1 (**a**); n≥3. (**b**) Genes involved in the Netrin signaling along with their log2(fold change) at 35 DPI; n=4. (**c**) Representative*

photomicrographs of serotonin (5-HT) staining of the sagittal sections of the spinal cord samples at 56 DPI. "X" indicates lentivirus injection site, and white line indicates hemisection site. n = 5; Scale bar = 100 μm.

II.5. Discussion

Limited neurogenesis, increased reactive astrogliosis and scar formation are the major barriers for neuroregeneration and functional recovery after SCI. In this study, we demonstrate that Gsx1 treatment promotes the activation of NSPCs and the generation of specific subtypes of interneurons (e.g., glutamatergic and cholinergic neurons). Importantly, Gsx1 expression inhibits reactive astrogliosis and glial scar formation, and leads to a dramatic locomotor functional recovery in mice with lateral hemisection SCI. Our RNA-Seq and RT-qPCR analysis reveals that Gsx1 alters the expression of genes associated with cell proliferation, NSPC activation, neurogenesis, astrogliosis and scar formation, which correlates with functional recovery after SCI.

Previous studies using transcription factors, e.g., Sox2 and NeuroD1 have shown successful induction of neurons [42, 71]. However, limited or no functional recovery have been reported. The failure of newly generated neurons for functional recovery may be attributed to the following aspects: 1) Sox2 and NeuroD1 are general neurogenic transcription factors, but not specific factors for spinal neuronal genesis; 2) Sox2-induced neurons resemble GABAergic interneurons [42]. The additional inhibitory interneurons might have caused further imbalance of the excitation/inhibition ratio; and 3) functional recovery may require the generation of various specific cell types, e.g., glutamatergic and cholinergic interneurons. A recent study has shown that spinal inhibitory interneurons act as a roadblock limiting the integration of descending inputs into relay circuits after injury

[78]. In support of this notion, we found that Gsx1 inhibits the generation of GABAergic interneurons. Thus, Gsx1-induced reduction of GABAergic interneurons may contribute to the restoration of the excitation/inhibition ratio.

Gsx1 is known to regulate Notch signaling via its interaction with a Notch1 enhancer [54]. At the embryonic stage, an increase in Gsx1 and Notch1 leads to a higher level of glutamate neurotransmitters [116]. Notch signaling is a canonical pathway required for NSPC proliferation and self-renewal, as well as prevention of untimely neuronal differentiation of NSPCs [117, 118]. In support of these observations, our RNA-Seq and RT-qPCR data show that Gsx1 transiently upregulates Notch and Nanog signaling pathways during an acute stage of SCI. These upregulated signaling pathways support the activation and expansion of endogenous NSPCs.

Our finding that Gsx1 reduces reactive astrogliosis and scar formation is consistent with functional recovery and such a role for Gsx1 has not been reported. In fact, the adult NSPCs give rise to mostly astrocytes after CNS injury [119, 120]. However, Gsx1 treatment significantly decreases the expression of genes associated with reactive astrocytes and scar forming astrocytes. It is thus likely that Gsx1-induced NSPC differentiation into neuronal lineage is on the expense of astrocyte lineage. Reduction in astrogliosis leads to attenuation of scar formation.

For Gsx1-induced neurons to be functional, they need to establish proper connections. In support of this notion, we found the upregulation of axon guidance signaling, Netrin signaling, CREB signaling pathway, and synaptogenesis. Thus, future research should investigate the therapeutic effects of manipulating Notch/Nanog, Netrin signaling, synapse

formation, and axonal guidance signaling pathways on locomotor functional recovery after SCI.

In summary, we have demonstrated that lentivirus-mediated Gsx1 expression in the injured spinal cord is sufficient to reduce glial scar, induce neurogenesis of specific interneurons, and improve locomotion after SCI. Thus, these findings indicate that Gsx1 is a promising therapeutic gene for the treatment of SCI and potentially for other central nervous related injuries as well.

II.6. Acknowledgements

We thank the Cai lab members for constructive comments and discussion. Dr. Kelvin Kwan and his lab helped with lentivirus production. Dr. KiBum Lee and his lab assisted with RT-qPCR analysis. This work was supported by the New Jersey Commission on Spinal Cord Research grant #15IRG006 (L.C.). M.P. and J.A. are recipients of NIH Biotechnology Pre-Doctoral Training Fellowship (T32GM008339). M.P. is also a recipient of the U.S. Department of Education GAANN Precision and Personalized Medicine Pre-Doctoral Training Fellowship (P200A150131).

Chapter III. Nkx6.1 attenuates glial scar formation and promotes neurogenesis after spinal cord injury

Note: This Chapter is reproduced from the manuscript that is submitted to Scientific Reports.

Misaal Patel, Jeremy Anderson, Shunyao Lei, Rebecca Risman, and Li Cai. Nkx6.1 attenuates glial scar formation and promotes neurogenesis after spinal cord injury. Scientific Reports (Submitted).

III.1. Abstract

Endogenous neural stem/progenitor cells (NSPCs) represents a promising cell source for damage repair and regeneration after spinal cord injury (SCI). Here we show that lentivirus-mediated Nkx6.1 expression in the adult injured mouse spinal cord promotes NSPC activation and cell proliferation in the acute phase of injury. In the chronic phase, Nkx6.1 increases the generation of specific spinal cord interneurons and reduces the number of reactive astrocytes and glial scar formation. Mechanistically, Nkx6.1 upregulates the sequential expression of genes involved in Nanog/Notch signaling pathways important for NSPC activation, and neurogenic pathways for axon and synapse formation. In the meantime, Nkx6.1 also downregulates genes involved in reactive astrocytes and glial scar formation. Thus, our study unveils a role of Nkx6.1 in adult NSPCs for neurogenesis and attenuation of glial scar formation after SCI.

III.2. Introduction

Endogenous neural stem progenitor cells (NSPCs) reside in the ependymal region around the central canal in the adult spinal cord and quickly become activated in response to the

spinal cord injury (SCI) [20, 66, 67]. However, the majority of injury-activated NSPCs differentiate into astrocytes and oligodendrocytes, while only a small percentage that differentiate into neurons [19, 20, 31, 68-70].

Despite extensive research, neuroregeneration and attenuation of the glial scar after SCI have still been extremely difficult. Studies have shown that resident non-neuronal cells can be converted to mature neurons by transcription factors (e.g., NeuroD1 and Sox2) [32, 71], suggesting the therapeutic potential in regenerative medicine. Furthermore, injury-induced reactive astrocytes (RAs) and chondroitin sulfate proteoglycans (CSPGs) constitute the majority of glial scars post-SCI, which are known to inhibit the axon regeneration and formation of local circuitry. Efforts are made to reduce glial scar by delivering chondroitinase ABCs at the injury site to digest CSPGs [27, 74]. An important next step is to identify genes/factors that can both promote neurogenesis and inhibit glial scar formation, which is required for the restoration of the damaged circuitry in the injured spinal cord.

Our previous study has established that NK6 Homeobox 1 (Nkx6.1) regulates Notch signaling in NSPCs [54]. Nkx6.1 is widely expressed by NSPCs within the neural tube [121]. It plays a critical role in ventral neural patterning and controls lineage specification of both neurons and glia during spinal cord development [58, 59]. In the adult mouse spinal cords, Nkx6.1^{+} ependymal cells retain the proliferative property of NSPCs [60]. In the injured spinal cord of zebrafish, V2 interneurons can be generated from Pax6 and Nkx6.1 expressing progenitors [61]. Nkx6.1 is also known to promote differentiation of NSPCs into mature neurons during development [62] and after spinal cord injury in turtles [63]. Based on these studies, we hypothesize that Nkx6.1 overexpression in the adult injured spinal cord will promote NSPC activation and neurogenesis.

In this study, we used a lentivirus-mediated gene delivery system to transduce Nkx6.1 into the spinal cord of the adult mice with lateral hemisection SCI. We found that Nkx6.1 expression expands the NSPC pool in the acute phase of an injury, and promotes the generation of mature cholinergic interneurons and inhibits glial scar formation in the chronic phase after SCI. Transcriptomic analysis revealed that Nkx6.1 upregulates the Notch and NANOG signaling pathways to promote NSPCs activation, upregulates genes associated with axon guidance, and downregulates the expression of genes associated with reactive astrocytes. These findings unveil a specific role of Nkx6.1 in the adult NSPCs for promoting neurogenesis and inhibiting reactive astrocytes and glial scar formation. Thus, Nkx6.1 represents a promising target gene to manipulate NSPCs for damage repair and tissue regeneration after SCI.

III.3. Materials and Methods

III.3.1. Lentivirus

pLenti-GIII-CMV-RFP-2A-Puro lentiviral vector with Nkx6.1-RFP (9947 bps) gene insert was purchased from Applied Biological Materials Inc. (Cat. # LV476460). Presence of gene in the lentiviral vector was verified using PCR followed by gel electrophoresis. A lentiviral vector expressing only RFP is used as a negative control (lenti-Ctrl-RFP). Human Embryonic Kidney (HEK293T) cells are cultured in high glucose Dulbecco's Modified Eagle Media (DMEM) supplemented with 10% fetal bovine serum (FBS), 1% nonessential amino acid (NEAA), and 1% Glutamax. Once the HEK293T cells are about 50-60% confluent, they are transfected with target vector (lenti-Nkx6.1-RFP or lenti-Ctrl-RFP), envelope plasmid (pMD2.G/VSVG, Addgene 12259), and 3rd generation packaging plasmids (pMDLg/pRRE, Addgene 12251 and pRSV-Rev, Addgene 12253). Virus containing supernatant is collected at 2 and 4 days post-transfection. Viral particles are

concentrated by polyethylene glycol 6000 (PEG6000) method [86] and titer is determined by infecting HEK293T cells [86].

III.3.2. Lateral Hemisection Spinal Cord Injury (SCI) and Lentivirus Injection

All experimental protocols were approved by the Institutional Animal Care and Use Committee (IACUC) and the Institutional Biosafety Committee at Rutgers University. All animal work was conducted in accordance with relevant guidelines and regulations of the IACUC. Young adult C57BL/6 mice (8-12 weeks-old) were used for this study. Mice were kept at 12-hour light/dark cycle and were blindly and randomly chosen for each treatment condition. Animals were divided into the following groups (3 animals/group): (1) Sham (No SCI but only exposing the spine), (2) mice received SCI and lenti-Ctrl-RFP treatment (SCI+Ctrl), and (3) mice received SCI and lenti-Nkx6.1-RFP treatment (SCI+Nkx6.1).

For the Sham, skin and muscle were cut exposing the spine. A lateral hemisection SCI performed by first exposing spinal cord around T9-T10 by laminectomy and then lateral cut on the left side of the spinal cord from the midline to the end. Immediately after the SCI, about 1-2 µl of lentiviral particles ($1x10^8$ TU/ml) were injected at the rate of 1 µL/min about 1 mm rostral and caudal to the injury site. The viral particle injection needle was left at the place for 2-3 minutes after the injection to avoid backflow. After surgery, animals from all three groups subcutaneously received pain killer (1 mg/kg Meloxicam) and antibiotics (50 mg/kg Cefazoline). Completeness of the hemisection was determined by paralysis in the left hind limb at the day-post injury (0 DPI) and 1 DPI.

III.3.3. Tissue Processing

Spinal cord tissues were harvested at 3, 14, and 56 DPI (n=3/group/time point). At each time point, mice were intracardially perfused with 1x (v/v) sterile phosphate buffer saline

followed by 4% (w/v) paraformaldehyde (PFA). About 5-6 mm of the spinal cord tissue containing the injury and injection sites was removed and fixed overnight with 4% PFA. Next day, fixed tissue is washed with 1x PBS and transferred to 30% (w/v) sucrose for dehydration for about 24 hours. Dehydrated tissue is embedded using Tissue-Tek® optimum cutting temperature (O.C.T.) and stored at -80ºC. At each time point, tissues were sagittally sectioned at 12 µm thickness using a cryostat (ThermoScientific).

III.3.4. Immunohistochemistry (IHC) and Image Analysis

IHC was performed based on a previously established protocol with minor modifications [54]. First, sagittally sectioned spinal cord tissue samples were treated with cold methanol for 10 mins at room temperature. Background signal was blocked by incubating samples with blocking solution (0.05% Triton X-100, 2% donkey serum, and 3% bovine serum albumin (BSA)). Samples were incubated with primary antibodies (Table III.1) in 1x (v/v) phosphate buffer saline (PBS) overnight at 4°C. Next day, samples are washed with 1x PBS and incubated with secondary antibodies (Table III.1) for 1 hour at room temperature. Samples are then washed with 1x PBS and incubated with DAPI (200ng/ml) for 5 mins followed by the final wash. Next slides are sealed with Cytoseal 60 (ThermoFisher Scientific 8310-4).

Immunostained fluorescent images were captured at the same exposure using Zeiss AxioVision Imager A.1 or confocal Zeiss LSM 800 microscope. At least five sections from each antibody/animal were imaged and analyzed around the injection/injury site. ImageJ [87, 88] automatic cell counter was used to count the total number of cells. Co-labeled cells were counted manually by an individual who was blinded to the treatment. Data are presented as the mean±standard error of the mean (SEM). Statistical significance between two conditions is calculated by Student's t-test and multi-group comparison are

performed using one-way ANOVA, followed by Tukey post-hoc test. A p-value less than 0.05 is considered statistically significant.

	Vendor, Catalog	Host Species	Type	RRID	Dilution
Primary Antibody					
CD68	Millipore Sigma, MAB1435	Mouse (Ms)	Monoclonal	AB_177576	1 : 100
Ki67	Abcam, ab15580	Rabbit (Rb)	Polyclonal	AB_443209	1 : 1000
Nestin	Abcam, ab6142	Mouse (Ms)	Monoclonal	AB_305313	1 : 200
Notch1	Abcam, ab8925	Rabbit (Rb)	Polyclonal	AB_306863	1 : 200
DCX	Santa Cruz Biotechnology, sc-8067	Goat (Gt)	Polyclonal	AB_2088491	1 : 100
PDGFRa	Abcam, ab61219	Rabbit (Rb)	Polyclonal	AB_2162341	1 : 100
NeuN	Millipore Sigma, MAB377	Mouse (Ms)	Monoclonal	AB_2298772	1 : 300
GFAP	Millipore Sigma, G3893	Mouse (Ms)	Monoclonal	AB_477010	1 : 400
Olig2	Millipore Sigma, AB9610	Rabbit (Rb)	Polyclonal	AB_570666	1 : 500
vGlut2	Millipore Sigma, AB2251-I	Guinea Pig (Gp)	Polyclonal	AB_2665454	1 : 1000
ChAT	Millipore Sigma, SAB2500236	Goat (Gt)	Polyclonal	AB_10603616	1 : 300
GABA	Millipore Sigma, A-2052	Rabbit (Rb)	Polyclonal	AB_477652	1 : 3000
CS56	Millipore Sigma, C8035	Mouse (Ms)	Monoclonal	AB_476879	1 : 200
Secondary Antibody					
Alexa Fluor 488 Dk anti Ms	Jackson Immuno Research, 715-545-150	-	Polyclonal	AB_2340846	1 : 200
Alexa Fluor 488 Dk anti Rb	Jackson Immuno Research, 711-545-152	-	Polyclonal	AB_2313584	1 : 200
Alexa Fluor 488 Dk anti Gt	Jackson Immuno Research, 705-545-003	-	Polyclonal	AB_2340428	1 : 200
Alexa Fluor 488 Dk anti Gp	Jackson Immuno Research, 706-545-148	-	Polyclonal	AB_2340472	1 : 200
Alexa Fluor 647 Dk anti Ms	Jackson Immuno Research, 715-605-150	-	Polyclonal	AB_2340862	1 : 200
Alexa Fluor 647 Dk anti Rb	Jackson Immuno Research, 711-605-152	-	Polyclonal	AB_2492288	1 : 200
Alexa Fluor 647 Dk anti Gt	Jackson Immuno Research, 705-605-003	-	Polyclonal	AB_2340436	1 : 200
Alexa Fluor 647 Dk anti Gp	Jackson Immuno Research, 706-605-148	-	Polyclonal	AB_2340476	1 : 200

Table III.1. A list of antibodies used in this study.

A list of antibodies along with the catalog, host species, type, RRID, and the dilution of each antibody used in this study. Ms = mouse, Rb = rabbit, Gt = goat, Gp = Guinea pig, Dk = donkey.

III.3.5. RNA Isolation

For RNA isolation, about 5 mm spinal cord tissue (containing the injury and the injection site) were extracted at 3 and 35 DPI. At least 3 samples for each condition per time points were harvested. Total RNA from spinal cord tissue is preserved by fast freezing the tissue samples in liquid nitrogen. Total RNA was isolated from spinal cord tissue using RNeasy Lipid Tissue Mini kit (Qiagen, #74804) using the manufacture's protocol. Total RNA was treated with DNase I (Qiagen) to eliminate genomic DNA contamination. The concentration and the quality of the total RNA is determined by NanoDrop Lite Spectrophotometer (ThermoScientific).

III.3.6. Quantitative real-time PCR (qPCR) and Analysis

From the total RNA, complementary DNA (cDNA) was synthesized using SuperScript III First-Strand Synthesis System (Invitrogen, #18080051) using the manufacture's protocol. qPCR was performed with Power SYBR™ Green PCR Master Mix and gene-specific primers (Table S2) using StepOnePlus Real-Time PCR system (Applied Biosystem). Glyceraldehyde 3-phosphate dehydrogenase (GAPDH) used as a housekeeping gene. The Levak method is used to calculate the fold change of SCI+Ctrl and SCI+Nkx6.1 groups normalized to Sham group.

III.3.7. Library Preparation and RNA-Seq Analysis

Quality control of the total RNA (using RNA 6000 Nano chip on the 2100 Bioanalyzer), library preparation (Illumina MiSeq) and RNA-Seq were performed by Admera Health (South Plainfield, NJ). The RNA-Seq was performed at 3 DPI and 35 DPI (n≥3/group/time point) using Illumina MiSeq using manufacturer's protocol. Each sample was sequenced as paired-end (2x150 bp) on the Illumina MiSeq platform and generated a total of 40 million reads per sample.

Quality of the raw fastq file was assessed using the FastQC (http://www.bioinformatics.babraham.ac.uk/projects/fastqc/). Once the sample passed quality control (QC) all sequences were aligned to the mouse reference genome, mm10, using STAR (version 2.0) [89]. The raw read counts were assembled as a matrix using HTSeq (version 0.6.0) [90] and normalized using the DESeq2 [91, 92], a R/Bioconductor package. Next, DESeq2 was used to call for differential expressed gene (DEGs; $p < 0.05$) from the counts matrix. The downstream pathway analysis was carried out using the

Ingenuity Pathway Analysis (IPA, QIAGEN, Inc., https://www.qiagenbioinformatics.com/products/ingenuity-pathway-analysis) [94].

III.4. Results

Given the established role of Nkx6.1 in neurogenesis [58], astrocyte progenitor specification [59], and in regulating Notch signaling [54] during the development of the spinal cord, it is likely that reactivating Nkx6.1 expression in the adult spinal cord will promote neural regeneration after SCI. To test this hypothesis, we performed lateral hemisection SCI at thoracic (T) 10 level in 8-12 weeks old young adult mice. Immediately after SCI, we delivered lentivirus encoding Nkx6.1 and a red fluorescent protein (RFP) reporter (lenti-Nkx6.1-RFP) ~1 mm rostral and caudal to the injury site (Figure III.1A and Figure III.2A). To control for the effect of lentivirus infection, we delivered a lentivirus encoding only the reporter RFP (lenti-Ctrl-RFP) as a control group (SCI+Ctrl). The successfulness and reproducibility of the lateral hemisection were determined by paralysis in the left hind limb at day-post injury (0 DPI) and 1 DPI. Next, we performed cellular and molecular analysis on spinal cord tissue samples using immunohistochemistry (IHC), RNA-Sequencing (RNA-Seq) (Figure III.3A), quantitative reverse transcription polymerase chain reaction analysis (qPCR) at various stages after SCI (Figure III.1B). We identified top 50 (25 upregulated and 25 downregulated) differentially expressed genes between Nkx6.1 treatment and control treatment (Table III.3). Lentivirus-mediated expression of Nkx6.1 in the spinal cord tissues at 3 days-post injury (DPI) was confirmed by qPCR (Figure III.2B).

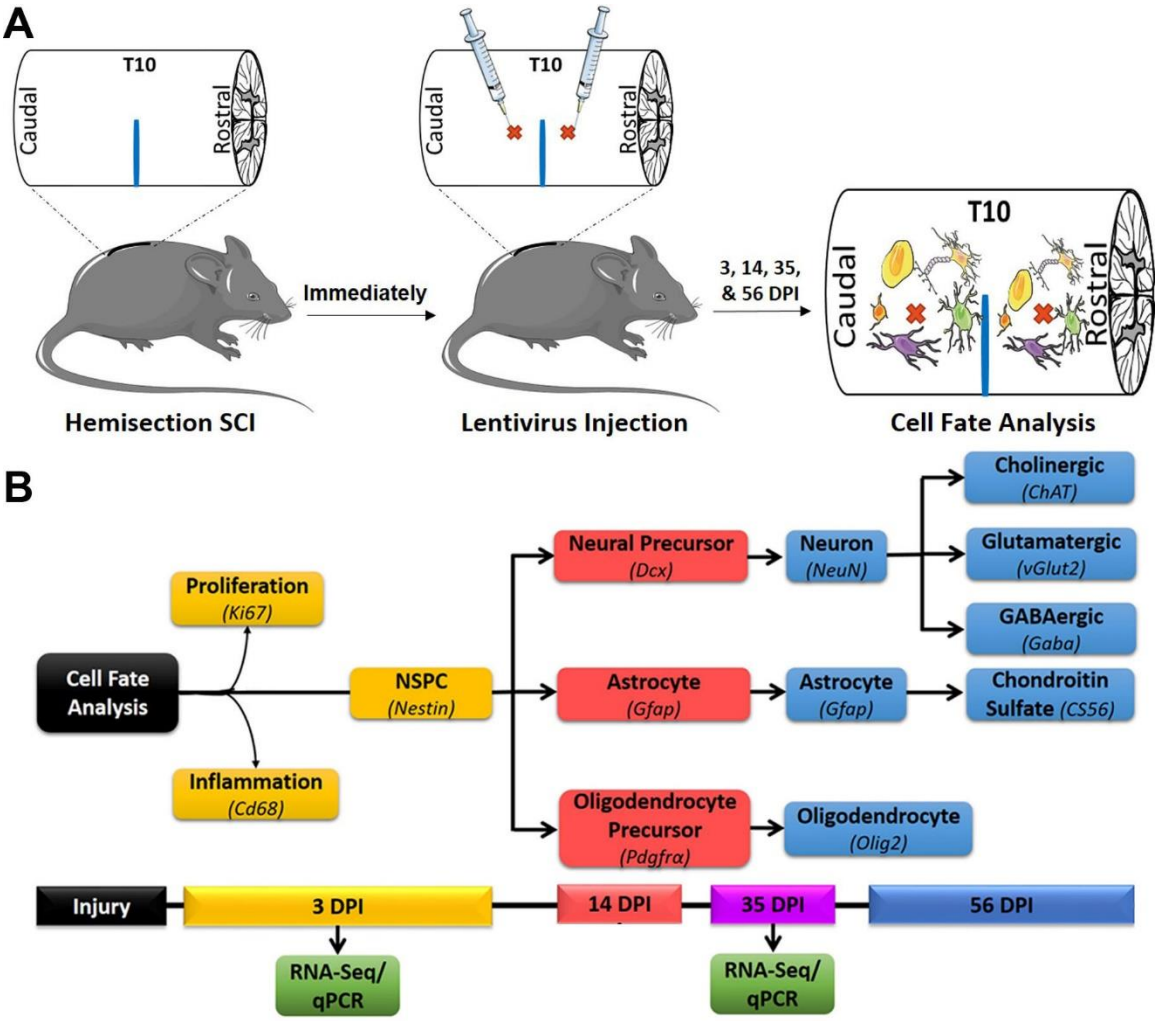

Figure III.1. Experimental Scheme.

*(**A**) Lateral hemisection SCI was performed on 8-12 weeks old mice at the thoracic vertebrae (T10) level followed by injection of lenti-Nkx6.1-RFP virus. Lentivirus encoding only the reporter RFP (lenti-Ctrl-RFP) serves as a control for viral infection. Animals received surgery to only expose the spine (Sham) were used as another control. Spinal cord segments (~5-6 mm) at the injection site were harvested at 3, 14, 35, and 56 DPI to determine cellular and molecular changes using immunohistochemistry (IHC), RNA-Seq, Ingenuity Pathway Analysis (IPA), and quantitative PCR (qPCR). (**B**) Schematic depiction of cell fate analysis following SCI and lentiviral injection. n=3/group/timepoint. DPI = days post injury.*

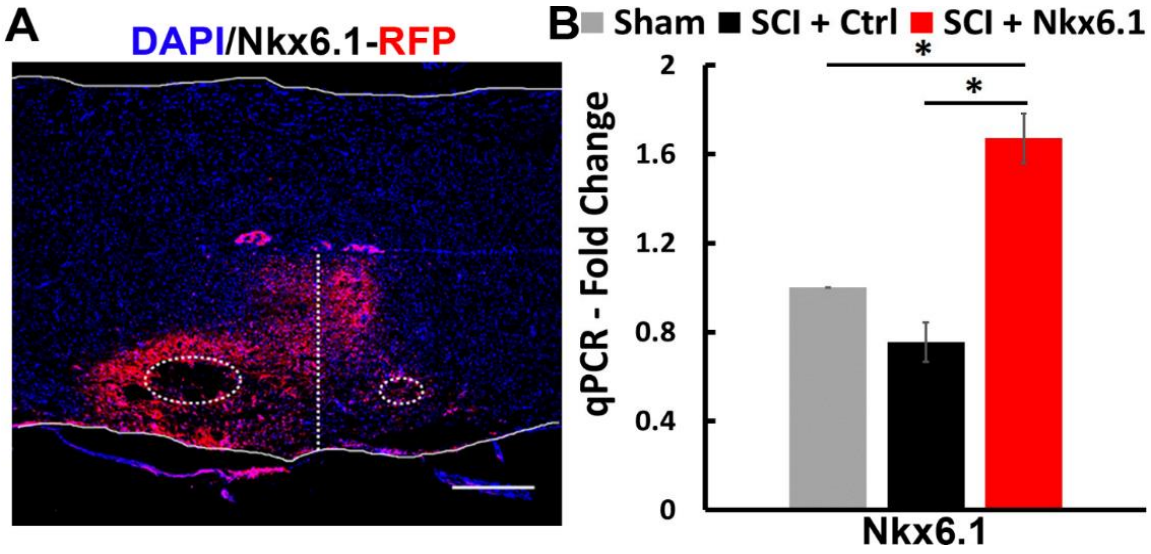

Figure III.2. Lentivirus expresses Nkx6.1 in the injured spinal cord.

*(**A**) Representative image of the injured spinal cord at 3 days post injury (DPI); scale bar = 500 µm. (**B**) RT-qPCR analysis indicating Nkx6.1 mRNA expression at 3 DPI, normalized to the Sham. n = 3/group; Mean ± SEM; * = p < 0.05; One-way ANOVA and Tukey post-hoc analysis.*

A

Time	SCI+Ctrl	SCI+Nkx6.1
3 DPI	n = 3	n = 3
35 DPI	n = 4	n = 3

B

	Differentially Expressed Genes (DEGs)		
	Total	Upregulated	Downregulated
3 DPI	3425	1749	1676
35 DPI	1973	699	1274

Figure III.3. Summary of RNA-Seq analysis.

*(**A**) Number of biological replicates used for each group (SCI+Ctrl and SCI+Nkx6.1) at 3 DPI and 35 DPI for RNA-Seq analysis. (**B**) Total number of differentially expressed genes (DEGs) that are upregulated and downregulated at 3 DPI and 35 DPI.*

3 DPI				35 DPI			
ID	Log2(Fold Change)	ID	Log2(Fold Change)	ID	Log2(Fold Change)	ID	Log2(Fold Change)
Col28a1	-2.5802	Plin4	1.8317	Clec4d	-1.7117	Hoxc13	1.4504
Ogn	-2.5055	Gdf15	1.8034	Cilp2	-1.4861	H2-Bl	1.2597
Ddn	-2.3369	Tmem52	1.8024	Atp6v0d2	-1.4396	Hoxd10	1.1292
Msln	-2.3253	AI506816	1.7968	Tlr8	-1.3987	Gramd2	1.0526
Slc13a4	-2.3043	Nxpe5	1.6645	Cd244	-1.3880	Hoxd11	1.0326
Cxcl11	-2.1156	A130077B15Rik	1.6490	Fam180a	-1.3823	4932441J04Rik	0.9998
Prx	-2.1147	Tmem82	1.5617	Itih2	-1.3823	Hoxa11	0.9935
Plekha4	-2.0711	Tlr1	1.5557	Msr1	-1.3819	Ckm	0.9796
Mpzl2	-2.0204	Hfe	1.5230	Sfrp4	-1.3742	Hoxd13	0.9525
Sostdc1	-1.9841	Fcrls	1.4835	Gpnmb	-1.3375	Dcstamp	0.9443
Pmp2	-1.9189	Galr3	1.4747	Wfdc17	-1.3371	Tecrl	0.9106
Slc6a13	-1.9143	Gm15708	1.4732	Trabd2b	-1.3312	9330175M20Rik	0.8743
Wnt6	-1.8900	G530011O06Rik	1.4513	Crabp2	-1.3300	Myh4	0.8669
Cdh1	-1.8632	Cd300a	1.4483	Dpp4	-1.3283	Ttc34	0.8662
Cldn19	-1.8135	Serpina3m	1.4410	Atp6v0a4	-1.3233	Avpr1a	0.8601
Ncmap	-1.7948	Lyz2	1.4349	Omd	-1.3175	Syt17	0.8554
Wif1	-1.7821	Lrrc25	1.4285	Twist1	-1.3114	Ppef1	0.8486
Sfrp4	-1.7721	Tcf23	1.3992	C2	-1.3094	Lrrc6	0.8287
Slc5a11	-1.7377	Kynu	1.3989	Anpep	-1.3049	Rad21l	0.8205
Osr1	-1.7377	B3gnt3	1.3895	Thbd	-1.3001	Foxr2	0.8175
Spon2	-1.689213	Gja5	1.38634	Mrc2	-1.299603	Hotair	0.816476
Smoc2	-1.669375	Serpina3j	1.383739	Cd5l	-1.298284	Irs4	0.812557
Pcdhb8	-1.64441	Stab1	1.381295	Stra6	-1.2977	Capn11	0.809789
Wnt4	-1.639732	Gm7173	1.374186	Mcoln3	-1.274189	Fam183b	0.805652
Mlip	-1.620607	Wdfy4	1.371852	Emilin1	-1.267752	Lhx2	0.797442

Table III.3. Top 50 differentially expressed genes.

Top 25 significantly ($p<0.05$) expressed upregulated (red) and top 25 downregulated (green) genes determined by RNA-Seq analysis from SCI+Ctrl and SC+Nkx6.1 treatment at 3 DPI and 35 DPI. $n\geq3$/group.

III.4.1. Nkx6.1 enhances cell proliferation during the acute phase of SCI

We first examined the effect of Nkx6.1 on cell proliferation via IHC using a proliferation marker Ki67 on sagittal sections of the spinal cord tissue samples in the following control and experimental groups: Sham (exposing the spine but no SCI; n=3), SCI+Ctrl (n=3), and SCI+Nkx6.1 (n=3) at 3 DPI (Figure III.4A). The number of $Ki67^+$ cells in the Sham group indicates the baseline level of proliferative cells in the adult spinal cord. We determined the percentage of $Ki67^+$ cells among the total number of cells ($DAPI^+$) (Figure III.4B) and among the virally transduced (RFP^+) cells (Figure III.4C) around the injury and injection site. Compared to the Sham group, we observed a significant increase in the percentage of $Ki67^+$ cells in the two injury groups (SCI+Ctrl and SCI+Nkx6.1), with the highest percentage of $Ki67^+$ cells in the SCI+Nkx6.1 group (Figure III.4B). Among the virally transduced cells, lenti-Nkx6.1 treatment leads to a significant increase in the percentage of $Ki67^+/RFP^+$ cells compared to the lenti-Ctrl treatment (Figure III.4C). The upregulation in cell proliferation was validated by measuring the mRNA level of Ki67 via qPCR analysis (Figure III.4D).

To identify Nkx6.1-induced key pathways affecting cell proliferation, we performed RNA-Seq analysis and identified 3425 genes that were differentially expressed ($p<0.05$) between the SCI+Ctrl (n=3) and SCI+Nkx6.1 (n=3) groups at 3 DPI (Figure III.3B, Figure III.5, Figure III.6). Ingenuity Pathway Analysis (IPA) revealed that Nkx6.1 treatment upregulated the Rac signaling pathway (Figure III.4E). Rac1 in the Rac signaling pathway plays role in stem cell proliferation and deletion of Rac1 leads to enhanced cell-cycle exits and reduction in self-renewal [122, 123]. Additionally, we identified an increase in the expression of genes associated with nerve growth factor (NGF) signaling (e.g., Pik3r5, Shc1, Rap1b), which are important in the proliferation of neuroepithelial cells [124, 125] (Figure III.4F). These results suggest that Nkx6.1 treatment promotes cell proliferation in

the injured spinal cord. Furthermore, we found attenuation of neuroinflammation due to the Nkx6.1 treatment compared to control treatment (Figure III.7).

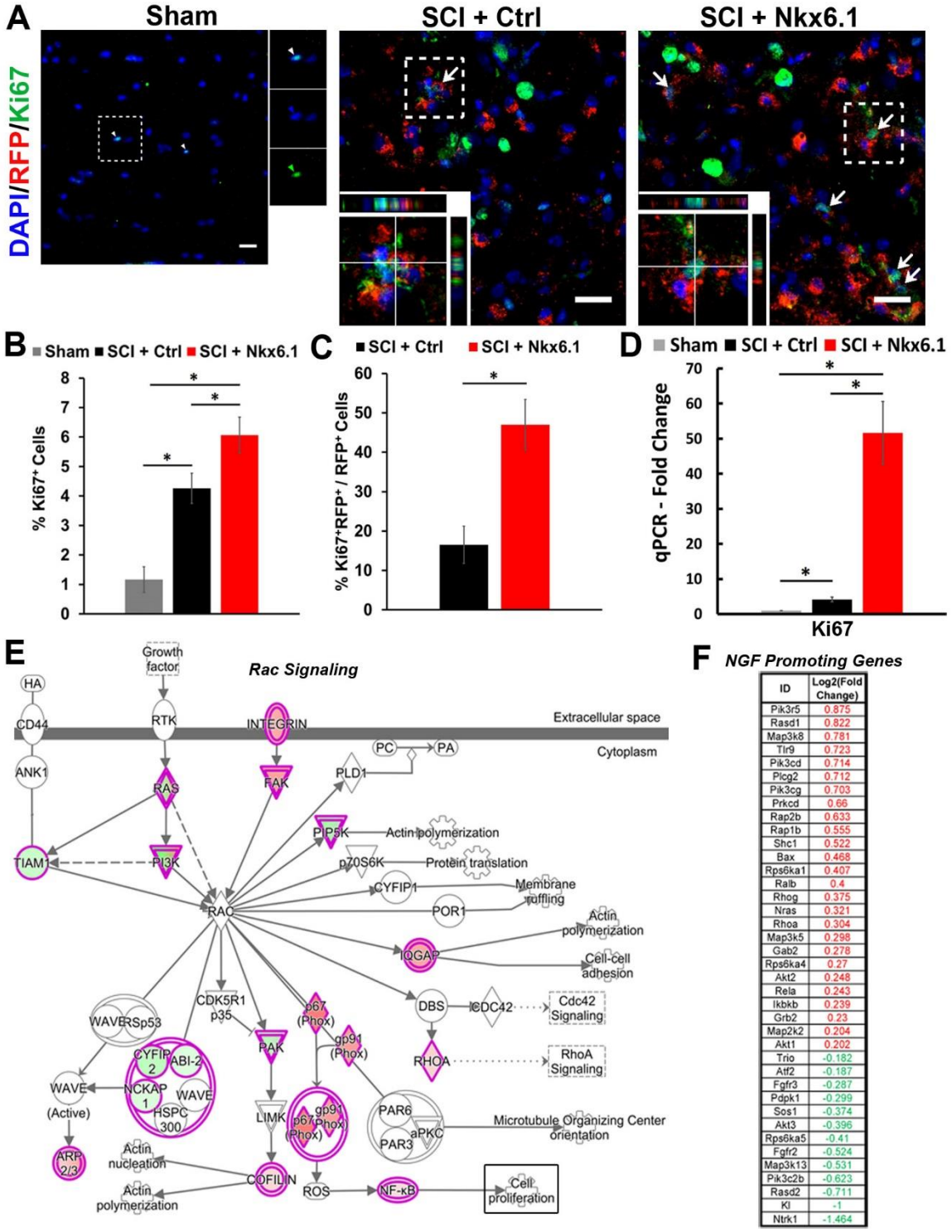

ID	Log2(Fold Change)
Pik3r5	0.875
Rasd1	0.822
Map3k8	0.781
Tlr9	0.723
Pik3cd	0.714
Plcg2	0.712
Pik3cg	0.703
Prkcd	0.66
Rap2b	0.633
Rap1b	0.555
Shc1	0.522
Bax	0.468
Rps6ka1	0.407
Ralb	0.4
Rhog	0.375
Nras	0.321
Rhoa	0.304
Map3k5	0.298
Gab2	0.278
Rps6ka4	0.27
Akt2	0.248
Rela	0.243
Ikbkb	0.239
Grb2	0.23
Map2k2	0.204
Akt1	0.202
Trio	-0.182
Atf2	-0.187
Fgfr3	-0.287
Pdpk1	-0.299
Sos1	-0.374
Akt3	-0.396
Rps6ka5	-0.41
Fgfr2	-0.524
Map3k13	-0.531
Pik3c2b	-0.623
Rasd2	-0.711
Kl	-1
Ntrk1	-1.464

Figure III.4. Nkx6.1 increases cell proliferation in the injured spinal cord.

*Spinal cord tissues were harvested 3 days post injury (3 DPI) and analyzed for proliferation marker, Ki67, using IHC. (**A**) Representative confocal images of the sagittal section around the injection site. Bottom left shows a higher magnification of orthogonal view of the area denoted by a white box. Arrows indicate the co-labeling of the virally transduced cells with Ki67. Scale bar = 20 µm. Quantification of the percentage of $Ki67^+$ cells among $DAPI^+$ cells (**B**) and among RFP^+ cells (**C**). (**D**) qPCR analysis of the mRNA level of Ki67, normalized to the Sham group. (**E**) Nkx6.1-induced upregulation (indicated by pink) in Rac signaling pathway and cell proliferation compared to SCI+Ctrl revealed by RNA-Seq and IPA analysis. (**F**) A list of differentially expressed genes known to promote nerve growth factor (NGF) signaling in the SCI+Nkx6.1 group compared to the SCI+Ctrl group. n = 3/group for IHC, RNA-Seq, and qPCR. Mean±SEM; One-way ANOVA followed by Tukey post-hoc test or Student's t-test and Student's t-test.*

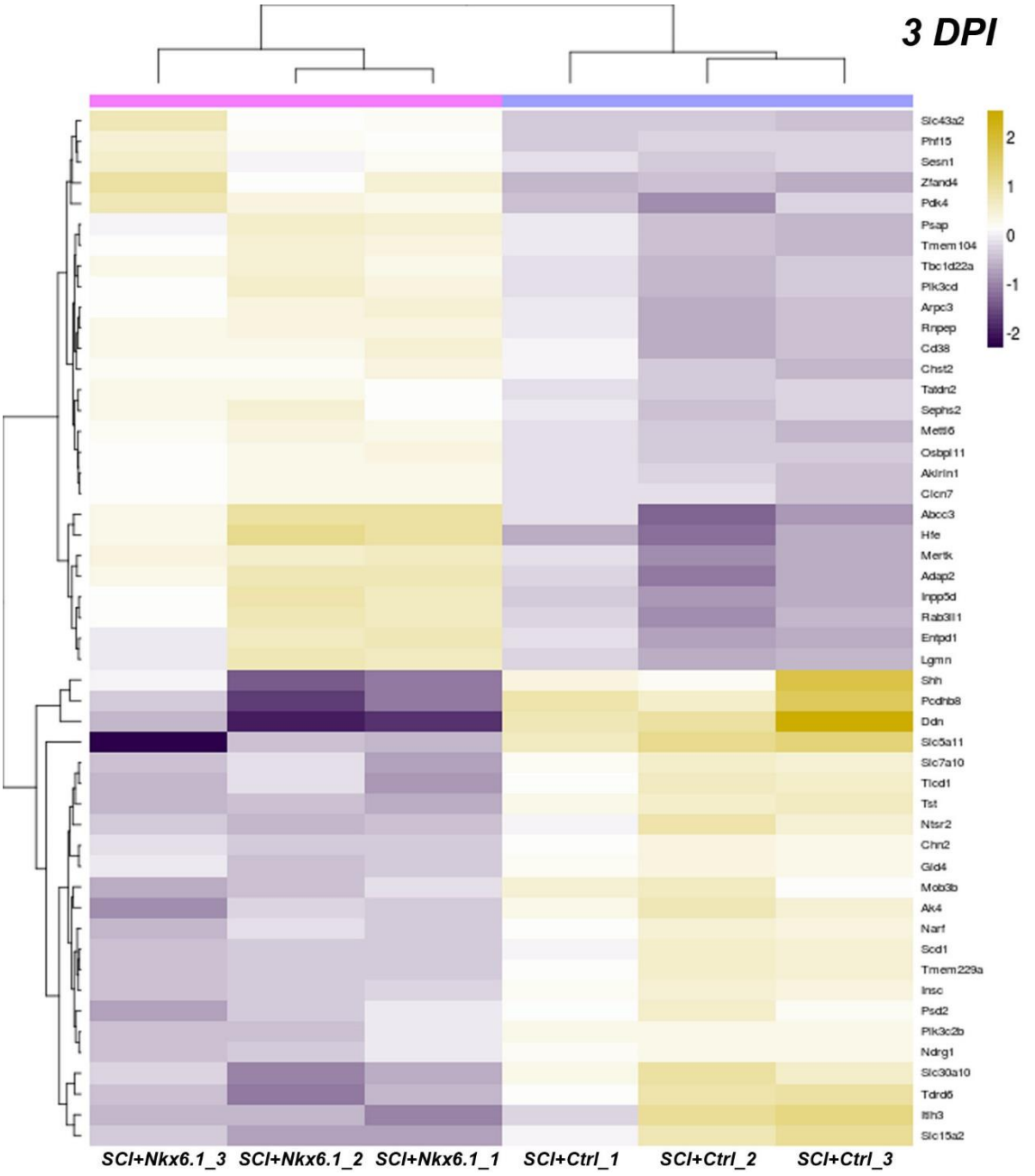

Figure III.5. Top 50 differentially expressed genes at 3 DPI.

Heat map generated by START (https://kcvi.shinyapps.io/START/) of the top 50 DEGs between the SCI+Ctrl and SCI+Nkx6.1 group at 3 DPI. Blue indicates downregulation and yellow indicates upregulation of the gene expression; n=3/group.

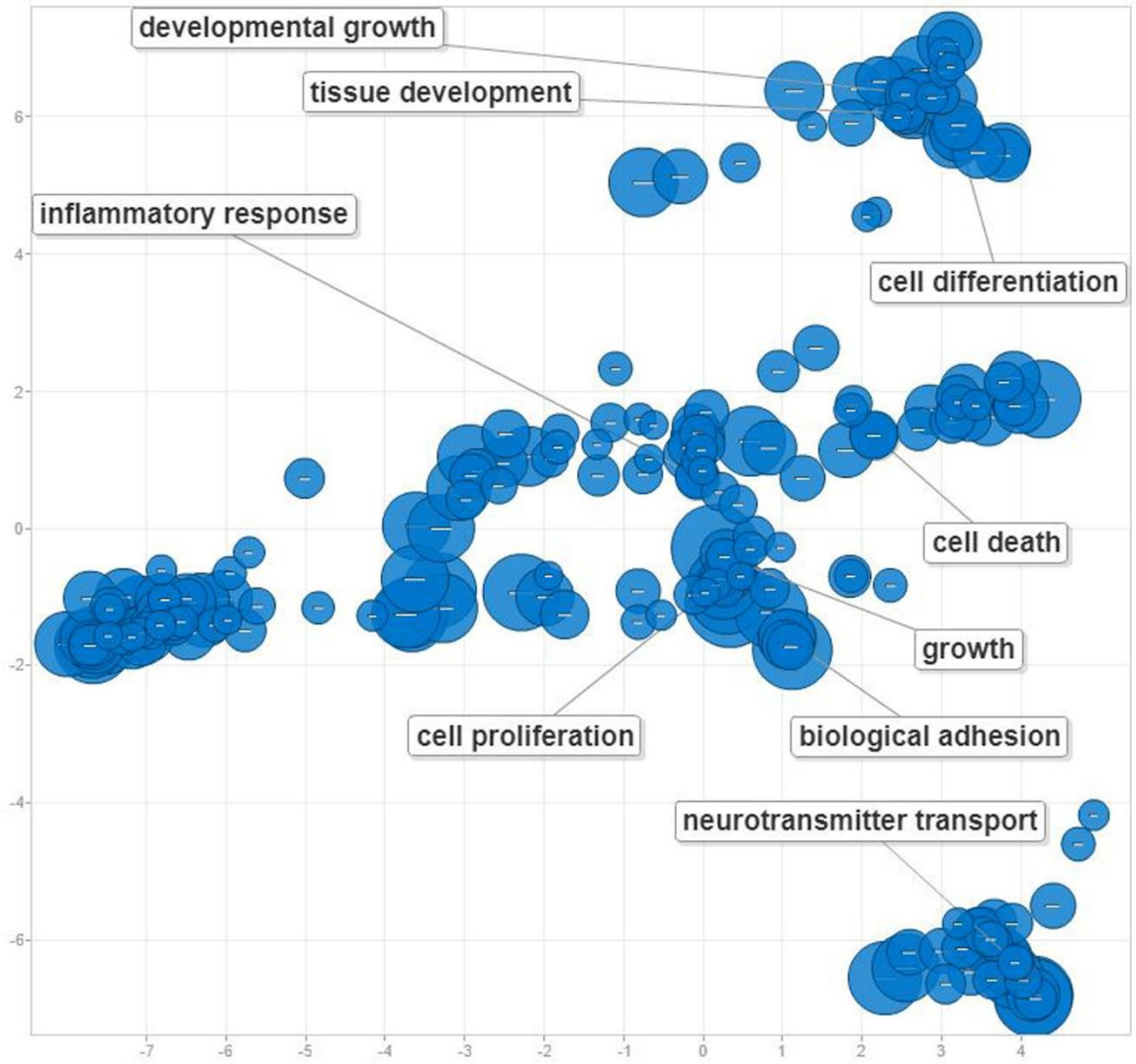

Figure III.6. Enrichment of gene ontology (GO) terms for differentially expressed genes at 3 DPI.

The biological process of the enrichment terms represented as a scatter the plot in a two-dimensional semantic space using REVIGO (http://revigo.irb.hr/) at 3 DPI. Circle size indicates the log10(p-value) of the GO terms.

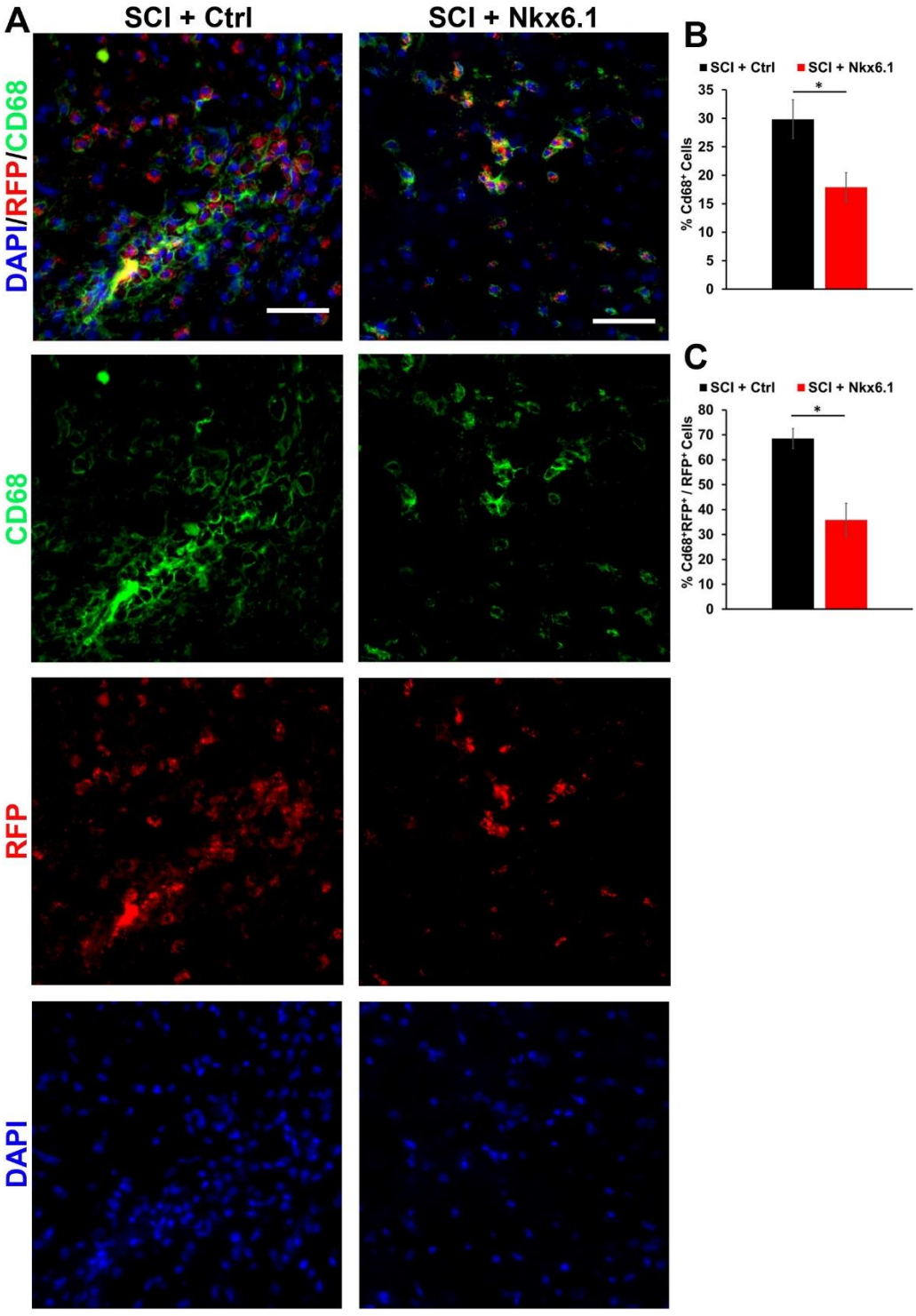

Figure III.7. Nkx6.1 attenuates neuroinflammation after SCI.

*(**A**) Representative image of the sagittal section of spinal cord tissue samples harvested at 3 DPI and analyzed for macrophage marker CD68; scale bar = 50 µm. Quantification*

*of percentage CD68$^+$ cells among the total number of cells (**B**) and among RFP$^+$ cells (**C**) around injury/injection site. n = 3/group. Mean±SEM; Student's t-test.*

III.4.2. Nkx6.1 increases NSPC activation through transient upregulation of Nanog and Notch signaling pathways at the acute phase of SCI

To investigate the effect of Nkx6.1 treatment on the level of NSPC activation after SCI, we conducted IHC analysis using a NSPC marker Nestin on sagittal sections of the spinal cord tissues at 3 DPI (Figure III.8A). An increased number of Nestin$^+$ cells was observed around the injury and injection sites compared to Sham animals, indicating activation of NSPCs after SCI (Figure III.8B). Among the virally transduced cells (RFP$^+$), lenti-Nkx6.1 treatment (n=3) significantly increased the percentage of Nestin$^+$/RFP$^+$ cells among RFP$^+$ cells compared to the lenti-Ctrl treatment (n=3) (Figure III.8C). The increase in the number of Nestin$^+$ cells were validated by measuring the mRNA level of Nestin through qPCR analysis (Figure III.8D).

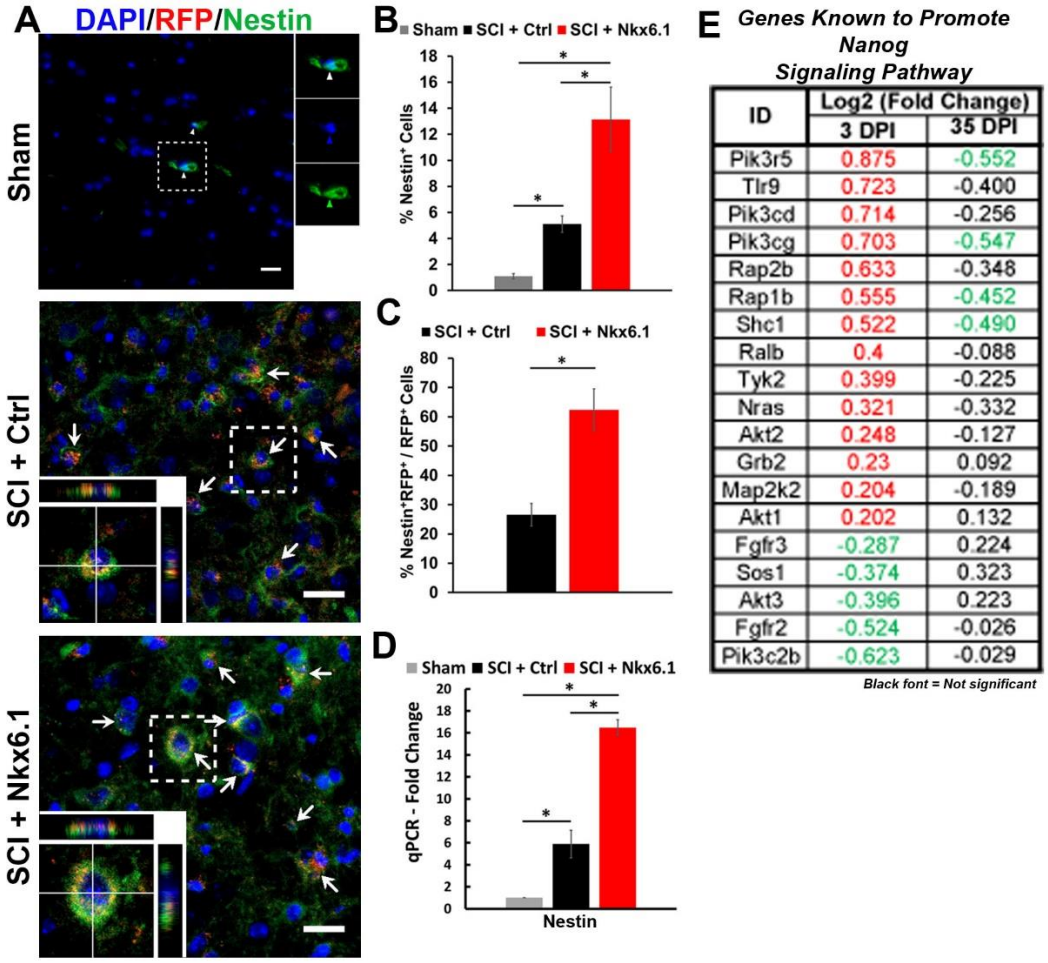

ID	Log2 (Fold Change)	
	3 DPI	35 DPI
Pik3r5	0.875	-0.552
Tlr9	0.723	-0.400
Pik3cd	0.714	-0.256
Pik3cg	0.703	-0.547
Rap2b	0.633	-0.348
Rap1b	0.555	-0.452
Shc1	0.522	-0.490
Ralb	0.4	-0.088
Tyk2	0.399	-0.225
Nras	0.321	-0.332
Akt2	0.248	-0.127
Grb2	0.23	0.092
Map2k2	0.204	-0.189
Akt1	0.202	0.132
Fgfr3	-0.287	0.224
Sos1	-0.374	0.323
Akt3	-0.396	0.223
Fgfr2	-0.524	-0.026
Pik3c2b	-0.623	-0.029

Figure III.8. Nkx6.1 increases NSPC activation in the injured spinal cord.

*Spinal cord tissues were harvested at 3 DPI and analyzed for NSPC marker, Nestin, using IHC. (**A**) Representative confocal images of the sagittal section around injection site. Bottom left shows a higher magnification of orthogonal view of the area denoted by a white box. Arrows indicate the co-labeling of the virally transduced cells with Nestin. Scale bar = 20 µm. Quantification of the percentage of Nestin$^+$ cells among DAPI$^+$ cells (**B**) and Nestin$^+$/RFP$^+$ cells among RFP$^+$ cells (**C**). (**D**) qPCR analysis of the mRNA level of Nestin, normalized to the Sham group. (**E**) A list of differentially expressed genes that are known to promote Nanog signaling pathway identified through RNA-Seq and IPA at 3 DPI and 35 DPI. n = 3/group for IHC, RNA-Seq, and qPCR. Mean±SEM; One-way ANOVA followed by Tukey post-hoc test or Student's t-test.*

To elucidate the mechanism of NSPC activation, we further investigated Nkx6.1-induced signaling pathways via RNA-Seq and IPA analysis. We found that Nkx6.1 treatment (n=3) upregulated genes known to promote Nanog signaling pathways at 3 DPI, and these genes were downregulated at 35 DPI (n≥3/group) (Figure III.8E). It has been shown that spinal cord-derived NSPCs express a number of genes associated with pluripotency, such as Nanog and Oct4 [103, 126, 127]. In addition, we also found an upregulation of genes in the Notch signaling (e.g., Ncstn, Psen1/2, Notch4, Furin, Rbpj) after lenti-Nkx6.1 treatment (n=4) compared to the lenti-Ctrl treatment (n=3) at 3 DPI, an acute phase of SCI (Figure III.9A-B). While in the chronic phase of SCI at 35 DPI, these genes were downregulated (Figure III.9B), indicating the activation of NSPCs occurred only in the acute phase after SCI. The Notch is an essential signaling pathway in maintenance of NSPCs [53]. Ncstn coded protein nicastrin and Psen1/2 are subunits of the γ-secretase complex that cleave and activate Notch receptors. Furin cleaves Notch1 and thus makes it biologically active [128-130]. Rbpj is a DNA-binding protein to Notch intracellular domain (NICD) that translocates the γ-secretase cleaved domain from the cytoplasm to nucleus. Rbpj binds to Notch1 forming a complex to enhance targeted gene expression [131]. We validated the upregulation of the key genes in the Notch signaling pathway (e.g., Notch1, Jag1, Jag2) and the downregulation of Delta1 (Del1) with lenti-Nkx6.1 treatment (n=3) compared to lenti-Ctrl treatment (n=3) via qPCR at 3DPI (Figure III.9C). The upregulation in Notch1 protein expression was confirmed by staining with anti-Notch1 antibody (Figure III.9D). An increase in the percentage of $Notch1^{+}$ cells among the RFP^{+} cells was observed in the lenti-Nkx6.1 treatment compared to the lenti-Ctrl treatment (Figure III.9E). These results reveal that Nkx6.1 promotes NSPC activation through transient upregulation of Nanog and Notch signaling pathways during the acute phase of SCI.

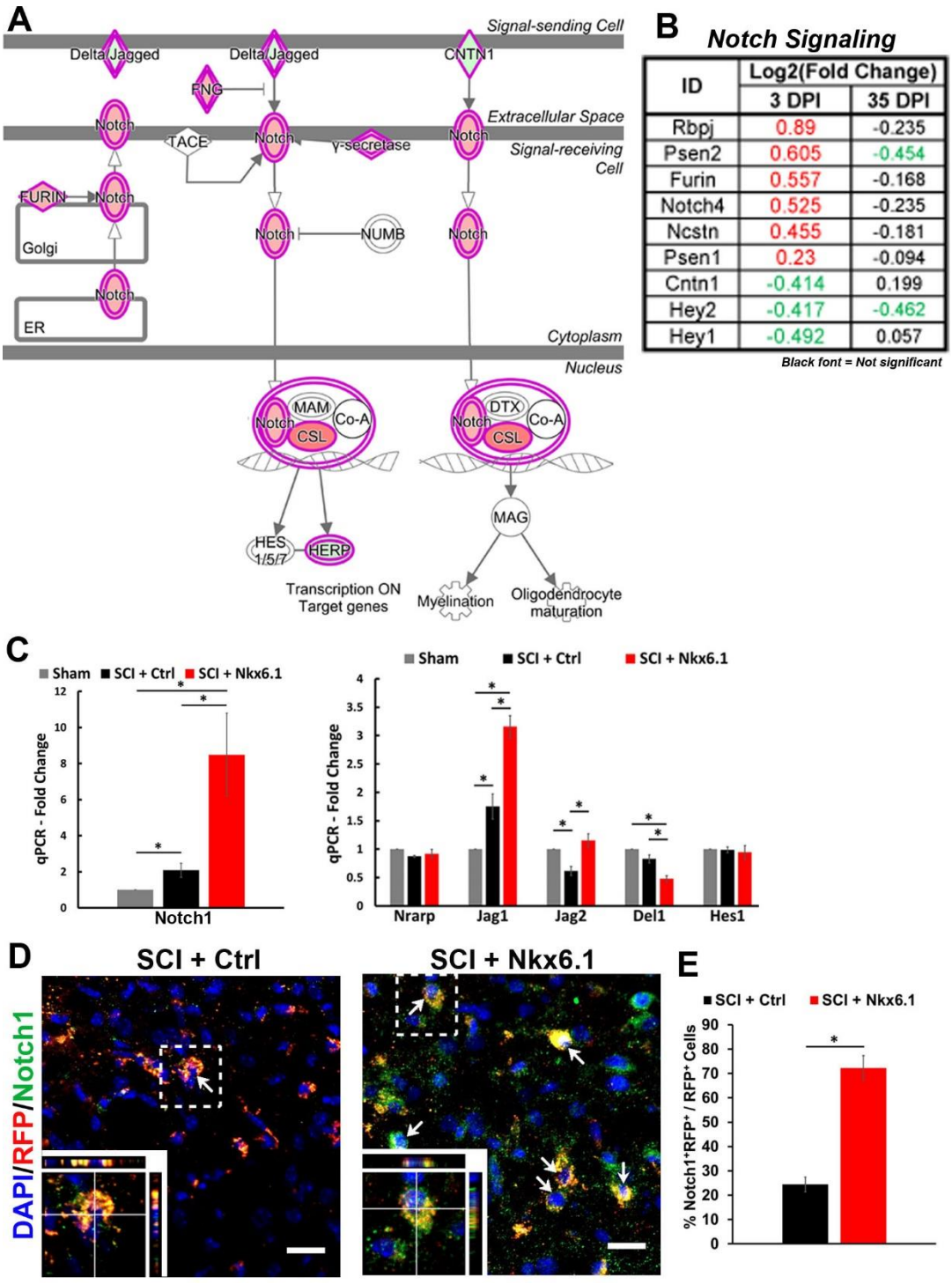

Figure III.9. Nkx6.1 transiently upregulates Notch signaling pathway at the acute phase of SCI.

*RNA-Seq and IPA analysis were performed on spinal cord tissue samples at 3 DPI (n=3/group) and 35 DPI (n≥3/group). (**A**) Nkx6.1-induced upregulation (indicated by pink)*

*in Notch signaling pathway compared to SCI+Ctrl. (**B**) A list of differentially expressed genes associated with Notch signaling pathway along with their log2(fold change) at 3 DPI and 35 DPI. (**C**) qPCR analysis of genes (Notch1, Nrarp, Jag1, Jag2, Del1, and Hes1) involved in the Notch signaling pathway, normalized to the Sham group. Representative confocal images (**D**) and quantification of the percentage of Notch1$^+$ cells among RFP$^+$ cells (**E**) at 3 DPI. Bottom left shows a higher magnification of orthogonal view of the area denoted by a white box. Arrows indicate the co-labeling of the virally transduced (RFP$^+$) cells with Notch1$^+$ cell; Scale bar = 20 μm; n = 3. Mean±SEM; One-way ANOVA followed by Tukey post-hoc test and Student's t-test.*

III.4.3. Nkx6.1 induces neurogenesis at the chronic phase of SCI

Injury-activated NSPCs predominately differentiate into astrocytes and oligodendrocytes, with only a small percentage that differentiate into neurons [19, 20, 31, 68-70]. To determine the fate of activated NSPCs after Nkx6.1 treatment, we performed IHC on spinal cord tissue samples at 14 DPI with an early neuronal progenitor/neuroblast marker doublecortin (DCX) (Figure III.10A), an astrocyte marker, GFAP, (Figure III.10B), and an oligodendrocyte progenitor marker, PDGFRa, (Figure III.10C). Since the majority (> 60%) of virally transduced (RFP$^+$) cells are expressing NSPC markers Nestin and/or Notch1 with the Nkx6.1 treatment, we tracked the fate of RFP$^+$ cells for fate analysis of NSPC at chronic stages. Compared to the lenti-Ctrl treatment (n=3), the lenti-Nkx6.1 treatment (n=3) significantly increased the DCX$^+$/RFP$^+$ cells and PDGFRa$^+$/RFP$^+$ cells among RFP$^+$ cells (Figure III.10D). Furthermore, some of the DCX$^+$ cells after Nkx6.1 treatment started to show small multipolar processes, a typical immature neuronal morphology (Figure III.10A). The percentage of GFAP$^+$/RFP$^+$ cells was found similar and decreased in PDGFRa$^+$/RFP$^+$ cells in the Nkx6.1 treatment and the Ctrl treatment (Figure III.10D). We analyzed the gene ontology of differentially expressed genes at 35 DPI betwee control

and Nkx6.1 treatment (Figure III.11), and REVIGO analysis indicates neurons and nervous system development, development of cellular processes, and signal transduction (Figure III.12). Furthermore, an increase in DCX$^+$ cells was also observed at 35 DPI with Nkx6.1 treatment (Figure III.10E). These results suggest that Nkx6.1 promotes NSPC differentiation towards neuronal over oligodendrocyte lineage, with no significant change in astrocyte lineage. The percent of RFP cells co-label with mature oligodendrocyte, marked by anti-Olig2 antibody, are not significantly different between Nkx6.1 and control treatment at 56 DPI (Figure III.13E).

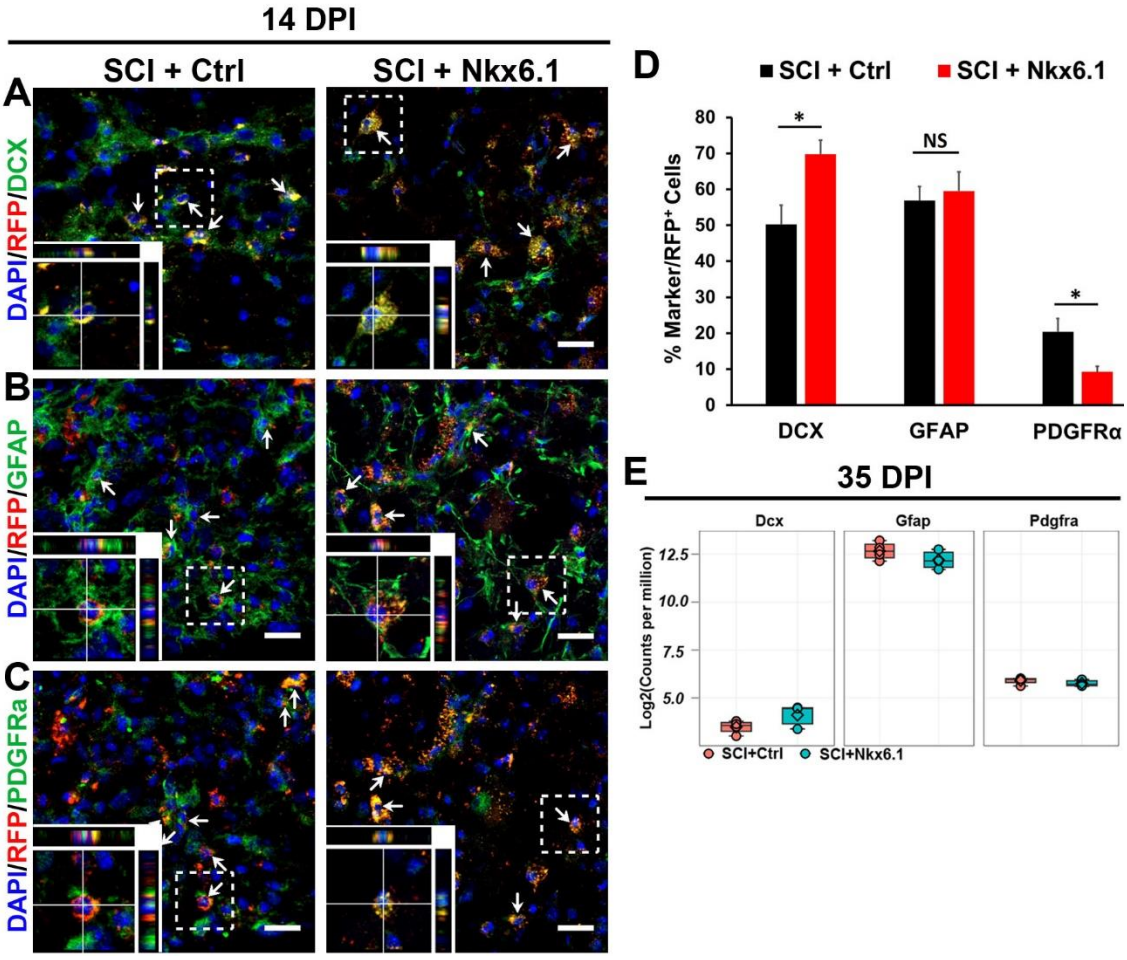

Figure III.10. Nkx6.1 induces neurogenesis in the injured spinal cord.

Representative confocal images of the sagittal section of spinal cord tissue samples harvested at 14 DPI and analyzed for an early neuronal progenitor marker Doublecortin

(DCX) (A), an astrocytic marker GFAP (B), and an oligodendrocyte progenitor marker PDGFRa (C). Bottom left shows a higher magnification of orthogonal view of the area denoted by a white box. Arrows indicate the co-labeling of the virally transduced (RFP+) cells with cell specific marker. Scale bar = 20 µm. (D) Quantification of virally transduced cells co-labeled with cell specific marker; n = 3. (D) Gene expression box plot of DCX, GFAP, and PDGFRa at 35 DPI between SCI+Ctrl and SCI+Nkx6.1 groups; n ≥ 3. Mean±SEM; Student's t-test.

Figure III.11. Top 50 differentially expressed genes at 35 DPI.

Heat map generated by START (https://kcvi.shinyapps.io/START/) of the top 50 DEGs between the SCI+Ctrl and SCI+Nkx6.1 group at 35 DPI. Blue indicates downregulation and yellow indicates upregulation of the gene expression; n=3 for the SCI+Nkx6.1 group and n=4 for the SCI+Ctrl group

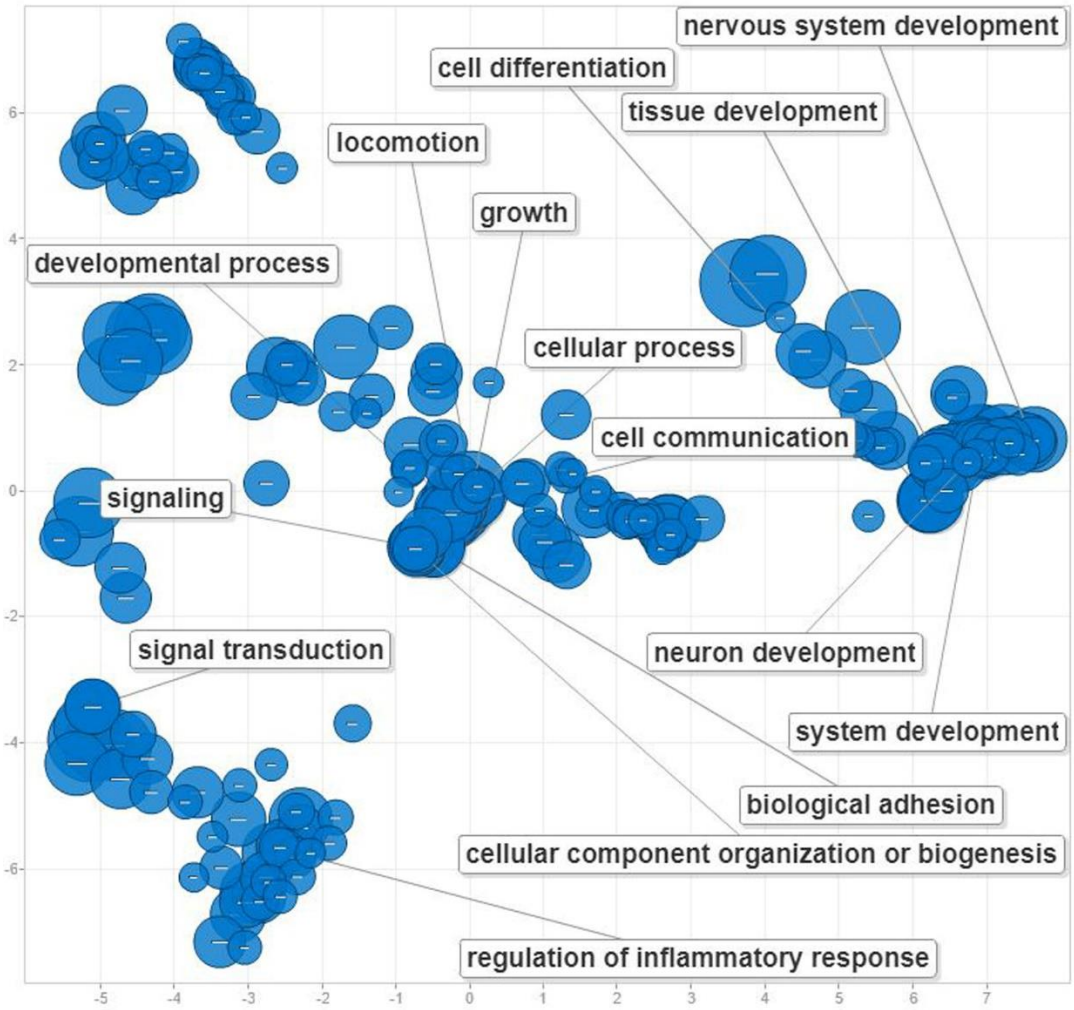

Figure III.12. Enrichment of gene ontology (GO) terms for differentially expressed genes at 35 DPI.

The biological process of the enrichment terms represented as a scatter the plot in a two-dimensional semantic space using REVIGO (http://revigo.irb.hr/) at 35 DPI. Circle size indicates the log10(p-value) of the GO terms.

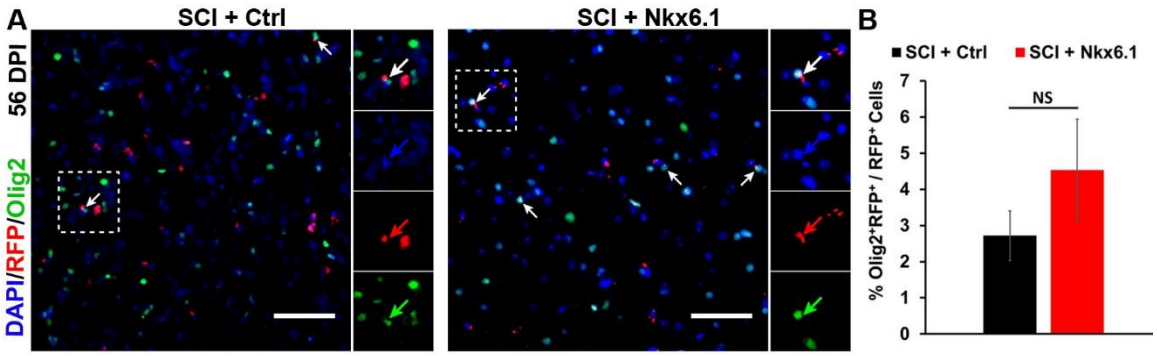

Figure III.13. Nkx6.1 does not change the number of oligodendrocytes after SCI.

*(**A**) Representative images of the sagittal section of spinal cord tissue samples at 56 DPI and analyzed for oligodendrocyte marker Olig2. Arrows in sagittal sections show co-expression and montage on the right of each of the image indicates separate channels for the region within the white box; scale bar = 50 µm. (**B**) Quantification of the percentage Olig2$^+$ cells among RFP$^+$ cells around the injury/injection site. n = 3/group. Mean±SEM; Student's t-test.*

III.4.4. Nkx6.1 promotes the generation of interneurons in the adult injured spinal cord

To further determine which specific subtype of neurons induced by Nkx6.1 treatment, we performed IHC analysis on spinal cord tissue samples at 56 DPI for a mature neuronal marker NeuN (Figure III.14A), a cholinergic neuronal marker Chat (Figure III.14B), a glutamatergic neuronal marker vGlut2 (Figure III.14C), and a GABAergic neuronal marker Gaba (Figure III.14D). Among the RFP$^+$ cells, we found a significant increase in the number of NeuN$^+$ and Chat$^+$ cells, with no significant difference in Gaba$^+$ cells after the lenti-Nkx6.1 treatment compared to the lenti-Ctrl treatment (Figure III.14E). The percentage of vGlut2$^+$/RFP$^+$ cells showed a slight increase but remained not significant (Figure III.14E).

To validate these findings, we performed qPCR analysis to measure the mRNA level of NeuN (Hrnbp3), vGlut (Slc17a6), Th (dopaminergic neuronal marker), Tph1 (serotonergic neuronal marker), and Chat at 35 DPI among the Sham (n=3), SCI+Ctrl (n=3), and SCI+Nkx6.1 (n=3) groups (Figure III.14F). The qPCR analysis indicated a significant upregulation in NeuN, vGlut, and Chat and a significant downregulation of Tph1 after the lenti-Nkx6.1 treatment compared to the lenti-Ctrl treatment (Figure III.14F). Furthermore, there was a slight increase in the mRNA expression of Th (Figure III.14F). From RNA-Seq and IPA analysis between the lenti-Nkx6.1 treatment and lenti-Ctrl treatment at 35 DPI, we identified upregulation of glutamate receptor signaling (Figure III.14G) and Gaba receptor signaling (Figure III.14H). These results indicate that Nkx6.1 promotes cholinergic neurons and decreases in serotonergic neurons after SCI.

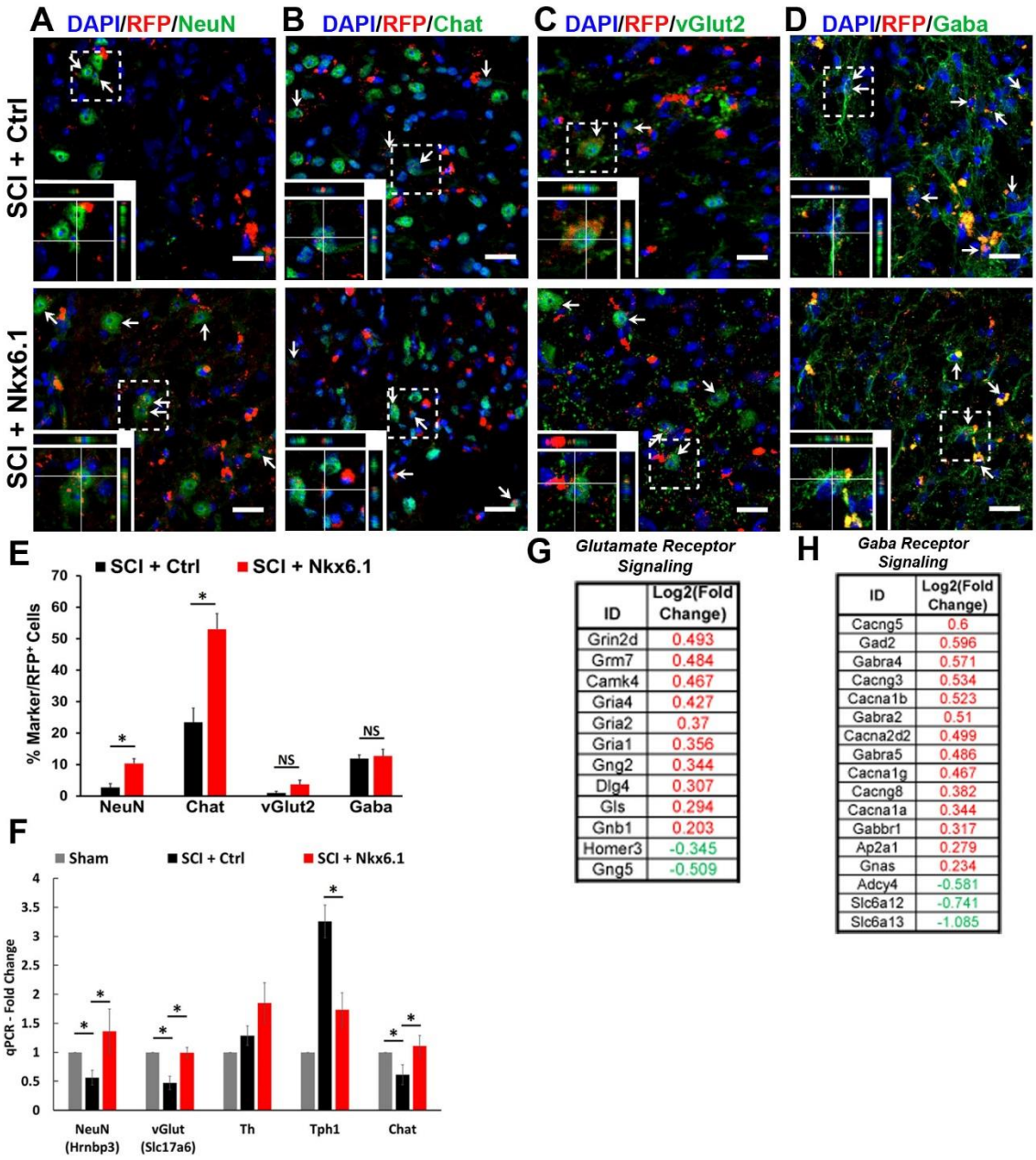

ID	Log2(Fold Change)
Grin2d	0.493
Grm7	0.484
Camk4	0.467
Gria4	0.427
Gria2	0.37
Gria1	0.356
Gng2	0.344
Dlg4	0.307
Gls	0.294
Gnb1	0.203
Homer3	-0.345
Gng5	-0.509

ID	Log2(Fold Change)
Cacng5	0.6
Gad2	0.596
Gabra4	0.571
Cacng3	0.534
Cacna1b	0.523
Gabra2	0.51
Cacna2d2	0.499
Gabra5	0.486
Cacna1g	0.467
Cacng8	0.382
Cacna1a	0.344
Gabbr1	0.317
Ap2a1	0.279
Gnas	0.234
Adcy4	-0.581
Slc6a12	-0.741
Slc6a13	-1.085

Figure III.14. Nkx6.1 induces cholinergic interneurons in the injured spinal cord.

*Representative confocal image of the sagittal section of spinal cord tissue samples harvested at 56 DPI and analyzed for a mature neuron marker NeuN (**A**), a cholinergic neuronal marker Chat (**B**), a glutamatergic neuronal marker vGlut2 (**C**), and a GABAergic neuronal marker Gaba (**D**). Bottom left shows a higher magnification of orthogonal view of the area denoted by a white box (**A**-**D**). Arrows indicate the co-labeling of the virally*

*transduced (RFP$^+$) cells with cell specific marker. Scale bar = 20 µm. (**E**) Quantification of virally transduced cells co-labeled with cell specific marker. (**F**) qPCR analysis of the genes associated with mature neurons and interneurons at 35 DPI. (**G**-**H**) Differentially expressed genes associated with glutamate receptor signaling (**G**) and Gaba receptor signaling (**H**) between the SCI+Ctrl and SCI+Nkx6.1 group identified by RNA-Seq and IPA analysis at 35 DPI. n ≥ 3/group. Mean±SEM; One-way ANOVA followed by Tukey post-hoc test or Student's t-test.*

Neurons need to form axons and synapses to be functional. To determine the ability of neurons to form synapses, we performed RNA-Seq, IPA, and qPCR analysis on spinal cord tissue samples at 35 DPI. We identified upregulation of the genes known to promote synaptogenesis (Figure III.15A) and a downregulation of the genes known to inhibit synaptogenesis (Figure III.15B). Furthermore, Nkx6.1 treatment promoted Netrin signaling, an essential signaling pathway for axon guidance, growth cone formation (Figure III.15C), and calcium signaling (Figure III.15D) at 35 DPI. Furthermore, our qPCR analysis identified an upregulation in the genes involved in synapse formation and axon guidance (e.g., Syn1, Ctnna1, Ntng1, and Col6a2) (Figure III.15E). Overall these results indicate that Nkx6.1 promotes the generation of specific subtypes of neurons, axon guidance, and synapse formation after SCI.

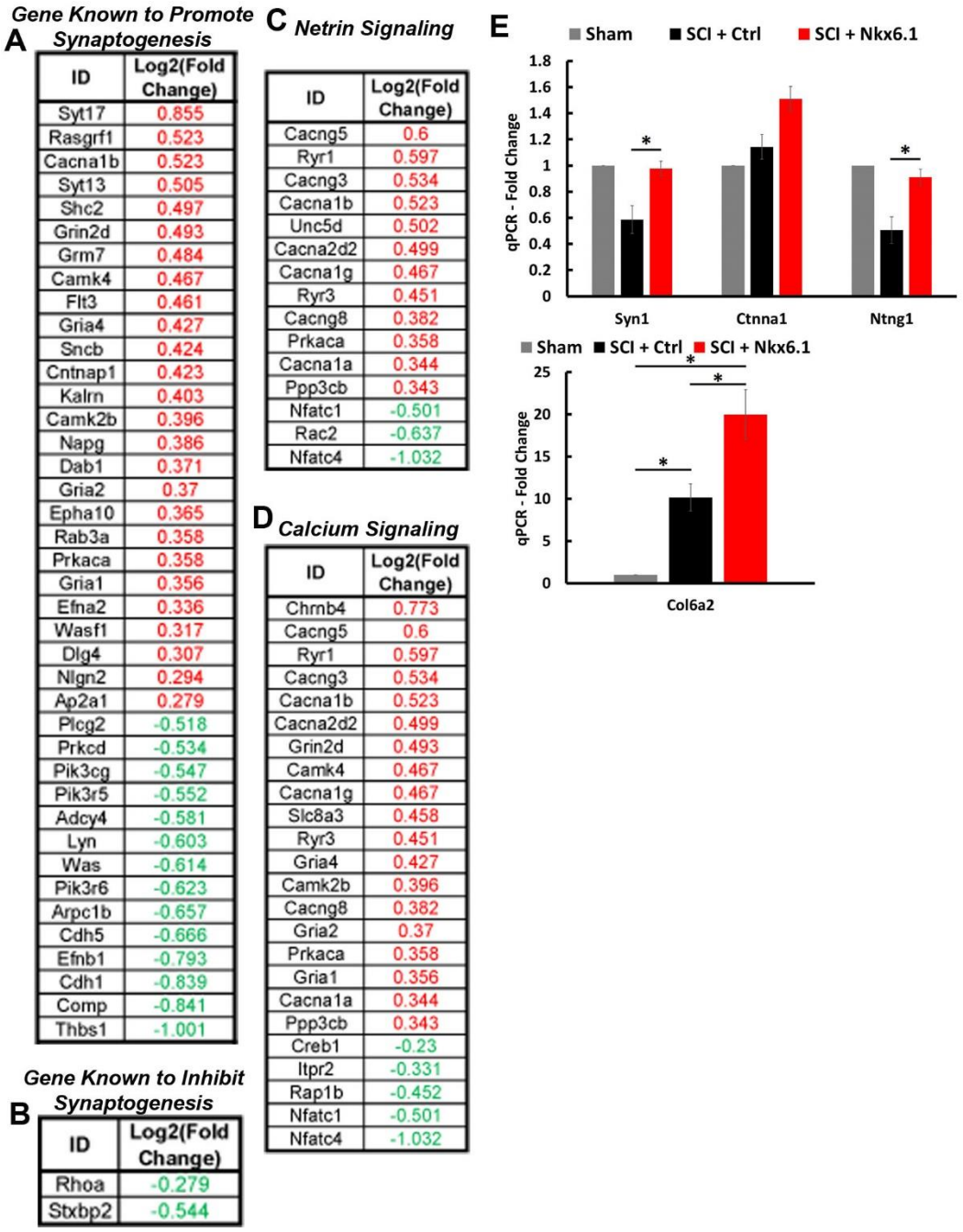

Figure III.15. Nkx6.1 upregulates axon signaling pathway in the injured spinal cord

*RNA-Seq and IPA analysis were performed on spinal cord tissue samples at 35 DPI. A list of differentially expressed genes, along with their expression (log2(fold change)), between the SCI+Ctrl and SCI+Nkx6.1 group that are known to promote (**A**) and inhibit (**B**) synaptogenesis, associated with Netrin signaling (**C**) and calcium signaling (**D**). (**E**) qPCR*

analysis of genes associated with axonal guidance (Syn1, Ctnna1, Ntng1, and Col6a2). n ≥ 3/group. Mean±SEM; One-way ANOVA followed by Tukey post-hoc test.

III.4.5. Nkx6.1 attenuates reactive astrocytes and glial scar formation

SCI activates native astrocytes to become reactive astrocytes (RA), which secrete chondroitin sulfate proteoglycan (CSPG) into the extracellular space [132]. RA and CSPG constitute to the formation of glial scar [133-136]. Glial scar inhibits transpassing axons and thus hindering the axon connections [15, 137, 138]. To determine Nkx6.1 treatment on astrogliosis and glial scar formation, we performed IHC using a RA marker GFAP (Figure III.16A) and a CSPG marker CS56 (Figure III.16B) at 56 DPI. The level of GFAP and CS56 expression in the Sham group established the baseline level of these proteins (Figure III.16A-B). Compared to the Sham, the two injury groups (SCI+Ctrl; n=3 and SCI+Nkx6.1; n=3) showed an increased level of GFAP and CS56 protein expression, with the highest level detected in the SCI+Ctrl group (Figure III.16C-D). However, with the Nkx6.1 treatment, there was a significant decrease in the percentage of area immunostained with GFAP and CS56 (Figure III.16C-D), indicating that Nkx6.1 treatment reduces astrogliosis and glial scar formation. Furthermore, our RNA-Seq analysis at 35 DPI showed a downregulation of the known RA (e.g., Ctnnb1 and Mmp13) [110] and glial scar forming genes (e.g., Il1b, Bmp4, Bmp6, Tgfb1) [139] with the lenti-Nkx6.1 treatment (n=3) compared to the lenti-Ctrl treatment (n=3) (Figure III.16E). Together, these results indicate that Nkx6.1 treatment inhibits RA and glial scar formation after SCI.

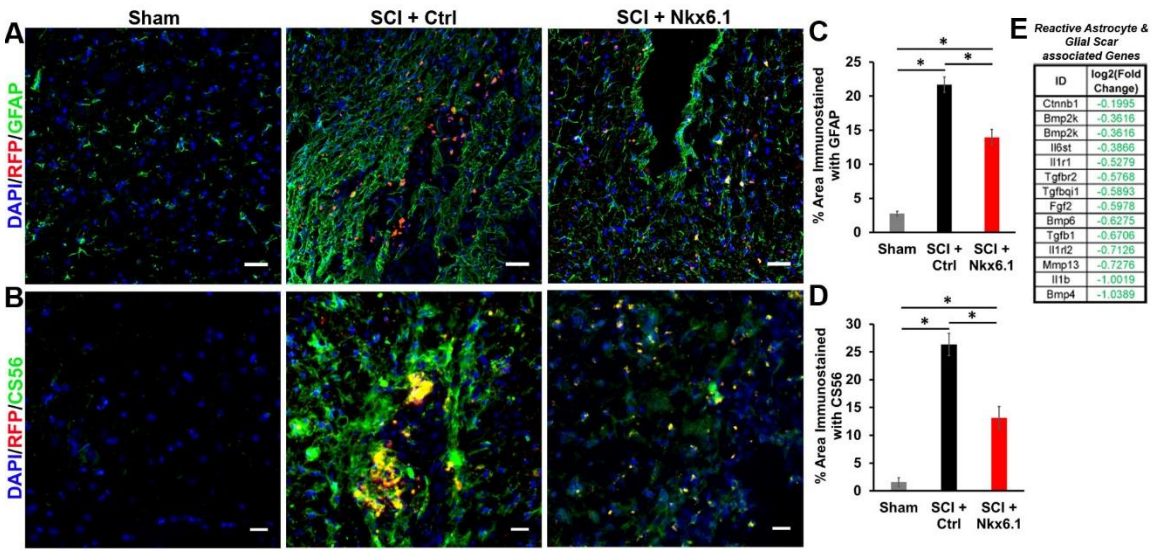

Figure III.16. Nkx6.1 attenuates the glial scar in the injured spinal cord.

*Representative confocal images of the sagittal section of spinal cord tissue samples at 56 DPI and analyzed for reactive astrocyte marker GFAP (**A**) and chondroitin sulfate proteoglycan (CSPG) marker CS56 (**B**). Quantification of the area immunostained with anti-GFAP (**C**) and anti-CS56 (**D**). (**E**) A list of differentially expressed genes and their log2(fold change) by RNA-Seq analysis between the SCI+Ctrl and SCI+Nkx6.1 group that are associated with reactive astrocyte (RA) and glial scar at 35 DPI. n ≥ 3. Mean±SEM; One-way ANOVA followed by Tukey post-hoc test.*

III.5. Discussion

Scar formation and the lack of neurogenesis are the two major issues that prevent tissue regeneration after SCI. In this study, using a lateral hemisection SCI model, we demonstrated that lentivirus-mediated Nkx6.1 gene delivery promotes cell proliferation (Figure III.4) and activation of endogenous NSPC (Figures III.8) by transient upregulation of Notch and Nanog signaling pathways (Figure III.9). Nkx6.1 expression promotes the generation of cholinergic neurons (Figure III.10, III.14, III.15) and attenuation of glial scar

formation (Figure III.16), which correlate well with the expression changes of genes involved in reactive astrocytes, synapse formation and axon growth.

Previous studies have shown that Nkx6.1 regulates Notch signaling during development of the spinal cord [54]. The Notch signaling pathway is known to play an essential role in stem cell self-renewal [117, 118]. It also actively functions in the post-injury neural regeneration by regulating spontaneous cell proliferation, neurogenesis, synapse formation, and axon remyelination [120, 140, 141]. Nanog signaling is another important pathway in stem cells. Nanog is expressed in the embryonic stem cells and plays an important role in self-renewal [142-144]. Nanog expression also found in NSPCs [126, 127]. A recent study showed that Nanog regulates the astrocyte cell proliferation after SCI, by interacting with cell-cycle protein CDK6 [145]. Our findings reveal that Nkx6.1 overexpression in the adult injured spinal cord upregulates key molecules in the Notch signaling pathway (e.g., Notch1, Notch4, Jag1, Rbpj) and Nanog signaling (e.g., Pik3r5, Tlr9, Pik3cd) (Figures III.8, III.9). Nkx6.1-induced activation of Notch and Nanog signaling pathways was in the acute phase of SCI, which leads to the expansion of endogenous NSPCs. This is consistent with the observation that Nkx6.1 increases the number of $Nestin^{+}$ NSPCs in the injured spinal cord (Figure III.8). In the chronic phase, Nkx6.1 expression increased the number of neurons (Figure III.10, III.14, III.15). Therefore, Nkx6.1 is a promising therapeutic gene for the treatment of SCI and other neurological diseases where regeneration of neurons are needed [146-148].

It is intriguing that Nkx6.1 reduces the reactive astrocytes and glial scar formation (Figure III.16). This is likely due to Nkx6.1 function in promoting NSPCs to differentiate into neurons at the expense of astroglial lineage. In support of this notion, we observed that Nkx6.1 promotes the generation of neurons (Figure III.14) and inhibition of astrocytes

(Figure III.16). In addition, it has been shown that Nkx6.1 affects differentiation of neuroepithelial cells into astrocyte precursors in the ventral spinal cord [59].

Previous studies have shown that ectopic expression of Nkx6.1 in native astrocytes ($GFAP^+$) failed to induce their conversion into neurons [32], suggesting Nkx6.1 may not be a potential factor for cell lineage reprogramming. In contrast, overexpression of Nkx6.1 in NSPCs induces neurogenesis (Figure III.10) and increases the number of cholinergic neurons (Figure III.14), supporting Nkx6.1 functions in cell fate choice and differentiation of NSPCs.

Major barriers for repair and regeneration after SCI also includes inflammatory response and the glial scar formation [109, 149, 150]. Glial scars form mechanical and chemical barriers for tissue repair and regeneration after SCI [109, 151]. Studies have shown that reducing the glial scar induces functional recovery. In this study, along with neurogenesis, we show the ability of Nkx6.1 in attenuating glial scar by downregulating RA [110] and CSPG (Figure III.16).

In summary, we demonstrate that the spinal cord neurogenic factor Nkx6.1 is able to reduce astroglial scar and induce neurogenesis to increase the number of cholinergic neurons in the injured spinal cord. This study provides evidence that Nkx6.1 might be a potential therapeutic target for SCI and other central nervous system related injuries.

III.6. Acknowledgements

We thank the Cai lab members for constructive comments and discussion. Dr. Kelvin Kwan and his lab for advice for lentivirus production. We would like to thank Dr. KiBum Lee and his lab for advice on qPCR analysis. This work was supported by the State of

New Jersey Commission on Spinal Cord Research 15IRG006 (L.C.). M.P. is a recipient of the U.S. Department of Education GAANN Precision and Personalized Medicine Pre-Doctoral Training Fellowship and NIH Biotechnology Pre-Doctoral Training Fellowship T32GM008339.

Chapter IV. Discussion

SCI results in physical disability and mental and economical burden to the patients. Primary phase of SCI occurs as a cause of an insult to the spinal cord, and it is only preventable. Primary SCI leads to acute to chronic injury in secondary phase of SCI, involving inflammation, neuronal cell death, glial scar formation, and loss of locomotor function. Currently there is no effective therapeutics for the treatment of SCI.

Immense challenges in developing treatment of SCI are promoting neurogenesis into specific types of interneurons and inhibiting glial scar. Interneurons are major components of neural circuits, and they enable cells to communicate between sensory and motor neurons. Many research projects are trying to either promote neurogenesis by cell reprogramming with overexpression of neurogenic transcription factors (e.g., Sox2, NeuroD1, and Olig2) in the injured spinal cord [42, 43, 71, 72]. In addition to limitation in neurogenesis, another big challenge in tissue repair and regeneration after SCI is the formation of glial scar. Glial scar is composed of injury activated astrocytes and CSPG. Glial scar forms around the injury site and inhibits axonal sprouting and growth. Many researches are focusing on attenuating glial scar to improve axonal connection and functional recovery in order to treat SCI [27, 73-75].

Since both increase in neurogenesis and attenuation of glial scar are assisting in locomotion recovery and thus treatment of spinal cord injury, we decided to develop a therapeutic treatment that would target both neurogenesis and inhibiting glial scar. Here in this project we focused on two different transcription factors, Gsx1 and Nkx6.1, involved in Notch signaling pathway for developing a treatment of SCI. Notch signaling pathway is one of the key signaling pathway in NSPC activation in CNS. Gsx1 and Nkx6.1 bind to the enhancer region of Notch1 gene, part of Notch signaling pathway, and determine the cell

fate during spinal cord development [54]. Gsx1 is expressed in the ventral region of the spinal cord and is known to control the fates of interneurons [64]. Whereas Nkx6.1 is found in the dorsal region of the spinal cord and is known to control the fate of both neurons and glia [58, 59]. We delivered Gsx1 and Nkx6.1 therapeutics through lentiviral delivery immediately after SCI.

Lentivirus-mediated Gsx1 expression (Chapter II) promotes NSPC activations and cell proliferation in acute stage after SCI. The activated NSPCs increasingly differentiates into immature neurons that matures into glutamatergic and cholinergic neurons. Additionally, with the Gsx1 treatment we see substantial decrease in the reactive astrocytes, scar forming astrocytes, and CSPG thus attenuating glial scar. We hypothesize that increase in glutamatergic and cholinergic neurons and decrease in GABAergic neurons and glial scar leads to significant increase in axon guidance signaling and synaptogenesis, eventually leading to functional recovery.

In comparison to Gsx1 treatment, lentivirus-mediated Nkx6.1 treatment (Chapter III) does not lead to significant improvement in functional locomotion. Even though Nkx6.1 treatment leads to endogenous NSPCs activation and proliferation after spinal cord injury, similar to Gsx1 treatment, activated NSPCs differentiates towards neuronal and astrocyte lineage. Immature neurons in chronic stage differentiate towards cholinergic neurons. Similar to Gsx1 treatment, with Nkx6.1 treatment there was a reduction in some reactive astrocytes and glial scar formation, however the extend of attenuation of glial scar is not as high as in with Gsx1 treatment. This supports our hypothesis regarding neurogenesis into specific types of interneurons and attenuation of glial scar might be essential in gaining functional recovery after SCI.

To understand the molecular mechanism of differential outcomes of Gsx1 and Nkx6.1, we next compared the RNA-Seq results from acute (3 DPI) and chronic (35 DPI) with Gsx1 and Nkx6.1 treatment. Our analysis indicates increase in Wnt signaling pathway, Notch3, and neural growth factor (NGF) expression with Nkx6.1 treatment compared to the Gsx1 treatment after 3 DPI. This indicates increase activation of endogenous NSPCs with Nkx6.1 compared to Gsx1. However, at chronic stage, we identified decrease in cell attachment, cell migration, neuroprotection, and neuron viability with Nkx6.1 treatment compared to control treatment. This indicates that mature neurons are not functional to attach, migrate, and transmit signals. We hypothesize that this might be also one of the factor of not having functional recovery with Nkx6.1 treatment in hemisection SCI models. Although further studies might be needed to fully characterize the transcription factors as potential therapeutics for the treatment of SCI, this analysis indicates huge potential of these two transcription factor in treatment of hemisection SCI in mouse model.

Chapter V. Future Direction

This study laid the ground work for determining Gsx1 and Nkx6.1 as potential therapeutic genes for the treatment of SCI. Since SCI and the other CNS injuries (e.g., traumatic brain injury) or neurodegenerative disease face similar challenges (e.g., limitation of neurogenesis and glial scar formation), this lentiviral-mediated therapeutic approach (Gsx1, Nkx6.1, or combination of both factors) might be applicable for the treatment of CNS injuries and neurodegenerative disease, with some modifications.

In this study we identified the potential of lentivirus-mediated transcription factors (e.g., Gsx1 and Nkx6.1) immediately after the SCI. However, under clinical setting it is very less likely that treatment is delivered immediately after the injury. To make this treatment clinically relevant, the next step of the project is to determine the therapeutic time window where this treatment is effective. If there is any variation in the efficacy of the treatment by delivery not immediately after SCI, then further characterization and better delivery system need to be optimized. Other challenge with this project is the lentiviral based gene delivery. Lentivirus based delivery system are not very clinically relevant models in the current gene therapy market due to their ability to integrate into the genome of both dividing and non-dividing cells. Adeno-associated virus (AAV), recombinant AAV (rAAV) vectors are commonly used gene delivery system for gene therapy products in the market and in clinical testing. The rAAV vectors lacks viral DNA and thus are safer for the gene delivery next generation gene delivery in patients. Other safer approach is to deliver the protein that encodes the gene of interest. However, with protein delivery, there is still more research needs to be performed to optimize the correct location and conjugate peptide for optimal cell penetration.

Although this project identified a novel gene therapeutic for the treatment of the SCI that could overcome SCI related challenges (e.g., neurogenesis and glia scar formation), further studies need to be performed to make Gsx1 treatment more clinically relevant.

Chapter VII. References

1. Benfey M, Aguayo AJ: **Extensive elongation of axons from rat brain into peripheral nerve grafts**. *Nature* 1982, **296**(5853):150-152.
2. David S, Aguayo AJ: **Axonal elongation into peripheral nervous system "bridges" after central nervous system injury in adult rats**. *Science* 1981, **214**(4523):931-933.
3. Richardson PM, Issa VM, Aguayo AJ: **Regeneration of long spinal axons in the rat**. *J Neurocytol* 1984, **13**(1):165-182.
4. Richardson PM, McGuinness UM, Aguayo AJ: **Axons from CNS neurons regenerate into PNS grafts**. *Nature* 1980, **284**(5753):264-265.
5. Hartkopp A, Bronnum-Hansen H, Seidenschnur AM, Biering-Sorensen F: **Survival and cause of death after traumatic spinal cord injury. A long-term epidemiological survey from Denmark**. *Spinal Cord* 1997, **35**(2):76-85.
6. **National Spinal Cord Injury Statistical Center, Facts and Figures at a Glance** 2019.
7. Zhang N, Fang M, Chen H, Gou F, Ding M: **Evaluation of spinal cord injury animal models**. *Neural Regen Res* 2014, **9**(22):2008-2012.
8. Norenberg MD, Smith J, Marcillo A: **The pathology of human spinal cord injury: defining the problems**. *J Neurotrauma* 2004, **21**(4):429-440.
9. Sroga JM, Jones TB, Kigerl KA, McGaughy VM, Popovich PG: **Rats and mice exhibit distinct inflammatory reactions after spinal cord injury**. *J Comp Neurol* 2003, **462**(2):223-240.
10. Zeman RJ, Wen X, Ouyang N, Rocchio R, Shih L, Alfieri A, Moorthy C, Etlinger JD: **Stereotactic radiosurgery improves locomotor recovery after spinal cord injury in rats**. *Neurosurgery* 2008, **63**(5):981-987; discussion 987-988.
11. Basso DM, Fisher LC, Anderson AJ, Jakeman LB, McTigue DM, Popovich PG: **Basso Mouse Scale for locomotion detects differences in recovery after spinal cord injury in five common mouse strains**. *J Neurotrauma* 2006, **23**(5):635-659.
12. Lee JH, Tigchelaar S, Liu J, Stammers AM, Streijger F, Tetzlaff W, Kwon BK: **Lack of neuroprotective effects of simvastatin and minocycline in a model of cervical spinal cord injury**. *Exp Neurol* 2010, **225**(1):219-230.
13. Van Meeteren NL, Eggers R, Lankhorst AJ, Gispen WH, Hamers FP: **Locomotor recovery after spinal cord contusion injury in rats is improved by spontaneous exercise**. *J Neurotrauma* 2003, **20**(10):1029-1037.
14. Kong X, Gao J: **Macrophage polarization: a key event in the secondary phase of acute spinal cord injury**. *J Cell Mol Med* 2017, **21**(5):941-954.
15. O'Shea TM, Burda JE, Sofroniew MV: **Cell biology of spinal cord injury and repair**. *J Clin Invest* 2017, **127**(9):3259-3270.
16. Sofroniew MV: **Dissecting spinal cord regeneration**. *Nature* 2018, **557**(7705):343-350.
17. Tran AP, Warren PM, Silver J: **The Biology of Regeneration Failure and Success After Spinal Cord Injury**. *Physiol Rev* 2018, **98**(2):881-917.
18. Assinck P, Duncan GJ, Hilton BJ, Plemel JR, Tetzlaff W: **Cell transplantation therapy for spinal cord injury**. *Nat Neurosci* 2017, **20**(5):637-647.
19. Barnabe-Heider F, Goritz C, Sabelstrom H, Takebayashi H, Pfrieger FW, Meletis K, Frisen J: **Origin of new glial cells in intact and injured adult spinal cord**. *Cell Stem Cell* 2010, **7**(4):470-482.
20. Meletis K, Barnabe-Heider F, Carlen M, Evergren E, Tomilin N, Shupliakov O, Frisen J: **Spinal cord injury reveals multilineage differentiation of ependymal cells**. *PLoS Biol* 2008, **6**(7):e182.

21. Rusanescu G, Mao J: **Immature spinal cord neurons are dynamic regulators of adult nociceptive sensitivity**. *J Cell Mol Med* 2015, **19**(10):2352-2364.
22. Vessal M, Aycock A, Garton MT, Ciferri M, Darian-Smith C: **Adult neurogenesis in primate and rodent spinal cord: comparing a cervical dorsal rhizotomy with a dorsal column transection**. *Eur J Neurosci* 2007, **26**(10):2777-2794.
23. Vessal M, Darian-Smith C: **Adult neurogenesis occurs in primate sensorimotor cortex following cervical dorsal rhizotomy**. *J Neurosci* 2010, **30**(25):8613-8623.
24. Goritz C, Dias DO, Tomilin N, Barbacid M, Shupliakov O, Frisen J: **A Pericyte Origin of Spinal Cord Scar Tissue**. *Science* 2011, **333**(6039):238-242.
25. Silver J, Schwab ME, Popovich PG: **Central nervous system regenerative failure: role of oligodendrocytes, astrocytes, and microglia**. *Cold Spring Harb Perspect Biol* 2014, **7**(3):a020602.
26. North HA, Pan L, McGuire TL, Brooker S, Kessler JA: **beta1-Integrin alters ependymal stem cell BMP receptor localization and attenuates astrogliosis after spinal cord injury**. *J Neurosci* 2015, **35**(9):3725-3733.
27. Bradbury EJ, Moon LD, Popat RJ, King VR, Bennett GS, Patel PN, Fawcett JW, McMahon SB: **Chondroitinase ABC promotes functional recovery after spinal cord injury**. *Nature* 2002, **416**(6881):636-640.
28. Shen Y, Tenney AP, Busch SA, Horn KP, Cuascut FX, Liu K, He Z, Silver J, Flanagan JG: **PTPsigma is a receptor for chondroitin sulfate proteoglycan, an inhibitor of neural regeneration**. *Science* 2009, **326**(5952):592-596.
29. Agrawal S, Schaffer DV: **In situ stem cell therapy: novel targets, familiar challenges**. *Trends Biotechnol* 2005, **23**(2):78-83.
30. Conti L, Cattaneo E: **Novel and immortalization-based protocols for the generation of neural CNS stem cell lines for gene therapy approaches**. *Methods Mol Biol* 2008, **438**:319-332.
31. Sabelstrom H, Stenudd M, Frisen J: **Neural stem cells in the adult spinal cord**. *Exp Neurol* 2014, **260**:44-49.
32. Matsui T, Akamatsu W, Nakamura M, Okano H: **Regeneration of the damaged central nervous system through reprogramming technology: basic concepts and potential application for cell replacement therapy**. *Exp Neurol* 2014, **260**:12-18.
33. Nishimura S, Yasuda A, Iwai H, Takano M, Kobayashi Y, Nori S, Tsuji O, Fujiyoshi K, Ebise H, Toyama Y *et al*: **Time-dependent changes in the microenvironment of injured spinal cord affects the therapeutic potential of neural stem cell transplantation for spinal cord injury**. *Mol Brain* 2013, **6**:3.
34. Gascon S, Murenu E, Masserdotti G, Ortega F, Russo GL, Petrik D, Deshpande A, Heinrich C, Karow M, Robertson SP *et al*: **Identification and Successful Negotiation of a Metabolic Checkpoint in Direct Neuronal Reprogramming**. *Cell Stem Cell* 2016, **18**(3):396-409.
35. Grande A, Sumiyoshi K, Lopez-Juarez A, Howard J, Sakthivel B, Aronow B, Campbell K, Nakafuku M: **Environmental impact on direct neuronal reprogramming in vivo in the adult brain**. *Nat Commun* 2013, **4**:2373.
36. Guo Z, Zhang L, Wu Z, Chen Y, Wang F, Chen G: **In vivo direct reprogramming of reactive glial cells into functional neurons after brain injury and in an Alzheimer's disease model**. *Cell Stem Cell* 2014, **14**(2):188-202.
37. Heinrich C, Bergami M, Gascon S, Lepier A, Vigano F, Dimou L, Sutor B, Berninger B, Gotz M: **Sox2-mediated conversion of NG2 glia into induced neurons in the injured adult cerebral cortex**. *Stem Cell Reports* 2014, **3**(6):1000-1014.

38. Liu Y, Miao Q, Yuan J, Han S, Zhang P, Li S, Rao Z, Zhao W, Ye Q, Geng J *et al*: **Ascl1 Converts Dorsal Midbrain Astrocytes into Functional Neurons In Vivo**. *J Neurosci* 2015, **35**(25):9336-9355.
39. Niu W, Zang T, Zou Y, Fang S, Smith DK, Bachoo R, Zhang CL: **In vivo reprogramming of astrocytes to neuroblasts in the adult brain**. *Nat Cell Biol* 2013, **15**(10):1164-1175.
40. Torper O, Ottosson DR, Pereira M, Lau S, Cardoso T, Grealish S, Parmar M: **In Vivo Reprogramming of Striatal NG2 Glia into Functional Neurons that Integrate into Local Host Circuitry**. *Cell Rep* 2015, **12**(3):474-481.
41. Torper O, Pfisterer U, Wolf DA, Pereira M, Lau S, Jakobsson J, Bjorklund A, Grealish S, Parmar M: **Generation of induced neurons via direct conversion in vivo**. *Proc Natl Acad Sci U S A* 2013, **110**(17):7038-7043.
42. Su Z, Niu W, Liu ML, Zou Y, Zhang CL: **In vivo conversion of astrocytes to neurons in the injured adult spinal cord**. *Nat Commun* 2014, **5**:3338.
43. Tan BT, Jiang L, Liu L, Yin Y, Luo ZR, Long ZY, Li S, Yu LH, Wu YM, Liu Y: **Local injection of Lenti-Olig2 at lesion site promotes functional recovery of spinal cord injury in rats**. *CNS Neurosci Ther* 2017, **23**(6):475-487.
44. Arvidsson A, Collin T, Kirik D, Kokaia Z, Lindvall O: **Neuronal replacement from endogenous precursors in the adult brain after stroke**. *Nat Med* 2002, **8**(9):963-970.
45. Ming GL, Song H: **Adult neurogenesis in the mammalian brain: significant answers and significant questions**. *Neuron* 2011, **70**(4):687-702.
46. Parent JM, Vexler ZS, Gong C, Derugin N, Ferriero DM: **Rat forebrain neurogenesis and striatal neuron replacement after focal stroke**. *Ann Neurol* 2002, **52**(6):802-813.
47. van Praag H, Schinder AF, Christie BR, Toni N, Palmer TD, Gage FH: **Functional neurogenesis in the adult hippocampus**. *Nature* 2002, **415**(6875):1030-1034.
48. Bonfanti L: **Adult Neurogenesis 50 Years Later: Limits and Opportunities in Mammals**. *Front Neurosci* 2016, **10**:44.
49. Goldman SA: **Stem and Progenitor Cell-Based Therapy of the Central Nervous System: Hopes, Hype, and Wishful Thinking**. *Cell Stem Cell* 2016, **18**(2):174-188.
50. Duan H, Song W, Zhao W, Gao Y, Yang Z, Li X: **Endogenous neurogenesis in adult mammals after spinal cord injury**. *Sci China Life Sci* 2016.
51. Zhao C, Teng EM, Summers RG, Jr., Ming GL, Gage FH: **Distinct morphological stages of dentate granule neuron maturation in the adult mouse hippocampus**. *J Neurosci* 2006, **26**(1):3-11.
52. Zhou ZD, Kumari U, Xiao ZC, Tan EK: **Notch as a Molecular Switch in Neural Stem Cells**. *Iubmb Life* 2010, **62**(8):618-623.
53. Imayoshi I, Sakamoto M, Yamaguchi M, Mori K, Kageyama R: **Essential roles of Notch signaling in maintenance of neural stem cells in developing and adult brains**. *J Neurosci* 2010, **30**(9):3489-3498.
54. Li Y, Tzatzalos E, Kwan KY, Grumet M, Cai L: **Transcriptional Regulation of Notch1 Expression by Nkx6.1 in Neural Stem/Progenitor Cells during Ventral Spinal Cord Development**. *Sci Rep* 2016, **6**:38665.
55. Ehm O, Goritz C, Covic M, Schaffner I, Schwarz TJ, Karaca E, Kempkes B, Kremmer E, Pfrieger FW, Espinosa L *et al*: **RBPJkappa-dependent signaling is essential for long-term maintenance of neural stem cells in the adult hippocampus**. *J Neurosci* 2010, **30**(41):13794-13807.
56. Sun YY, Li L, Liu XH, Gu N, Dong HL, Xiong L: **The spinal notch signaling pathway plays a pivotal role in the development of neuropathic pain**. *Mol Brain* 2012, **5**:23.

57. Dias TB, Yang YJ, Ogai K, Becker T, Becker CG: **Notch signaling controls generation of motor neurons in the lesioned spinal cord of adult zebrafish**. *J Neurosci* 2012, **32**(9):3245-3252.
58. Sander M, Paydar S, Ericson J, Briscoe J, Berber E, German M, Jessell TM, Rubenstein JL: **Ventral neural patterning by Nkx homeobox genes: Nkx6.1 controls somatic motor neuron and ventral interneuron fates**. *Genes Dev* 2000, **14**(17):2134-2139.
59. Zhao X, Chen Y, Zhu Q, Huang H, Teng P, Zheng K, Hu X, Xie B, Zhang Z, Sander M *et al*: **Control of astrocyte progenitor specification, migration and maturation by Nkx6.1 homeodomain transcription factor**. *PLoS One* 2014, **9**(10):e109171.
60. Fu H, Qi Y, Tan M, Cai J, Hu X, Liu Z, Jensen J, Qiu M: **Molecular mapping of the origin of postnatal spinal cord ependymal cells: evidence that adult ependymal cells are derived from Nkx6.1+ ventral neural progenitor cells**. *The Journal of comparative neurology* 2003, **456**(3):237-244.
61. Kuscha V, Frazer SL, Dias TB, Hibi M, Becker T, Becker CG: **Lesion-induced generation of interneuron cell types in specific dorsoventral domains in the spinal cord of adult zebrafish**. *J Comp Neurol* 2012, **520**(16):3604-3616.
62. Briscoe J, Sussel L, Serup P, Hartigan-O'Connor D, Jessell TM, Rubenstein JL, Ericson J: **Homeobox gene Nkx2.2 and specification of neuronal identity by graded Sonic hedgehog signalling**. *Nature* 1999, **398**(6728):622-627.
63. Fabbiani G, Rehermann MI, Aldecosea C, Trujillo-Cenoz O, Russo RE: **Emergence of Serotonergic Neurons After Spinal Cord Injury in Turtles**. *Front Neural Circuits* 2018, **12**:20.
64. Mizuguchi R, Kriks S, Cordes R, Gossler A, Ma Q, Goulding M: **Ascl1 and Gsh1/2 control inhibitory and excitatory cell fate in spinal sensory interneurons**. *Nat Neurosci* 2006, **9**(6):770-778.
65. Cheesman SE, Eisen JS: **gsh1 demarcates hypothalamus and intermediate spinal cord in zebrafish**. *Gene Expr Patterns* 2004, **5**(1):107-112.
66. Lacroix S, Hamilton LK, Vaugeois A, Beaudoin S, Breault-Dugas C, Pineau I, Levesque SA, Gregoire CA, Fernandes KJ: **Central canal ependymal cells proliferate extensively in response to traumatic spinal cord injury but not demyelinating lesions**. *PLoS One* 2014, **9**(1):e85916.
67. McDonough A, Martinez-Cerdeno V: **Endogenous proliferation after spinal cord injury in animal models**. *Stem Cells Int* 2012, **2012**:387513.
68. Mothe AJ, Tator CH: **Proliferation, migration, and differentiation of endogenous ependymal region stem/progenitor cells following minimal spinal cord injury in the adult rat**. *Neuroscience* 2005, **131**(1):177-187.
69. Sabelstrom H, Stenudd M, Reu P, Dias DO, Elfineh M, Zdunek S, Damberg P, Goritz C, Frisen J: **Resident neural stem cells restrict tissue damage and neuronal loss after spinal cord injury in mice**. *Science* 2013, **342**(6158):637-640.
70. Zai LJ, Wrathall JR: **Cell proliferation and replacement following contusive spinal cord injury**. *Glia* 2005, **50**(3):247-257.
71. Chen W, Zhang B, Xu S, Lin R, Wang W: **Lentivirus carrying the NeuroD1 gene promotes the conversion from glial cells into neurons in a spinal cord injury model**. *Brain Res Bull* 2017, **135**:143-148.
72. Li H, Chen G: **In Vivo Reprogramming for CNS Repair: Regenerating Neurons from Endogenous Glial Cells**. *Neuron* 2016, **91**(4):728-738.

73. Dias DO, Kim H, Holl D, Werne Solnestam B, Lundeberg J, Carlen M, Goritz C, Frisen J: **Reducing Pericyte-Derived Scarring Promotes Recovery after Spinal Cord Injury**. *Cell* 2018, **173**(1):153-165 e122.
74. Cafferty WB, Yang SH, Duffy PJ, Li S, Strittmatter SM: **Functional axonal regeneration through astrocytic scar genetically modified to digest chondroitin sulfate proteoglycans**. *J Neurosci* 2007, **27**(9):2176-2185.
75. Fitch MT, Silver J: **CNS injury, glial scars, and inflammation: Inhibitory extracellular matrices and regeneration failure**. *Exp Neurol* 2008, **209**(2):294-301.
76. Courtine G, Song B, Roy RR, Zhong H, Herrmann JE, Ao Y, Qi J, Edgerton VR, Sofroniew MV: **Recovery of supraspinal control of stepping via indirect propriospinal relay connections after spinal cord injury**. *Nat Med* 2008, **14**(1):69-74.
77. Rossignol S, Frigon A: **Recovery of locomotion after spinal cord injury: some facts and mechanisms**. *Annu Rev Neurosci* 2011, **34**:413-440.
78. Chen B, Li Y, Yu B, Zhang Z, Brommer B, Williams PR, Liu Y, Hegarty SV, Zhou S, Zhu J *et al*: **Reactivation of Dormant Relay Pathways in Injured Spinal Cord by KCC2 Manipulations**. *Cell* 2018, **174**(6):1599.
79. Gong S, Zheng C, Doughty ML, Losos K, Didkovsky N, Schambra UB, Nowak NJ, Joyner A, Leblanc G, Hatten ME *et al*: **A gene expression atlas of the central nervous system based on bacterial artificial chromosomes**. *Nature* 2003, **425**(6961):917-925.
80. Pei Z, Wang B, Chen G, Nagao M, Nakafuku M, Campbell K: **Homeobox genes Gsx1 and Gsx2 differentially regulate telencephalic progenitor maturation**. *Proc Natl Acad Sci U S A* 2011, **108**(4):1675-1680.
81. Chapman H, Riesenberg A, Ehrman LA, Kohli V, Nardini D, Nakafuku M, Campbell K, Waclaw RR: **Gsx transcription factors control neuronal versus glial specification in ventricular zone progenitors of the mouse lateral ganglionic eminence**. *Dev Biol* 2018, **442**(1):115-126.
82. Lopez-Juarez A, Howard J, Ullom K, Howard L, Grande A, Pardo A, Waclaw R, Sun YY, Yang D, Kuan CY *et al*: **Gsx2 controls region-specific activation of neural stem cells and injury-induced neurogenesis in the adult subventricular zone**. *Genes Dev* 2013, **27**(11):1272-1287.
83. Wang B, Long JE, Flandin P, Pla R, Waclaw RR, Campbell K, Rubenstein JL: **Loss of Gsx1 and Gsx2 function rescues distinct phenotypes in Dlx1/2 mutants**. *J Comp Neurol* 2013, **521**(7):1561-1584.
84. Wang B, Waclaw RR, Allen ZJ, 2nd, Guillemot F, Campbell K: **Ascl1 is a required downstream effector of Gsx gene function in the embryonic mouse telencephalon**. *Neural Dev* 2009, **4**:5.
85. Chen K, Deng S, Lu H, Zheng Y, Yang G, Kim D, Cao Q, Wu JQ: **RNA-seq characterization of spinal cord injury transcriptome in acute/subacute phases: a resource for understanding the pathology at the systems level**. *PLoS One* 2013, **8**(8):e72567.
86. Kutner RH, Zhang XY, Reiser J: **Production, concentration and titration of pseudotyped HIV-1-based lentiviral vectors**. *Nat Protoc* 2009, **4**(4):495-505.
87. Rueden CT, Schindelin J, Hiner MC, DeZonia BE, Walter AE, Arena ET, Eliceiri KW: **ImageJ2: ImageJ for the next generation of scientific image data**. *BMC Bioinformatics* 2017, **18**(1):529.
88. Schneider CA, Rasband WS, Eliceiri KW: **NIH Image to ImageJ: 25 years of image analysis**. *Nat Methods* 2012, **9**(7):671-675.

89. Dobin A, Davis CA, Schlesinger F, Drenkow J, Zaleski C, Jha S, Batut P, Chaisson M, Gingeras TR: **STAR: ultrafast universal RNA-seq aligner**. *Bioinformatics* 2013, **29**(1):15-21.
90. Anders S, Pyl PT, Huber W: **HTSeq--a Python framework to work with high-throughput sequencing data**. *Bioinformatics* 2015, **31**(2):166-169.
91. Love MI, Huber W, Anders S: **Moderated estimation of fold change and dispersion for RNA-seq data with DESeq2**. *Genome Biol* 2014, **15**(12):550.
92. Anders S, Huber W: **Differential expression analysis for sequence count data**. *Genome Biol* 2010, **11**(10):R106.
93. Zhao C, Deng W, Gage FH: **Mechanisms and functional implications of adult neurogenesis**. *Cell* 2008, **132**(4):645-660.
94. Kramer A, Green J, Pollard J, Jr., Tugendreich S: **Causal analysis approaches in Ingenuity Pathway Analysis**. *Bioinformatics* 2014, **30**(4):523-530.
95. Supek F, Bosnjak M, Skunca N, Smuc T: **REVIGO summarizes and visualizes long lists of gene ontology terms**. *PLoS One* 2011, **6**(7):e21800.
96. Horky LL, Galimi F, Gage FH, Horner PJ: **Fate of endogenous stem/progenitor cells following spinal cord injury**. *J Comp Neurol* 2006, **498**(4):525-538.
97. Johansson CB, Momma S, Clarke DL, Risling M, Lendahl U, Frisen J: **Identification of a neural stem cell in the adult mammalian central nervous system**. *Cell* 1999, **96**(1):25-34.
98. Izon DJ, Aster JC, He Y, Weng A, Karnell FG, Patriub V, Xu L, Bakkour S, Rodriguez C, Allman D *et al*: **Deltex1 redirects lymphoid progenitors to the B cell lineage by antagonizing Notch1**. *Immunity* 2002, **16**(2):231-243.
99. Pirot P, van Grunsven LA, Marine JC, Huylebroeck D, Bellefroid EJ: **Direct regulation of the Nrarp gene promoter by the Notch signaling pathway**. *Biochem Biophys Res Commun* 2004, **322**(2):526-534.
100. Shi Y, Whetstine JR: **Dynamic regulation of histone lysine methylation by demethylases**. *Mol Cell* 2007, **25**(1):1-14.
101. Kawamata S, Du C, Li K, Lavau C: **Overexpression of the Notch target genes Hes in vivo induces lymphoid and myeloid alterations**. *Oncogene* 2002, **21**(24):3855-3863.
102. Hatakeyama J, Bessho Y, Katoh K, Ookawara S, Fujioka M, Guillemot F, Kageyama R: **Hes genes regulate size, shape and histogenesis of the nervous system by control of the timing of neural stem cell differentiation**. *Development* 2004, **131**(22):5539-5550.
103. Lee SH, Jeyapalan JN, Appleby V, Mohamed Noor DA, Sottile V, Scotting PJ: **Dynamic methylation and expression of Oct4 in early neural stem cells**. *J Anat* 2010, **217**(3):203-213.
104. Brown JP, Couillard-Despres S, Cooper-Kuhn CM, Winkler J, Aigner L, Kuhn HG: **Transient expression of doublecortin during adult neurogenesis**. *J Comp Neurol* 2003, **467**(1):1-10.
105. Gleeson JG, Lin PT, Flanagan LA, Walsh CA: **Doublecortin is a microtubule-associated protein and is expressed widely by migrating neurons**. *Neuron* 1999, **23**(2):257-271.
106. Couillard-Despres S, Winner B, Schaubeck S, Aigner R, Vroemen M, Weidner N, Bogdahn U, Winkler J, Kuhn HG, Aigner L: **Doublecortin expression levels in adult brain reflect neurogenesis**. *Eur J Neurosci* 2005, **21**(1):1-14.
107. Bovolenta P, Wandosell F, Nieto-Sampedro M: **CNS glial scar tissue: a source of molecules which inhibit central neurite outgrowth**. *Prog Brain Res* 1992, **94**:367-379.
108. Rolls A, Shechter R, Schwartz M: **The bright side of the glial scar in CNS repair**. *Nat Rev Neurosci* 2009, **10**(3):235-241.

109. Silver J, Miller JH: **Regeneration beyond the glial scar**. *Nat Rev Neurosci* 2004, **5**(2):146-156.
110. Hara M, Kobayakawa K, Ohkawa Y, Kumamaru H, Yokota K, Saito T, Kijima K, Yoshizaki S, Harimaya K, Nakashima Y *et al*: **Interaction of reactive astrocytes with type I collagen induces astrocytic scar formation through the integrin-N-cadherin pathway after spinal cord injury**. *Nat Med* 2017, **23**(7):818-828.
111. Zamanian JL, Xu L, Foo LC, Nouri N, Zhou L, Giffard RG, Barres BA: **Genomic analysis of reactive astrogliosis**. *J Neurosci* 2012, **32**(18):6391-6410.
112. Moore DL, Goldberg JL: **Multiple transcription factor families regulate axon growth and regeneration**. *Dev Neurobiol* 2011, **71**(12):1186-1211.
113. Perrin FE, Noristani HN: **Serotonergic mechanisms in spinal cord injury**. *Exp Neurol* 2019, **318**:174-191.
114. Faden AI, Gannon A, Basbaum AI: **Use of serotonin immunocytochemistry as a marker of injury severity after experimental spinal trauma in rats**. *Brain Res* 1988, **450**(1-2):94-100.
115. Camand E, Morel MP, Faissner A, Sotelo C, Dusart I: **Long-term changes in the molecular composition of the glial scar and progressive increase of serotoninergic fibre sprouting after hemisection of the mouse spinal cord**. *Eur J Neurosci* 2004, **20**(5):1161-1176.
116. Alaynick WA, Jessell TM, Pfaff SL: **SnapShot: spinal cord development**. *Cell* 2011, **146**(1):178-178 e171.
117. Ables JL, Breunig JJ, Eisch AJ, Rakic P: **Not(ch) just development: Notch signalling in the adult brain**. *Nat Rev Neurosci* 2011, **12**(5):269-283.
118. Pierfelice T, Alberi L, Gaiano N: **Notch in the vertebrate nervous system: an old dog with new tricks**. *Neuron* 2011, **69**(5):840-855.
119. Faulkner JR, Herrmann JE, Woo MJ, Tansey KE, Doan NB, Sofroniew MV: **Reactive astrocytes protect tissue and preserve function after spinal cord injury**. *J Neurosci* 2004, **24**(9):2143-2155.
120. Benner EJ, Luciano D, Jo R, Abdi K, Paez-Gonzalez P, Sheng H, Warner DS, Liu C, Eroglu C, Kuo CT: **Protective astrogenesis from the SVZ niche after injury is controlled by Notch modulator Thbs4**. *Nature* 2013, **497**(7449):369-373.
121. Cai J, Xu X, Yin H, Wu R, Modderman G, Chen Y, Jensen J, Hui CC, Qiu M: **Evidence for the differential regulation of Nkx-6.1 expression in the ventral spinal cord and foregut by Shh-dependent and -independent mechanisms**. *Genesis* 2000, **27**(1):6-11.
122. Fuchs S, Herzog D, Sumara G, Buchmann-Moller S, Civenni G, Wu X, Chrostek-Grashoff A, Suter U, Ricci R, Relvas JB *et al*: **Stage-specific control of neural crest stem cell proliferation by the small rho GTPases Cdc42 and Rac1**. *Cell Stem Cell* 2009, **4**(3):236-247.
123. Leone DP, Srinivasan K, Brakebusch C, McConnell SK: **The rho GTPase Rac1 is required for proliferation and survival of progenitors in the developing forebrain**. *Dev Neurobiol* 2010, **70**(9):659-678.
124. Cattaneo E, McKay R: **Proliferation and differentiation of neuronal stem cells regulated by nerve growth factor**. *Nature* 1990, **347**(6295):762-765.
125. Xu L, Zhou S, Feng GY, Zhang LP, Zhao DM, Sun Y, Liu Q, Huang F: **Neural stem cells enhance nerve regeneration after sciatic nerve injury in rats**. *Mol Neurobiol* 2012, **46**(2):265-274.
126. Sundberg M, Andersson PH, Akesson E, Odeberg J, Holmberg L, Inzunza J, Falci S, Ohman J, Suuronen R, Skottman H *et al*: **Markers of pluripotency and differentiation in human**

neural precursor cells derived from embryonic stem cells and CNS tissue. *Cell Transplant* 2011, **20**(2):177-191.
127. Vincent PH, Benedikz E, Uhlen P, Hovatta O, Sundstrom E: **Expression of Pluripotency Markers in Nonpluripotent Human Neural Stem and Progenitor Cells**. *Stem Cells Dev* 2017, **26**(12):876-887.
128. Qiu H, Tang X, Ma J, Shaverdashvili K, Zhang K, Bedogni B: **Notch1 Autoactivation via Transcriptional Regulation of Furin, Which Sustains Notch1 Signaling by Processing Notch1-Activating Proteases ADAM10 and Membrane Type 1 Matrix Metalloproteinase**. *Molecular and Cellular Biology* 2015, **35**(21):3622-3632.
129. Beel AJ, Sanders CR: **Substrate specificity of gamma-secretase and other intramembrane proteases**. *Cell Mol Life Sci* 2008, **65**(9):1311-1334.
130. Hemming ML, Elias JE, Gygi SP, Selkoe DJ: **Proteomic profiling of gamma-secretase substrates and mapping of substrate requirements**. *PLoS Biol* 2008, **6**(10):e257.
131. Wang H, Zang C, Taing L, Arnett KL, Wong YJ, Pear WS, Blacklow SC, Liu XS, Aster JC: **NOTCH1-RBPJ complexes drive target gene expression through dynamic interactions with superenhancers**. *Proc Natl Acad Sci U S A* 2014, **111**(2):705-710.
132. McKeon RJ, Jurynec MJ, Buck CR: **The chondroitin sulfate proteoglycans neurocan and phosphacan are expressed by reactive astrocytes in the chronic CNS glial scar**. *J Neurosci* 1999, **19**(24):10778-10788.
133. Rhodes KE, Fawcett JW: **Chondroitin sulphate proteoglycans: preventing plasticity or protecting the CNS?** *J Anat* 2004, **204**(1):33-48.
134. McKeon RJ, Hoke A, Silver J: **Injury-induced proteoglycans inhibit the potential for laminin-mediated axon growth on astrocytic scars**. *Exp Neurol* 1995, **136**(1):32-43.
135. Jones LL, Margolis RU, Tuszynski MH: **The chondroitin sulfate proteoglycans neurocan, brevican, phosphacan, and versican are differentially regulated following spinal cord injury**. *Exp Neurol* 2003, **182**(2):399-411.
136. Windle WF, Chambers WW: **Regeneration in the spinal cord of the cat and dog**. *J Comp Neurol* 1950, **93**(2):241-257.
137. Barnabe-Heider F, Frisen J: **Stem cells for spinal cord repair**. *Cell Stem Cell* 2008, **3**(1):16-24.
138. Fawcett JW, Asher RA: **The glial scar and central nervous system repair**. *Brain Res Bull* 1999, **49**(6):377-391.
139. Wang H, Song G, Chuang H, Chiu C, Abdelmaksoud A, Ye Y, Zhao L: **Portrait of glial scar in neurological diseases**. *Int J Immunopathol Pharmacol* 2018, **31**:2058738418801406.
140. Givogri MI, de Planell M, Galbiati F, Superchi D, Gritti A, Vescovi A, de Vellis J, Bongarzone ER: **Notch signaling in astrocytes and neuroblasts of the adult subventricular zone in health and after cortical injury**. *Dev Neurosci* 2006, **28**(1-2):81-91.
141. LeComte MD, Shimada IS, Sherwin C, Spees JL: **Notch1-STAT3-ETBR signaling axis controls reactive astrocyte proliferation after brain injury**. *Proc Natl Acad Sci U S A* 2015, **112**(28):8726-8731.
142. Mitsui K, Tokuzawa Y, Itoh H, Segawa K, Murakami M, Takahashi K, Maruyama M, Maeda M, Yamanaka S: **The homeoprotein Nanog is required for maintenance of pluripotency in mouse epiblast and ES cells**. *Cell* 2003, **113**(5):631-642.
143. Chambers I, Colby D, Robertson M, Nichols J, Lee S, Tweedie S, Smith A: **Functional expression cloning of Nanog, a pluripotency sustaining factor in embryonic stem cells**. *Cell* 2003, **113**(5):643-655.

144. Boyer LA, Lee TI, Cole MF, Johnstone SE, Levine SS, Zucker JP, Guenther MG, Kumar RM, Murray HL, Jenner RG *et al*: **Core transcriptional regulatory circuitry in human embryonic stem cells**. *Cell* 2005, **122**(6):947-956.
145. Gu J, Ni Y, Xu L, Xu H, Cai Z: **Nanog interact with CDK6 to regulates astrocyte cells proliferation following spinal cord injury**. *Biochem Biophys Res Commun* 2016, **469**(4):1097-1103.
146. Stenudd M, Sabelstrom H, Frisen J: **Role of endogenous neural stem cells in spinal cord injury and repair**. *JAMA Neurol* 2015, **72**(2):235-237.
147. Yang H, Lu P, McKay HM, Bernot T, Keirstead H, Steward O, Gage FH, Edgerton VR, Tuszynski MH: **Endogenous neurogenesis replaces oligodendrocytes and astrocytes after primate spinal cord injury**. *J Neurosci* 2006, **26**(8):2157-2166.
148. Yang Z, Zhang A, Duan H, Zhang S, Hao P, Ye K, Sun YE, Li X: **NT3-chitosan elicits robust endogenous neurogenesis to enable functional recovery after spinal cord injury**. *Proc Natl Acad Sci U S A* 2015, **112**(43):13354-13359.
149. Block ML, Zecca L, Hong JS: **Microglia-mediated neurotoxicity: uncovering the molecular mechanisms**. *Nat Rev Neurosci* 2007, **8**(1):57-69.
150. Popovich PG, Guan Z, Wei P, Huitinga I, van Rooijen N, Stokes BT: **Depletion of hematogenous macrophages promotes partial hindlimb recovery and neuroanatomical repair after experimental spinal cord injury**. *Exp Neurol* 1999, **158**(2):351-365.
151. Yu XJ, Bellamkonda RV: **Dorsal root ganglia neurite extension is inhibited by mechanical and chondroitin sulfate-rich interfaces**. *J Neurosci Res* 2001, **66**(2):303-310.